# Investigating factors influencing UAS task automation in dynamic environments

**HE Van Rensburg**

**orcid.org 0000-0002-3396-0249**

Dissertation accepted in partial fulfilment of the requirements for the degree *Master of Science in Computer Science* at the North-West University

| | |
|---|---|
| Supervisor: | Mr H Foulds |
| Assistant Supervisor: | Prof L Drevin |

Graduation May 2020

22984542

# ACKNOWLEDGEMENTS

I wish to thank my supervisors for their guidance, support, inspiration, patience and everything I was able to learn from them during this time.

Thank you also to

Prof Suria Ellis at the Statistical Consultation Services of the NWU Potchefstroom Campus for your friendliness, encouragement and assistance with the statistics of this study

Dr Isabel Swart for proof reading and language editing

All my colleagues at the School for Computer Science and Information Systems at the NWU Potchefstroom Campus for your inspiration, friendliness and willingness to help

My parents, Ray and Jetty van Rensburg, and my siblings, Olga, Martin, Jacob, and Pierre for your love, motivation and support throughout the study

J'Retha Rossouw for your encouragement, listening to my concerns, and helping me see the light during all the tough times and

Finally, I would like to thank my Creator that made this all possible.

# ABSTRACT

UAS (Unmanned Aerial System) technology and capabilities have greatly improved which means that there are increased application possibilities and various industries in diverse fields are starting to show interest in UAS implementations. The problem with widespread implementations is that not all industries have a skilled UAS operator or pilot with a license. More often than not, these industries are not necessarily interested in flying the UAS, but only in the data collected or specific task undertaken by the UAS. Thus, it is more important for UASs to perform automated tasks without placing a huge burden on the operator or pilot, to be able to focus on the task at hand. The problem is that most commonly available UASs that support autonomous tasks are influenced by external factors that are not always compensated for. In this study, external factors influencing the UAS task environment are investigated in literature to determine the most significant factor. The most significant factor that influences UAS task automation and performance is identified as wind therefore experiments were conducted to illustrate its effects. The UAS performed automated flight experiments to predetermined waypoints along a chosen flight path. The data collected from the UAS flight logs, as well as the weather station was analysed to illustrate and determine the influence of wind on the UAS flight, and how it affected the accuracy of the automated flight in terms of deviation from the planned flight path between the waypoints, the time it took to reach the waypoints, as well as the drift sustained when hovering. These results are used to make recommendations for conducting autonomous UAS flights in dynamic environments with wind, to improve the accuracy and applicability in diverse applications.

*Keywords*:

UAS, UAV, Wind, Automation, Control, Weather, Environment, Experiment, Unmanned, Dynamic, Conditions, Applications, System, Aerial, Aircraft

# OPSOMMING

UAS (*Unmanned Aerial System*) tegnologie en funksionaliteit het baie verbeter, wat beteken dat daar baie meer toepassingsmoontlikhede is en verskeie industrieë belangstelling begin toon vir UAS implementerings in diverse velde. Die probleem met wydverspreide implementerings is dat alle industrieë nie 'n opgeleide UAS-operateur of -vlieënier met 'n lisensie het nie. Hierdie industrieë stel meer dikwels nie noodwendig belang in die vlieg van die UAS nie, maar stel slegs belang in die data wat ingesamel word of die spesifieke taak wat deur die UAS verrig word. Daarom is dit belangriker vir die UAS om take outomaties te kan uitvoer sonder om 'n geweldige las op die vlieënier of beheerder te plaas en eerder op die taak te kan fokus. Die probleem is dat die algemeenste beskikbare UAS wat outonome take ondersteun deur eksterne faktore beïnvloed word waarvoor daar nie altyd voorsiening gemaak word nie. In hierdie studie word die skynbare eksterne faktore in die literatuur ondersoek om die invloedrykste eksterne faktor te bepaal. Die invloedrykste faktor wat die UAS geoutomatiseerde taakprestasie beïnvloed, is geïdentifiseer as wind, dus is eksperimente uitgevoer word om die gevolge daarvan te illustreer. Die UAS het die vlugeksperimente outomaties uitgevoer deur na voorafbepaalde punte op 'n roete te vlieg. Die data wat uit die UAS-vluglogboek sowel as die weerstasie ingesamel is, is ontleed om die invloed van wind op die UAS-vlug te illustreer en te bepaal hoe dit die outonome uitgevoerde vlugroete beïnvloed het om voorspelling en verbetering van outonome UAS-vluguitvoering en praktiese toepasbaarheid in diverse implementerings te ondersteun.

*Sleutelterme*:

UAS, UAV, Wind, Outomatisering, Beheer, Weer, Omgewing, Eksperiment, Onbemande, Dinamies, Omstandighede, Toestande, Toepassings, Stelsel, Lugvaartuig, Vliegtuig

# TABLE OF CONTENTS

# LIST OF TABLES

# LIST OF FIGURES

## LIST OF CODE SNIPPETS

# CHAPTER 1 – INTRODUCTION

*An introduction to the research study, providing background on key terminology, including the problem statement and substantiation, the aim and objectives, as well as an overview of the structure of the study.*

## 1.1 Background and problem description

Unmanned aircraft have gained popularity in various fields of application, especially with the exponential advancement of unmanned aircraft technology and constantly improving capabilities, promoting commercial interest. There is, however, often a degree of confusion regarding the terms and names used to describe unmanned aircraft. An Unmanned Aerial Vehicle (UAV) is a generic term, commonly referred to as a drone, used for aerial vehicles that have no pilot on board and are controlled remotely or by an on-board computer (Dalamagkidis, 2015b). An Unmanned Aerial System (UAS) consists of a UAV, the ground control station and the communications medium working together as a comprehensive system (Dalamagkidis, 2015b). UAS is the preferred term adopted by regulators, the American Federal Aviation Administration (FAA) and in industry when referring to the overarching system, whereas UAV refers to the vehicle itself.

UAS capabilities have greatly improved, increasing the demand for UAS applications (Clothier *et al.*, 2007). UAS technologies have become cheaper, lighter and the use of these technologies are becoming more popular in a wide variety of environments, leading to increased commercial interest (Leong, 2015; Bouabdallah *et al.*, 2007). UASs are commonly used in situations and environments deemed too dangerous or risky for pilots to enter or operate within (Chee & Zhong, 2013; Watts *et al.*, 2012). Due to the progress of UAS technology, UAS implementations have diversified in various fields of application and environments, such as surveillance (Casbeer *et al.*, 2006; Puri, 2005), safety and security (Leong, 2015; Goodrich *et al.*, 2008), disaster and emergency management (Quaritsch *et al.*, 2010; Ameri *et al.*, 2009; Metni & Hamel, 2007), exploration and mapping (Bryson & Sukkarieh, 2009; Rathinam *et al.*, 2007), and agriculture (Rasmussen *et al.*, 2013; Zhang & Kovacs, 2012; Grenzdörffer *et al.*, 2008).

UASs are used in fields and environments for various practical purposes with the main goal being data collection, and image and video collection. Therefore, regardless of the application or environment, specialists are predominantly interested in gathering data for a specific task, rather than focusing on the chore of flying the UAV safely (Rasmussen *et al.*, 2013). Traditionally, UAS applications have a human operator who is responsible for flying the UAV to collect the required

data. This approach was enhanced as technology allowed an additional controller to simultaneously communicate with the UAS, allowing a second operator to control the camera and focus on data collection, while the other operator focuses on flying the UAS as required for the specific application. Although an original approach, this is not practically favourable, since an additional operator is required for collecting imagery and data. This reliance on operators is an aspect of concern, since trained UAS operators are not always available (Fern & Shively, 2009). Therefore, researchers aim to improve autonomous UAS control and flight management efficiency in order to minimize the need for a human operator or human intervention in UAS flight.

UAS applications are often reliant on the automation of specific tasks to reduce the burden placed on an operator. An example of this is the *Return to Home* (RTH) functionality of many commonly available UASs which enables the UAV to fly back to the take-off location, or predefined home location. The RTH functionality often assumes a static environment, not compensating for collisions that might occur. This RTH functionality of particularly the DJI Phantom 3 professional used in this study is a static implementation that does not compensate for any obstacles or collisions that might occur, whereas the UAV merely ascends to a pre-set altitude, adjusts direction towards the recorded home position and flies back (DJI, 2016). Commonly available automation implementations are heavily reliant on human operators to plan and manage flights, as well as being available and alert to take control in unsafe or potentially hazardous situations to safely return and land the UAV.

Some UAS applications make use of limited automation implementations that struggle to maintain a steady flight path, since they do not compensate for dynamic environmental factors (Yang *et al.*, 2013). These automation implementations have difficulty in executing objectives precisely as planned, causing a deviation in the flight path that can potentially result in hazardous situations, since dynamic environmental factors are not compensated for (Yang *et al.*, 2013). Manual and automated flights are rarely performed in static environments in practice, but rather predominantly in dynamic and unpredictable environments. Therefore, the overall objective is improving UAV control and flight accuracy by improving automation implementations to easily navigate through dynamic and unpredictable environments and reducing the burden placed upon human operators.

UAS performance and reliability are influenced by dynamic environmental factors, such as unknown wind conditions (Jordan, 2015; Månsson & Stenberg, 2014; Orr *et al.*, 2005). Any environmental factors that influence performance and reliability will also influence UAS task automation. Since UASs operate in real-world environments that are subject to dynamic conditions, such as changing climate conditions and communications interference, the UAS task environment is unavoidably influenced by these conditions. Another factor influencing widespread

UAS task automation is possible collisions with static or dynamic objects (Surakul *et al.*, 2015; Patel, 2011). In practical UAS applications, potentially hazardous situations ranging from unknown static objects in static environments to moving objects in dynamic environments may result in collisions, causing property damage or harm if not compensated for.

The abovementioned factors influencing UAS task automation make it clear that it is not enough to only consider static environments. Automating UAS control in dynamic environments is still in the early stages of development and more research is needed in this field to reduce the cognitive burden placed on UAS operators (Lin *et al.*, 2019; Belkhouche, 2009). This research study will focus on identifying prominent factors in dynamic UAS task environments and to what extent the most significant factors influence the automation of UAS tasks.

## 1.2 Research aims and objectives

The aim of this research study is to investigate environmental factors influencing the automation of UAS tasks in dynamic environments.

To achieve the aim of this research study, the following objectives are set:

- Explore UAS technologies, control methods and automation in literature;
- Investigate literature relating to environmental factors influencing the UAS task environment and review existing automation methods that may address these factors;
- Identify the most significant environmental factor, as well as UAS task automation methods that can be used to evaluate the identified environmental factor in dynamic UAS task environments;
- Conduct experiments to illustrate the influence and/or significance of the identified environmental factor on automated UAS tasks;
- Evaluate the influence of the identified environmental factor on the completion of the automated tasks by comparing the planned flight path to the actual flight path from the experimental results obtained in a dynamic environment; and
- Propose possible solutions that may improve UAS task automation to address the identified environmental factor.

## 1.3 Overview of chapters

An overview of the chapters in this study is listed below to provide an outline of the content and a short description to offer a holistic view of the study and show how it is structured.

- **Chapter 1 – Introduction:** An introduction to the research study, providing background on key terminology, including the problem statement and substantiation, the aim and objectives, as well as an overview of the structure of the study.
- **Chapter 2 – Research method:** A description of the research paradigm, methods and design methodologies used for the research study, as well as the experimental design, providing a framework that guided this study.
- **Chapter 3 – Literature review:** An overview and discussion of topics relevant to this research study, including an investigation into the environmental factors influencing UAS task automation in dynamic environments.
- **Chapter 4 – Experiments:** An introduction to the hardware and software used, as well as how various experiments are implemented to highlight and demonstrate the relevance and effect of wind on UAS task automation.
- **Chapter 5 – Results:** In this chapter, the results of the experiments conducted in the study and how UAS task automation is affected by windy environmental conditions are presented. A description is provided on how the consolidation and segmentation were performed to obtain the relevant data, whereafter a description of the statistical techniques used to analyse the data and a presentation of the results obtained from the analysis are provided.
- **Chapter 6 – Discussion and conclusion:** A brief summary of the research, methods and implementation of the study, as well as a discussion and interpretation of the results, what implications these results have on UAS task automation in dynamic environments and opportunities for future work.

# CHAPTER 2 – RESEARCH METHOD

*A description of the research paradigm, methods and design methodologies used for the research study, as well as the experimental design, providing a framework that guided this study.*

## 2.1 Introduction and overview

The term “research” can be defined as the systematic investigative process into existing sources of facts and knowledge, with the purpose of discovering new facts and knowledge by studying these materials and sources in order to establish facts and to reach new conclusions (Stevenson, 2015; Shuttleworth & Wilson, 2008). “A paradigm is a set of shared assumptions or ways of thinking about some aspects of the world” (Oates, 2006). Therefore, a research paradigm is concerned with various ways of approaching research and the different assumptions researchers make in their efforts to establish facts and gain knowledge.

There are three major types of research paradigms namely positivism, interpretivism and critical theory. In this research study, a positivistic paradigm will be followed for the evaluation of UAS task automation in dynamic environments. An experimental design research strategy was used in order to obtain data to better understand the effect and influence of the identified dynamic environmental factor on the automation of UAS tasks. This experimental UAS design strategy was used to plan and manage, as well as to set up and perform UAS flight experiments. The results from these experiments are used to understand the effect and to measure the influence of the identified environmental factor on UAS task automation.

This chapter contains a detailed description of the research paradigm and its fundamental characteristics, why it is suitable for this research study and how it was implemented to approach the research and gain knowledge are outlined. In the next section, a description of the positivistic paradigm, followed by its unique characteristics, criticisms, methods, data gathering, data analysis and conclusion is presented. The research method provides insight into the theoretical background and practical applicability of the method on this particular research study.

## 2.2 Positivistic paradigm

The paradigm of positivism can be defined as a shared assumption about the nature of the world (Oates, 2006). The positivistic paradigm underlies the scientific method, which means that it is concerned with making scientific observations and performing various experiments. According to

Oates (2006), this paradigm has two basic assumptions; firstly, that the world is not random, it is ordered by laws and patterns that this method seeks to discover. Secondly, Oates makes the assumption that the world can be investigated in an objective manner, where personal experience and/or feelings do not affect the exploration and fact discovery, and that the world can be investigated rationally.

According to Oates (2006), this method consists of an iterative cycle and there are three basic techniques to take into consideration when applying the scientific method which include reductionism (breaking complex components into more manageable components), repeatability (recurring experiments must yield the same results), and refutation (if repeatability is not an option, it should be supported with evidence to support the refutability).

### 2.2.1 Characteristics

As defined in the previous section, the positivistic paradigm is mainly concerned with, but is not limited to making scientific observations and performing experiments. Positivistic researchers make use of a variety of other research strategies to support their study, where the main emphasis is on their shared view of the world and how to gain information on it, and not on the specific research strategy used (Oates, 2006). These shared assumptions and worldview held by positivistic researchers have the following characteristics in common (Oates, 2006):

- **The world exists independently of humans:** As the view of this paradigm believes that the world is not random and that certain laws and patterns govern the world around us, this characteristic refers to just that in the sense that human beings are separate from the components or subject under investigation;

- **Measurements and modelling:** According to Oates (2006), it is the discovery of this independent world with the use of hypothesis theory. This is the process of conducting experiments by making observations and capturing measurements to construct models of the discovery made. Validity and reliability are instinctively associated with this characteristic;

- **Objectivity:** This highlights the fact that no emotional bias or interference is present and that the study can be conducted without the worry of personal values or beliefs of the participants or any person involved in the study affecting the results obtained;

- **Hypothesis testing**: This characteristic is unique to positivism where a theory, proposition or initial idea is presented which is further discussed, tested, interpreted, and proven or disproven through the extensive research conducted;

- **Quantitative data analysis:** This is the characteristic relating to the measurements and modelling, as well as the hypothesis testing, where the resulting observations of the investigation are analysed by mathematic and statistical modelling of the results; and

- **Universal laws:** Positivistic research looks for patterns, universal laws, and generalisations in order to prove the research findings of the study independent of the researcher.

The characteristics of the positivistic paradigm have now been highlighted, but in order for other academics to accept and use the research, one still has to assess the quality of the research conducted (Oates, 2006). The quality assurance and validity of the conducted research are based on the following criteria (Oates, 2006):

- **Objectivity** – whether or not the research is completely unbiased and free from any preference or personal beliefs of the researcher who conducted the research study;

- **Reliability** – whether or not the correct research procedures were followed, the instruments calibrated, and the data used in the correct and appropriate way;

- **Internal validity** – whether or not the right questions were asked and data collected to produce an accurate and coherent study from the right sources; and

- **External validity** – whether or not the study has generalisability factors to support different situations, and that patterns and general laws were taken into consideration.

These characteristics, along with the quality assurance criteria, provide a framework shaping the paradigm of positivism. This paradigm, however, does have some critique to be cognisant of as described in the next section.

### 2.2.2 Critiques

Since positivistic research is greatly involved with the natural world and aspects of it, there are a few criticisms that have to be taken into consideration. According to Oates (2006), there are five criticisms which include reductionism, repetition, which is not always possible, generalisation that may sometimes not be desirable, the fact that the world is perceived differently by other people,

and that general laws and patterns may be observable in the social world, but are in fact made by people. More detail on these five criticisms is described in the list below (Oates, 2006):

- Reductionism is the process of breaking complex components into more manageable components to study. Positivistic researchers marked the fact that in some situations, external factors simply cannot be excluded, since the holistic view will then be lost in situations where no facet or component can be excluded;

- Repetition is not always possible with positivistic research where the environment can change and yield different results. A popular example in the field of computer science is the change or advancement of hardware and software used to conduct a particular study;

- Generalisation may sometimes not be desirable, since the specific positivistic research study may be conducted in a unique environment that is distinctive to that study;

- Perception relates to the fact that the world is perceived in a different way by different people, making some people interpret similar things in completely different ways even when the results indicate similar findings; and

- General laws and patterns give the illusion that they are observable in the social world, when they are in fact the creations of people.

These criticisms have demerged over time, and should be taken into consideration when conducting research in the paradigm of positivism.

### 2.3 Research methods

A research method can be defined as a strategy created through philosophic assumptions and paradigms involved in order to support the research subject and lead to proper data acquisition and processing (Myers, 1997).

There are a variety of different research methods under each of the research paradigms that is uniquely related to that specific paradigm (Guo & Sheffield, 2008). In general, the positivistic paradigm makes use of methods, such as questionnaires and experiments, where the observations of the investigation are statistically analysed by mathematical and statistical modelling of the results.

According to Oates (2006), there are a variety of research strategies, referred to as methods, where those associated with the positivistic paradigm include methods, such as experiments,

surveys, case studies, action research, as well as design and create. To gain a better understanding and determine which will be most suitable for the purpose of this research study each of these research methods is briefly described below.

**Design and create,** the primary focus of the design and creation research strategy is solving complicated real-world problems by the development of computer science and information system products, which are contextually referred to as artefacts (Hevner & Chatterjee, 2010; Oates, 2006). With the design science research method, design and create, a designer answers questions that are appropriately related to human problems via the design and development of new artefacts. These artefacts are beneficial and of course essential in thoroughly understanding the situation or problem at hand (Hevner & Chatterjee, 2010).

**Action research** can be made use of in all three types of research paradigms. Existing theories are typically tested using action research that involves a critical reflection of a particular approach or action taken by the participants who indirectly become co-researchers in understanding their actions in order to learn from them (Hofstee, 2006).

**Case studies** are not particularly common in positivistic research, but can certainly be used in situations where theories or hypotheses have to be proven or disproven. Case studies also help to identify unmentioned assumptions and agendas that are accepted as true (Oates, 2006).

**Surveys** can also be viewed as a type of experiment in the sense that information is gathered with the aim of identifying patterns of the world, which the researcher should assume exist (Oates, 2006). Surveys enable researchers to gain a wider perspective of the topic under investigation.

**Experiments** are widely used in positivistic research, especially when theories and hypotheses are tested to obtain data to be translated into valuable information in order to understand the specific study or investigation underway into a topic or aspect of the world (Oates, 2006). Experiments are used to explain the outcome of some activity, theory or hypothesis observed in a particular environment to better understand and be able to explain the effect or behaviour of that outcome.

The primary research methods briefly described above provide the generalised application of each method. The most suitable method for the purpose of this research study is experiments that will be discussed further in the next section.

## 2.4 Experimental design

Experiments are widely used in positivistic research, especially when theories and hypotheses are tested to obtain data to be translated into valuable information in order to understand the specific study or investigation underway into a topic or aspect of the world (Oates, 2006). Field experiments are the result of combining traditional laboratory experiments and field work (Gerber & Green, 2008). The purpose of field experiments is to resemble the natural environment as closely as possible by conducting the experiments in the typical environment in which it is ordinarily functioning.

The experimental UAS design, in this exploratory research study, will be in the form of field experiments conducted to assess the influence of identified environmental factors on the automation of UAS tasks. A number of these experiments will be conducted, observed, documented, evaluated, and the results from the evaluation will be used to determine if there is a relationship or some correlation between the particular outcome of the experiments and the identified environmental factor influencing UAS task automation in dynamic environments based on the data observed from the experiments.

### 2.4.1 Data gathering

Data gathering in the positivistic research paradigm depends on the particular research method(s) used to conduct the study as described in the previous section. These methods are used to guide and support the research subject leading to proper data gathering of the aspect under investigation. Mathematical and statistical data analysis is then performed on the gathered data, described in the next section, after which new knowledge and facts can be extracted to produce valuable information on the specific topic under investigation (Oates, 2006).

Quantitative data is collected from the field experiments conducted to support the research study. These experiments are uniquely set up to be able to easily repeat the experiment as the environment changes, to measure the factors influencing UAS task automation. The experimental data collection consists of three main sources, namely waypoint data, flight log data, and weather data. The waypoint data is a collection of coordinates specified by the ground control station software of the particular task to be completed or flight path that must be followed. The flight log data contains all the sensory data from the UAV, specifically the coordinates of each point in time during these flights. Weather data is collected to provide information about the particular location or environment in which the experiments are conducted.

The specifics of the data gathering process are discussed in detail in Chapter 5. All these data sources are consolidated in MATLAB R2018a and stored for further analysis.

### 2.4.2 Data analysis

This is closely related to the specific methods used in the research study as described earlier, with the main focus of data gathering and consolidation, then mathematically and statistically interpreting the gathered data in order to provide facts and other valuable information to support the theories or assumptions with which the research study started off (Oates, 2006). All the data for this study that was consolidated in MATLAB R2018a and stored are further be used to determine if there is a relationship or some correlation between the particular outcome of the experiments and the identified environmental factor influencing UAS task automation in dynamic environments. Before the data analysis phase, the gathered data needs to be organised for the particular analysis to be done. The organised data are exported from MATLAB R2018a as CSV files that can be imported into the IBM SPSS Statistics software platform used for statistical analysis of the data. The specific statistical methods used include descriptive statistics, as well as bivariate statistics that are comprehensively discussed in Chapter 5.

## 2.5 Conclusion

Through the completion of this extensive study on the dominant research paradigm in the field of computer sciences, the paradigm of positivism, it is made clear what this specific paradigm entails. In this chapter, it is made evident that the positivistic paradigm underlies the scientific method, and is concerned with making scientific observations and performing experiments.

The distinctive characteristics of the positivistic paradigm that have been discussed fit perfectly with the requirements and nature of this research study. Some criticisms that should be taken into consideration when conducting positivistic research have been highlighted, as well as a description of the methods, data gathering and data analysis available to be used when conducting a study using the positivistic research paradigm. The unique environments in which the positivistic paradigm should be used are highlighted and applied throughout the research process to support this particular study.

In the next chapter, an overview and discussion of the literature pertaining to the topics relevant to this research study is undertaken. The literature survey attempts to address the first three objectives of this study as specified in Section 1.2, to provide a thorough understanding of all the necessary aspects in literature in order to identify the factors influencing UAS task automation in dynamic environments.

# CHAPTER 3 – LITERATURE REVIEW

*An overview and discussion of topics relevant to this research study, including an investigation into the environmental factors influencing UAS task automation in dynamic environments.*

## 3.1 Introduction

In this chapter, a discussion on literature relevant to this particular study is provided. Firstly, an introduction and background on aerial vehicles and the terms UAV and UAS are provided, followed by the components and various technologies typically present in UASs. Thereafter a look into basic UAS control methods to attain movement from an aerial vehicle and an investigation into automation in UASs are provided. Several applications for UASs in a wide variety of environments are described, followed by an investigation into dynamic environmental factors influencing UAS task automation, including weather conditions, atmospheric conditions, radio frequency interference, and other obstacles in order to determine the most significant factors influencing the UAS task environment.

Historically, unmanned aircraft have been primarily used for military operations due to their expensive price tag and high operating costs (Dalamagkidis, 2015a). However, because of the advancement of technology, these unmanned aircraft became smaller and more affordable which sparked interest in the civilian market. With these small unmanned aircraft now being accessible to academics, researchers and a larger part of the population, developments improved, which provided new possibilities and applications in various environments.

## 3.2 UAS technologies, control methods and automation

The significant advancement in technology over the last decade has opened up a vast number of opportunities and possibilities, especially when it comes to aerial vehicles (AVs) and UASs. In this section, some background and terminology (3.2.1) are provided, and UAS technologies (3.2.2), various control methods (3.2.3), a comparison of autonomously controlled systems (3.2.4), as well as unique UAS applications (3.2.5) are explored.

### 3.2.1 Background and terminology

There is often some confusion about the terms and names used to describe unmanned aircraft. A UAV is a generic term, commonly referred to as a drone, used for aerial vehicles that have no human pilot on board and are controlled remotely or by an on-board computer (Dalamagkidis,

2015b). A UAS consists of a UAV, the ground control station and the communications medium working together as a comprehensive system (Dalamagkidis, 2015b). UAS is the preferred term adopted by regulators, the American FAA and in industry.

There are two main types of UAS, fixed-wing systems and multirotor systems (Marcaccio *et al.*, 2016). Multirotor systems are AVs operating on multiple propellers with the main advantage being the high level of manoeuvrability compared to a conventional helicopter with a single propeller (Månsson & Stenberg, 2014). A quad rotor, usually referred to as a quadcopter, is classified as a type of multirotor UAV that is equipped with exactly four rotors that are evenly spaced around the centre that makes it possible for the quad rotor to not only fly, but also hover, take off and land vertically and is therefore classified as a Vertical Take-Off and Landing (VTOL) aircraft (Vaswani *et al.*, 2014).

The intended application and focus of this research is on UASs with a quad rotor UAV. These have a number of advantages in environments where abilities, such as agility, hovering, and limited space are important.

### 3.2.2 Technologies

UAS technologies have become cheaper and lighter and the use of these technologies is becoming more popular in a wide variety of environments (Leong, 2015). According to Bouabdallah (2007), the simple construction and control of a quad rotor UAV, and the increase in carrying capability, also referred to as a payload, are the fundamental advantages that are responsible for the increased commercial interest and diverse application of these types of UAV. There are, however, some drawbacks, such as the weight, size and high energy consumption that are of concern, but the advantages outweigh them by far.

With the advancement of UAS technologies, a diverse range of solutions suited for different environments and conditions are available together with a combination of components to achieve the desired solution for a specific environment, condition, or application. The various technologies and an overview of components typically present in UAV are briefly described in the sections that follow.

#### 3.2.2.1 Power sources and propulsion

All UAVs require some source of power to enable flight. UAVs can have different power sources to enable propulsion, such as an internal combustion engine, or they can be battery powered or solar-powered (Lee *et al.*, 2015). Depending on the environment and the conditions, different power sources are considered to suit the specific application. These power sources can therefore

be categorised into two classes, namely electrically-powered systems and internal combustion engine systems (Brandt, 2015).

For electrically-powered systems (batteries), Lithium polymer (LiPo) batteries are most commonly used in UAV technology, since they provide the best combination of energy, power density and lifetime (Saha *et al.*, 2011). These systems are more efficient than internal combustion engine systems, but have the major drawback of shorter flight times. Internal combustion engines have a much longer flight time and can quickly be refuelled between flights, whereas electrically-powered systems require a considerable length of time to recharge between flights or additional batteries need to be ready, charged and exchanged between flights.

Using internal combustion engines for longer flights is less expensive than the electrical counterpart because less weight is required and internal combustion engines use their fuel during flight, therefore the aircraft weight also decreases during flight (Brandt, 2015). Electrically-powered systems also produce much less noise than internal combustion engine systems, they are more reliable, easier to operate and can be controlled with a higher degree of precision than internal combustion engine systems. Multirotor UAVs almost exclusively make use of electrically-powered systems, mainly because they are more reliable and respond faster to instructions and commands.

#### 3.2.2.2 Navigation systems and sensors

UAVs require information about their current position and various other components to be able to navigate to another location or to change the orientation of the UAV. The sensors used for positioning and movement provide information about the current position, orientation, and state of the UAV at all times. This information is provided to the control system of the UAV and can also be used to automate predefined tasks is discussed in Section 3.2.4.

The Global Positioning System (GPS) is the standard for determining the exact position in terms of latitude, longitude and elevation. Based on the intended use and application of the UAS, there are some UAVs equipped with GPS sensors, while others make use of image processing algorithms to determine their position and enable navigation (Bender *et al.*, 2016). Smaller recreational UAVs are usually not equipped with GPS sensors, but due to the advancement of technology, these sensors are becoming more affordable thereby making the addition of GPS sensors more appealing to manufacturers.

A magnetometer is a sensor that is used to measure the earth's magnetic field that is depicted as a digital compass (FAA, 2016) and used to determine the course of the AV in terms of navigational

components. In aviation, North is expressed as 360º instead of 0º. Cardinal directions are North (N), East (E), South (S), West (W) at 90º angles, where ordinal, also known as inter-cardinal directions are northeast (NE), southeast (SE), southwest (SW) and northwest (NW). The cardinal and ordinal directions together form what is known as the eight principal directions at 45º angles which provides eight points of precision for determining direction. When these eight points of precision are further subdivided, it provides sixteen points of precision at 22.5º angles such as North-northeast (NNE) between North (N) and Northeast (NE).

The accelerometer is a component that measures linear acceleration. This measurement indicates the immediate change in direction as the force of acceleration in a particular direction (FAA, 2016). That force of acceleration is the straight line movement measured in each of the three axes X, Y, and Z. Rotational movement, on the other hand, is referred to as the rate of angular change and is measured by a device called a gyroscope. The gyroscope measures the movement around, instead of along each of the three axes as the accelerometer.

A barometer is a pressure sensor used to measure the atmospheric pressure in order to establish the altitude of the UAV (FAA, 2016). An altimeter is similar to a barometer in that it is used to measure the atmospheric pressure, but it is able to measure the change in pressure, therefore a change in altitude of an object above a certain level. Atmospheric pressure is higher at lower altitudes; therefore altimeters are calibrated at sea level where the atmospheric pressure is the highest. At sea level the atmospheric pressure is 101.325 kilopascal (kPa), also known as one standard atmosphere.

Recently, UASs are more frequently equipped with ultrasonic sensors. These sensors are used to measure distances by using sound waves. Ultrasonic sensors measure the time it takes for a sound wave to bounce back in order to calculate the distance, e.g.:

*Distance = (speed * time taken) / 2*

According to Bohn (1988), weather conditions also affect ultrasonic sensing as temperature and humidity affect the speed of sound in air. These ultrasonic sensors can be used along with the other positioning sensors to orient the UAV. Other sensors used to measure distance include laser and LIDAR sensors, usually to determine the distance to the ground or other objects.

#### 3.2.2.3 Flight control

The control system enables overarching control of a UAS and comprised of essential control components and a variety of other components. Essential control components include the electronic speed controller, the flight controller and the radio control (RC) transmitter or equivalent

data transmitter that communicates with the UAV in order to send instructions and receive sensor information (FAA, 2016).

The flight controller is essentially a programmable microcontroller that controls the entire aircraft and all the accompanying sensors. The flight controller is in charge of regulating motor speeds via the Electronic Speed Controller (ESC) to make it possible to steer and navigate, controlling the camera and other payloads, storing and executing waypoints and contains fail-safe operations and controls. The ESC has the purpose to vary an electric motor's rotational speed and direction in which it rotates.

The RC transmitter and receiver unit make it possible to take manual control of the UAV by moving the sticks on the transmitter. Most modern transmitters use the 2.4 GHz or 5 GHz frequency band for communication. The number of individual actions that the transmitter controls is referred to as R/C channels. For a quad rotor to attain movement, the minimum number of R/C channels is 4 where channel 1 is for thrust (elevation), channel 2 for yaw (*rotation*), channel 3 for pitch (f*orward and backward lean*) and channel 4 for roll (*left and right lean*). These movement controls are described in detail in Section 3.2.3.1.

#### 3.2.2.4 Camera systems

Most UAVs make provision for or are equipped with some sort of camera system to record or transmit a video feed. The camera systems found on UAVs are used to collect imagery data, to provide feedback to the control system and pilot, and are commonly used for aerial mapping, monitoring, photography and filming (Linchant *et al.*, 2015; Jordan, 2015). Some UAVs make use of an additional camera located at the bottom of the aerial vehicle as an additional positioning sensor for stability and improved take-off and landing performance.

Components that form part of the camera systems commonly found on UAVs are the gimbal, and sometimes an additional camera, such as a GoPro. Some UASs provide dual control of the UAV, where both controllers can be connected to the UAV and assigned different roles, such as one controlling the movement while the other controller is able to take control of the camera.

#### 3.2.2.5 Summary

Of the variety of technologies featured in UAVs, there are some common sensors and equipment that assist and improve the elegance and correctness of UAV flight and others to gather information about the flight and environment in which the flight is conducted. Various sensors commonly present on board a UAV have been described in order to achieve a better understanding of what enables a UAV to navigate the way it does. This section also provided

insight to what sensory data is available opening the window to a wide range of applications in different fields as discussed in Section 3.2.5. The background on technologies and an overview of the components typically found in UAVs have been established. In the next section, basic control methods and how they are used to control the movement of UAVs is discussed.

### 3.2.3 Control methods

A UAV moves from one point in the air to another with a combination of basic flight controls allowing a change in position, orientation or motion. Along with the basic flight controls, a Proportional Integral Derivative (PID) controller is used to reduce the effect of disturbances and to improve overall UAV control. These movement controls are described in the sections below.

#### 3.2.3.1 Basic flight control

Movement and motion controls are fundamental to UAV control. All aerial vehicles function and move freely in three dimensional spaces and are able to move from one point in space (position) to another. Therefore, the ability of changing position, orientation and rotation at any point in time makes it clear that UAVs function and operate in six degrees of freedom (6DoF) space.

The 6DoF is composed of the ability to move forwards/backwards (surge), up/down (heave), left/right (sway), roll, pitch and yaw. According to Wang and Liu (2018), a UAV is under-actuated in the sense that each movement (degree of freedom) cannot be controlled in isolation, but rather indirectly with a combination of the main movement controls in order to control the position of the UAV.

According to Månsson and Stenberg (2014), there are four main controls to attain movement from any multirotor UAV – Roll, Pitch, Yaw and Thrust. These main controls are illustrated for a quad rotor UAV in Figure 3-1 (Månsson & Stenberg, 2014).

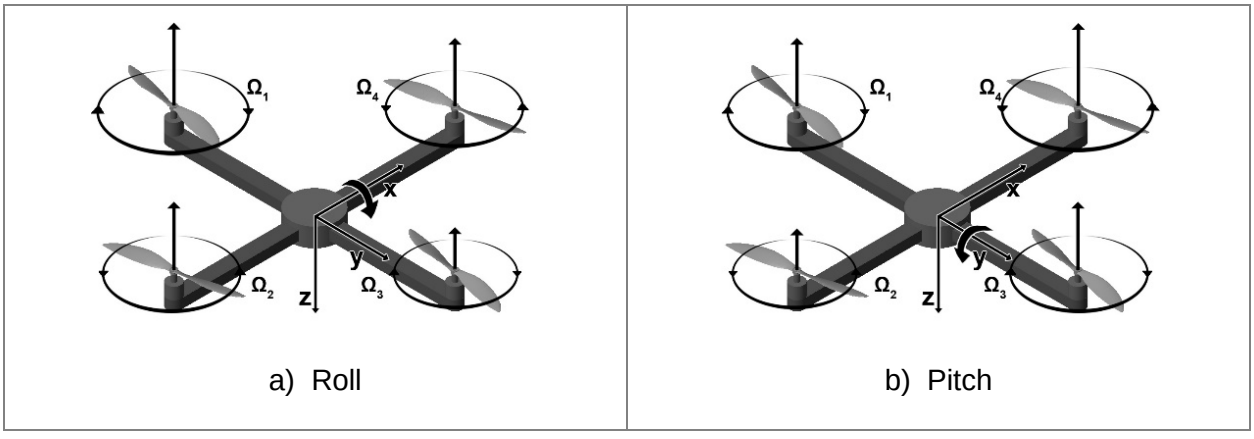


a) Roll

b) Pitch

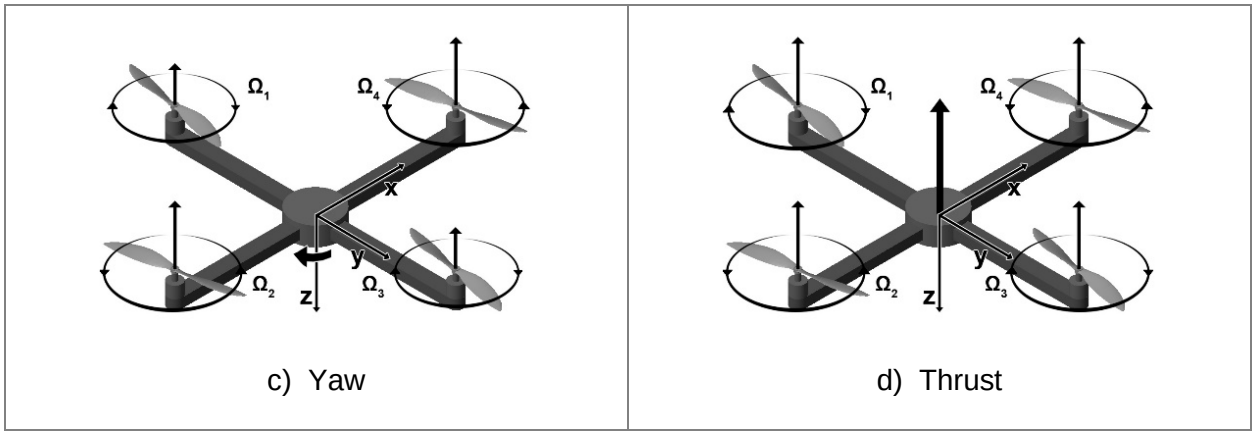


c) Yaw

d) Thrust

**Figure 3-1: Main motion controls for a quadrotor UAV (Månsson & Stenberg, 2014)**

The four main controls to attain movement from any multirotor UAV are described with specific reference to a quad rotor UAV based on the figures above.

1. **Roll** – Moves the quadrotor left or right by tilting diagonally downwards to the left to move left, and tilting diagonally downwards to the right to move right (Figure 3-1 a).
2. **Pitch** – Tilting the quadrotor forwards and backwards for movement (Figure 3-1 b).
3. **Yaw** – Rotating the quadrotor clockwise and counterclockwise (Figure 3-1 c).
4. **Thrust** – Moving the quadrotor up and down (Figure 3-1 d).

Basic UAS flight control is described along with the four main movements above. During flight, these movement controls work in unison for flight along a specific path, or simply to move from one point to another. This movement or change in position is achieved by the PID controller described in the next section.

#### 3.2.3.2 PID control

The PID controller is a control loop feedback mechanism that measures sensor information and calculates the desired output by combining the proportional, integral and derivative coefficients (movements) in order to obtain the desired actuator output for optimal control of the UAV. The PID controller is universally applied in industrial applications and extensively used for UAV control (Gärtner & Johansson, 2017).

A PID controller comprises three components that include a Set Point (SP), where the desired direction, location, motion, movement or related performance measure is specified. The second is the Controller Output (CO) that controls actuator output, such as the propeller's motor speed and the third component provides sensor information feedback called the Process Variable (PV).

The PID operates by comparing the PV to the SP to get the difference between them, called the error rate, in order to determine the correct CO to achieve the desired results.

Proportional control is achieved by only changing the CO with regard to the error rate that may result in an offset to the SP. Integral control will constantly try to adjust the change in, and rate of change in the CO in order to reduce the error between the PV and the SP. If Proportional control and Integral control are combined, offset to the SP can be eliminated. Derivative control is mainly used for motion control and is very sensitive to noise making it react faster to changes. Derivative control changes the CO, based on the rate of change of the error between the PV and the SP. The components and functioning of the PID controller are illustrated in Figure 3-2 (Gärtner & Johansson, 2017).

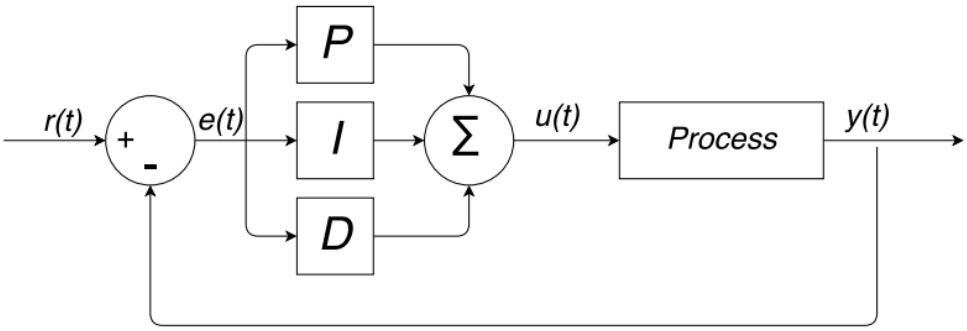


**Figure 3-2: PID controller (Gärtner & Johansson, 2017)**

The PID controller is therefore a combination of the proportional, integral and derivative control actions as depicted in Figure 3-2. This type of controller is widely used for UAV control, since it reduces the time taken to react to- and recover from disturbances, therefore reducing the effect and improving overall UAV control.

### 3.2.4 Automation in UAS

UASs are difficult to control, and not everyone has the resources to send a person or an employee for official training to become a certified UAS operator. According to Fern and Shively (2009), widespread use of UASs is limited by the availability of trained operators. Therefore by automating the task of controlling UAS flight, the need for trained operators can be minimised or even eliminated.

Automation in the general sense is any mechanical device, technique, method or system that functions, operates or controls a process automatically without continuous input from an operator, minimalizing human intervention and increasing reliability and efficiency. Automation has become an integral part in the field of aviation. As described by Rasmussen *et al.* (2013), the major

challenge is to enable a UAV to fly autonomously in order to focus on the specific task at hand, such as taking photos and collecting relevant data instead of being absorbed by the demanding task of flying the UAV safely and as required.

For a UAV to become autonomous it requires making use of all the data provided by the sensors to combine it into useful information to guide and control the UAV (Ross *et al.*, 2008). More data available to the control program produces a higher chance that the UAV will be capable of flying without human intervention thus increasing its level of autonomy (Ross *et al.*, 2008).

Ten levels of autonomy were proposed by Clough (2002), classified as Autonomous Control Levels (ACL) that specify the involvement of human operators. These levels were, however, proposed as a response to UAV autonomy advancements aimed at military applications that were simplified to four levels specifically aimed at civilian applications. These four levels of UAV autonomy, also referred to as operational modes were introduced by Huang (2004):

- **Remotely piloted** – human pilot usually with line of sight;
- **Teleoperation** – human pilot in control that can specify waypoints as the situation allows;
- **Semi-autonomous** – UAV performs the flight based on the pre-planned task or objective specified by a human pilot who is able to monitor all sensor information and take over control at any point in the event of an unanticipated condition or undesired situation; and
- **Fully autonomous** – UAV is in complete control, where a task or objective is provided and the UAV determines how to accomplish it. The UAV is also in control of sensor information in order to adjust to unanticipated conditions or undesired situations.

The aim is to make these UAVs completely autonomous so that they can determine how to complete a task or objective and not be limited by human intervention and restricted by the distance between the operator and the UAV (Caplinger, 2015). Restrictions on computational power, energy-efficient and light-weight sensors that can be equipped to UAVs present a great challenge in achieving autonomy (Tomic *et al.*, 2012). These restrictions however, become less of a concern as they are addressed by the technology advancements.

Some UAS applications are often reliant on the automation of specific tasks. An example of this is the RTH functionality of the DJI Phantom 3 drone. This RTH is a static implementation that does not compensate for any obstacles or collisions that might occur and the UAS merely ascends to a pre-set altitude, adjusts direction towards the recorded home position and flies back (DJI, 2016).

Most applications attempt to make use of some or limited automation, but struggle to maintain a steady flight path and execute objectives precisely as planned, causing the error margin to increase and creating potentially hazardous situations, since they do not compensate for dynamic environmental factors (Yang *et al.*, 2013).

The general automation implementations available are heavily reliant on human operators to plan and manage the flight and take control in unsafe or potentially hazardous situations. However, human errors are one of the main causes of UAV accidents. According to a study by Oncu and Yildiz (2014), 65% of UAV accidents were associated with human-related influences and errors. Therefore, further advancement in automation to take over control in situations where humans are prone to making errors is imperative.

An example of a UAS compensating for dynamic and potentially hazardous situations is the *Vision and Infrared Sensing System* of the DJI Inspire 2. This system is able to detect possible collisions in three directions (forward, upward and downward) and to adjust its path accordingly by flying around it, adjusting the elevation and going over or by entering a hover state where the UAV holds its position for the operator or pilot to take over control (DJI, 2017).

UAS automation rarely occurs within static environments in practice, but rather in dynamic and unpredictable environments as discussed in Section 3.3. Therefore, the overall objective is to improve UAV control and flight management efficiency by introducing automation to easily navigate through dynamic and unpredictable environments and to reduce the dependence on human operators.

### 3.2.5 UAS applications

UAS capabilities have greatly improved, increasing the demand for UAS applications (Clothier *et al.*, 2007). There are commercially available UASs that come ready-to-fly (RTF) out of the box. These commercially available UASs are equipped with various technologies that can be used for a range of applications. These applications can be divided and identified according to their main purpose in two categories, namely, recreational or professional UASs.

#### Recreational

Recreational UASs are more commonly found in toy stores and are far less expensive compared to UAVs in the other categories. These smaller recreational UASs typically make use of a proprietary controller with minimum functionality that is associated only with that specific

UAV. Some of the newer recreational UASs allow control via a mobile device using Wi-Fi technology for communication.

According to Martinez (2019), commonly available UASs for recreation include the Altair Aerial 818 Plus Hornet, Altair Aerial AA108, Altair Aerial Falcon, Hubsan H501S X4, Altair Aerial Outlaw SE and some older recreational UASs, namely the Syma X5C, Hubsan X5, Blade Nano QX, LaTrax Alias and Proto X.

Racing UASs are recreational UASs that are also small in size, optimised for speed and agility, and commonly equipped with a camera. The camera on racing UASs is not to capture images, but rather specifically to provide FPV (First-Person View) for an operator to orientate and control the UAV. With FPV control, the pilot typically wears a head-mounted display, also referred to as a Virtual Reality (VR) headset presenting a live video stream from the perspective of the UAV.

Commonly available racing UASs include the TBS Vendetta, IRC Vortex, Lumenier QAV, Eachine Racer, with the top-rated racing UASs currently the Force1 DYS XDR220 and the Parrot Disco FPV RC (Martinez, 2019).

**Professional**

Sensor UASs have the main purpose of collecting sensory data from any of the UAS components as described in Section 3.2.2 or any other sensory equipment connected to the UAS for unique application purposes. A camera UAS can also be identified as a sensor UAS where the sensory data collected is in the form of images or videos. These UASs are considered to be of a higher professional standard and more expensive than recreational UASs. Some of these camera UASs have a built-in or on-board camera system, while others are manufactured without a camera attached, supporting specific equipment to be attached for imagery purposes, such as a gimbal and camera specific to the unique application.

Most commonly available camera UASs include the DJI Phantom 3, DJI Phantom 4, DJI Inspire 1, DJI Inspire 2, DJI Mavic, DJI Mavic Pro, Yuneec Breeze, Yuneec Q500 4K, Yuneec Typhoon H 4K, 3DR Solo, Parrot AR, and Parrot Bebop, with the top camera UASs currently being the DJI Inspire 2 and the Yuneec H520 (Martinez, 2019).

Actuator UASs were originally developed by the military to deliver resources to troops situated in difficult-to-reach areas (Boucher, 2015). These UASs have a commercial application as a courier service to deliver packages or post, such as UASs used for the delivery of medical supplies to remote locations (Ackerman & Strickland, 2018). Amazon is working on their delivery drones that they want to deploy, but are waiting on the finalisation of regulatory and legal issues, as well as

the privacy and safety concerns that are currently preventing the implementation thereof (Burzichelli, 2016).

As UAS technologies and capabilities improve and costs come down, demand for UAS applications in various environments increases (Clothier *et al.*, 2007). A UAS is traditionally used in situations and environments deemed too dangerous or risky for human pilots to enter or in which to operate (Chee & Zhong, 2013; Watts *et al.*, 2012). However, due to the progress in UAS technology, UAS applications have diversified in a wide variety of environments, such as:

- **Surveillance** – surveying land and crops (Pederi & Cheporniuk, 2015), forest fires (Casbeer *et al.*, 2006), traffic and transportation surveillance (Puri, 2005), wildlife monitoring (Linchant *et al.*, 2015);
- **Safety and security** – sea, wilderness and various other search and rescue operations (Leong, 2015; Goodrich *et al.*, 2008);
- **Disaster and emergency management** – situation assessment and inspection (Quaritsch *et al.*, 2010; Ameri *et al.*, 2009; Metni & Hamel, 2007), post-disaster assessment (Cione *et al.*, 2016; Adams *et al.*, 2014; Adams & Friedland, 2011);
- **Exploration and mapping** – river and coastline exploration and geological mapping of their boundaries (Jordan, 2015; Rathinam *et al.*, 2007), simultaneous localisation and mapping in GPS-denied environments (Bryson & Sukkarieh, 2009); and
- **Agriculture** – yield prediction, cost effective and convenient remote sensing (Rasmussen *et al.*, 2013; Grenzdörffer *et al.*, 2008), precision agriculture (Pederi & Cheporniuk, 2015; Zhang & Kovacs, 2012).

All the above-mentioned UAS applications have unique environments and conditions; however, these applications are all interrelated through the fact that they occur in natural real-world environments that are subject to change. Each application may differ according to its sensitivity and position accuracy required for the specific task in the sense that some require centimetre or even millimetre accuracy, while others are able to complete tasks without that level of accuracy. These changing environments in which most applications occur need to be investigated to determine which factors influence UAS task automation in these dynamic environments.

### 3.3 Factors influencing UAS task environment

UAS task environments differ from application to application, but they have one thing in common, namely that they mostly operate in real-world environments that are subject to change. These changing environments can be due to changing weather conditions, atmospheric conditions, objects in the task environment, signal interferences, other devices and UASs.

The biggest concern to UAS operation and flight is weather conditions, with windy conditions being one of the major factors influencing the stability and performance of UAS task completion (Jordan, 2015; Yang *et al.*, 2012; Orr *et al.*, 2005). Weather conditions are known to influence UAS operation, but it is not always clear to what extent the performance is hindered. Communication frequency interferences are also known to be a major factor of concern influencing the UAS task environment (Fabra *et al.*, 2017).

In this section, several factors influencing UAS flight and communications are discussed, including communications interference, atmospheric conditions and various weather conditions in order to determine the most significant factors influencing the UAS task environment and therefore UAS task automation.

### 3.3.1 Communications interference

Radio Frequency Interference (RFI), also known as Electromagnetic interference (EMI), is described as the electromagnetic radiation or noise of radio frequency energy on other electrical devices which may interfere with or interrupt the normal functioning of an electronic device (Bellavia *et al.*, 2015). UASs operate in a complex real-world environment with electromagnetic influences affecting the UAS's communications and control (Jia *et al.*, 2019). With the increase in the number of devices and UASs in the already electromagnetically-polluted environment, researchers should further investigate interference-resistant design and optimisation of UAS communications (Jia *et al.*, 2019). Various studies have been done on the influence of electromagnetic interference on UAS communications (Jia *et al.*, 2019; Bellavia *et al.*, 2015). To control or reduce RFI, it is recommended that radio transmitting components be placed as far away from other electronic components as possible. This is, however, not always possible, especially with a UAV that is small in size with all electronic components compacted closely together.

Commercially available UASs most commonly make use of the 2.4 GHz and 5 GHz radio frequency band (Wi-Fi) for communications. Fabra *et al.* (2017) investigated the impact of UAV communications interference on the 2.4 GHz frequency band and identified several factors influencing the communications link. These factors include, amongst others, the distance between the UAV and the controller, data packet size, antenna positioning and the vibrations as a result of increased power applied to the motors to generate lift. Nekrasov *et al.* (2019) performed a similar study on performance analysis using the 2.4 GHz frequency band and indicated similar factors affecting UAS communication in the air, thus providing recommendations to minimise the communications interference or loss.

Wireless computer networks make use of Wi-Fi technology that most commonly operate on the 2.4 GHz frequency band. Therefore, major congestion is experienced in cities and built-up areas with many electronic devices and networks which can lead to unstable or even loss of connectivity. To overcome the congestion issues, some UASs provide the ability to make use of the newer, less congested 5 GHz frequency band, especially when congestion or substantial noise is detected on the 2.4 GHz band (Ganti & Kim, 2015). However, not all UASs support the 5 GHz frequency band and if it is supported, there are advantages and disadvantages to consider when choosing a frequency band for each specific application. The main differences between the 2.4 GHz and 5 GHz frequency band are the speed, range, bandwidth of channels and the number of users on the frequency band. The 5 GHz frequency band has a higher speed, is less congested and provides more non-overlapping channels than the 2.4 GHz frequency band.

Additional to the main differences highlighted above, line of sight is generally important with these wavelengths, especially when it comes to airborne UAS control. An obstruction in the direct line of sight may cause signal interference, since the signal has to travel through or around obstacles in its path. The 2.4 GHz frequency band is more capable of travelling through obstacles than the 5 GHz frequency band (Ganti & Kim, 2015). The communications interferences are, however, mitigated to some extent by providing the ability to disperse the UAS's communications across multiple channels over the frequency bands (Gutierrez *et al.*, 2017). Since RFI detection sensors are very expensive and therefore reserved for professional and military applications, UAS manufacturers try to mitigate the expected influence rather than measure the actual RFI (Nguyen *et al.*, 2018).

Commonly encountered communication interference experienced by recreational UAS pilots include power lines that produce high EMI that influences or may even disrupt communications completely (Jia *et al.*, 2019; Bellavia *et al.*, 2015). Additionally, video cameras, such as a GoPro may affect communication, since video transmission is on the same frequency band (2.4 GHz) as the UAS controls and communication transmission adding to the congestion. However apparent, these interferences are mitigated by incorporating autonomous RTH functionality (DJI, 2016) that can be activated whenever the interference is of such a magnitude that it could possibly affect UAS task execution or communications.

### 3.3.2 Air density

AV performance is significantly affected by the density of air (FAA, 2016). As air becomes less dense, it produces less lift, since thin air applies less force on the wing or propeller, resulting in reduced propeller efficiency and therefore reduced net thrust. The density of air is most

significantly affected by variations in temperature and altitude, but other factors, such as humidity, also affect the air density.

The International Civil Aviation Organisation (ICAO) has established a worldwide standard for the variable air density called the International Standard Atmosphere (ISA) which describes the standard atmosphere at sea level to be 15ºC (degrees Celsius) with a surface pressure (air density) of 29.92 inches of mercury (Hg) or 1013.2 millibars (FAA, 2016). The surface pressure describes the density of the air. Air is considered a gas and can consequently expand or be compressed, therefore closer to the earth's surface, air is more compressed than further away, since there is more air pushing down compressing the air and increasing the density (FAA, 2016). This means that the air density will decrease with an increase in altitude.

As indicated by the definition of a standard atmosphere, temperature is closely related to air density. Raising the temperature of any substance or material, subsequently decreases its density. According to Ryaciotaki-Boussalis and Guillaume (2015), air temperature affects the performance of AVs, since temperature fluctuations affect the air density, whereas less dense air produces less lift and thrust, therefore reduced flight performance. As the air temperature increases, air density decreases.

Humidity refers to the amount of water vapour present in air. Humidity is expressed as a percentage relative to the maximum amount of water vapour the air can hold. This is therefore commonly referred to as relative humidity (FAA, 2016). Water vapour is lighter than air, meaning that as the relative humidity increases and holds more water vapour, the air becomes less dense. Therefore, the air density decreases as humidity increases.

It is clear that the density of the air is associated with, and has an indirect relationship with the temperature of the air, as well as the amount of water vapour, expressed as relative humidity, present in the air.

### 3.3.3 Temperature

According to Ryaciotaki-Boussalis and Guillaume (2015), air temperature affects the performance of AVs because temperature fluctuations affect the air density and as previously described, less dense air produces less lift and thrust therefore reduced flight performance. However, temperature does not only affect air density as described previously, but may also affect various other UAS sensors and components, resulting in reduced flight performance. Moreover, high temperatures may cause some sensors and electrical components to potentially overheat or malfunction.

Battery capacity and performance are predominantly affected by ambient temperatures, as well as the stress applied by the rate at which power is withdrawn or restored (Leuchter & Bauer, 2015). When ambient temperature rises, air becomes less dense and motors have to work harder to generate more lift. Motors working harder results in higher immediate power consumption, inducing battery stress, affecting the battery capacity and therefore resulting in shorter flight times (Saha *et al.*, 2011). On the other hand, when ambient temperature decreases, battery efficiency also decreases. Battery levels decrease less smoothly in colder ambient temperatures and may suddenly drop to a critically low capacity and force the ESC (Electronic Speed Controller) to cut out the motors that could potentially cause an accident (Leuchter *et al.*, 2016). According to Dapper e Silva *et al.* (2018), more research is required on the influence of temperature on UAS sensors, especially on differential pressure sensors in order to introduce the temperature component to increase the accuracy of the sensor measurements.

### 3.3.4 Precipitation, Fog, Humidity

Rain, fog and humidity are generally not preferred atmospheric conditions, depending on the specific AV and its capabilities of withstanding these conditions. Most UASs do not handle any form of moisture well, with some exceptions of UASs purposefully designed to operate in such environments and conditions.

As discussed in the previous section, humidity refers to the amount of water vapour present in air. A hot atmosphere has a greater capacity to hold water vapour than a cold atmosphere, resulting in a higher probability for humid conditions. Humid conditions are not as bad as rain or fog, but long-term exposure could result in damage to the UAS. These conditions are not only damaging to the UAV and all its electrical components, but also affect the wireless signals between the UAV and the controller (Rizk *et al.*, 2018).

There are certain applications, such as river mapping and water sports that require the UAS to be water resistant to some degree in order to be able to perform the required task without running the risk of losing the UAV due to water damage. Liardon *et al.* (2018) designed and created a waterproof UAS capable of landing in water and being able to float due to the specific application and typical operating environment.

Apart from some exceptions, as described earlier, most UASs do not handle any form of moisture well. Therefore, it is advisable to always check the predicted precipitation, fog and humidity probability and intensities in the area where the flight is planned before conducting the flight to avoid unfavourable situations. These conditions affect the visibility and the operator may not be able to see the UAV properly.

### 3.3.5 Wind

UAVs operate in real-world environments, therefore the biggest concern to UAV operation and flight is weather conditions, especially windy conditions influencing the stability and performance of UAS task completion (Qian & Liu, 2019; Jordan, 2015; Selecký *et al.*, 2013; Yang *et al.*, 2012; Orr *et al.*, 2005). High wind speeds make it difficult to manoeuvre a UAV and to maintain a stable position. According to Jordan (2015), high wind speeds critically limit UAV control and reduce overall flight time due to increased battery consumption as the UAV constantly tries to stabilise and maintain its position during high wind speeds. These conditions are difficult and sometimes even impossible for UAVs to operate within and it is therefore important to address the effects of wind on UAV environments (Ayhan *et al.*, 2018; Selecký *et al.*, 2013).

With wind being a major concern that is not always compensated for, as a rule, it is important for the operator to check the maximum flight speed of the UAV and make sure it exceeds the maximum predicted wind speed where a specific flight is planned. The speed of a UAV is measured relative to airspeed. For example, if the maximum speed of a UAV is 40 km/h and the wind speed is 40 km/h, flying directly into the wind, the UAV will theoretically not move and remain at its current location relative to the ground. This also applies in the opposite direction when the maximum speed of the UAV is 40 km/h and the wind speed is 40 km/h, if the UAV were to be flying in the same direction as the wind, it will theoretically be moving at 80 km/h relative to the ground. Therefore, high wind speeds may exceed the physical limits of the UAV, making it unable to counteract and maintain flight or hold its position (Månsson & Stenberg, 2014). The UAV reacts differently to control inputs when it is constantly affected by the wind to the extent that a simple 90º turn can be performed completely differently from another, depending on whether it is a turn up-wind, into the wind, or a turn down-wind, in the direction in which the wind is blowing.

It is not enough to simply consider the average, maximum and minimum wind speeds of the UAV task environment, but especially important to pay attention to the anticipated wind gusts in the specific location where flights are planned (Pappu *et al.*, 2017). With high wind gusts, the motors may have to aggressively adjust the rotational speed up to maximum voltage that may be less than what is required to maintain flight and possibly cause the UAV to tumble (Månsson & Stenberg, 2014). Therefore, as a rule, UAV task environments where wind gusts may exceed the maximum speed of the UAV should be avoided.

As described previously, high wind speeds affect the battery life of a UAV as it constantly tries to stabilise and maintain its position. Therefore high wind speeds have an effect on the over-all flight time, as reduced battery life leads to reduced flight time (Jordan, 2015). This means that the

planned flight path will be influenced in terms of the distance it can cover during regular conditions compared to the distance during high wind conditions. Orr *et al.* (2005) recommend that forecasted wind data should be used during flight planning to calculate the optimal flight path instead of only calculating the optimal flight path relative to the position on a map.

Due to the physical design and restricted power, these UAVs are greatly affected and subject to wind disturbances. The flight stability and accuracy are influenced by high winds causing a deviation from the flight plan (Schiano *et al.*, 2014). Since the stability of the UAV and its ability to maintain a position are influenced, the ability to capture quality videos and photos will also be affected. Even a slight breeze of 14 kilometres per hour (km/h) can considerably affect the effectiveness of UAV task completion (Orr *et al.*, 2005). The planned flight path may have to be reoriented so that the starting point of the flight is located up-wind or down-wind, depending on the flight requirements to ensure the task can be completed in time and according to plan. Another aspect of concern is the take-off and landing location, which has to be shielded against windy conditions, since the UAV is so close to the ground that it can easily tumble and crash when trying to compensate for the affecting winds.

It becomes clear that the effectiveness of UAV task completion is greatly affected by and subject to favourable wind conditions. The influence wind has on various aspects of UAS task completion should be taken into consideration when planning and executing experiments (Ayhan *et al.*, 2018). This is especially important with fully autonomous flight where no human operator can take over control and compensate for these dynamic conditions.

### 3.4 Approaches to address the effect of wind

As evident in literature and discussed in Section 3.3.5, it is clear that wind is a major factor of concern and the effectiveness of UAS task automation is greatly affected by and subject to favourable wind conditions. In this section, various approaches from different studies found in literature are discussed in an attempt to compensate for the effect of wind on UAS task automation.

There have been various studies conducted to measure and possibly mitigate the influence of wind on UAS performance in high wind conditions. According to Biradar (2014), the ideal way is to fly directly into the wind during windy conditions. This is in most cases not possible since the objective is to fly along a specific flight path or to fly around an obstacle. An approach that relates to some extent is to identify the best starting point for a planned flight based on the wind direction. If the flight path is oriented in such a way that the majority of the flight is up-wind, then it will not

be as efficient as when the majority of the flight is down-wind in the same direction in which the wind is blowing.

Another strategy to address wind disturbances on UASs, is to explicitly take them into consideration during flight planning and to implement the predicted wind disturbances into the control algorithms. Schiano *et al.* (2014) attempt to perform wind estimations without additional expensive wind sensors to a UAS, and try to compensate by including those estimations in the control algorithms. Liu *et al.* (2013) propose a control algorithm making use of wind estimates to fly at a trimming angle to compensate for the wind component perpendicular to the flight. Yang *et al.* (2013) propose a control framework to improve performance in gusty environments when compared to the PID controller discussed in Section 3.2.3.2.

Selecký *et al.* (2013) highlighted the importance of addressing the effects of wind on UASs and reviewed various algorithms attempting to address this issue to some extent. Their research showed that most proposed algorithms provided sub-optimal solutions or would have to apply a computationally intensive recalculation beforehand whenever the environment or wind conditions change. Therefore, to take the wind disturbances into account, it is important to firstly obtain this data, perform calculations and make estimations as to how it can possibly affect the UAV before it can be implemented in the control algorithms. However, for small UAVs with limited computational capabilities, this is not always possible.

According to Biradar (2014), there are various wind estimation methods that predominantly make use of GPS sensors and airspeed sensors to predict the wind speed and direction. Due to the expensive price tag, most UASs do not have any sensors directly measuring wind speed or direction and therefore have to make wind estimations (Schiano *et al.*, 2014). Because of the lack of dedicated sensors available, the corrections to compensate for wind disturbance tend to be inaccurate and cause the UAV to drift from the planned flight path (Biradar, 2014).

Wind drift is an occurrence caused by the wind affecting and causing a displacement in the flight path of an aerial vehicle. This is most notably observed when the wind blows perpendicular to the flight path or at any angle from the side of the flight path, depending on the wind speed and the relative air speed of the aerial vehicle. These conditions are identified and commonly referred to as crosswinds. In the presence of a crosswind, if an AV were to aim at a specific waypoint or destination in the distance, the aerial vehicle would drift off its intended course in the same direction in which the wind was blowing.

This effect of wind drift is illustrated in Figure 3-3 below where the planned flight path is in a straight line from one waypoint to the next (red circles). But with the presence of wind, a

displacement in the flight path is caused. The wind direction is shown in green, the black line and arrow shows the heading of the aerial vehicle, the blue line shows the actual flight path, and the angle between the heading and the actual flight path is known as the drift angle.

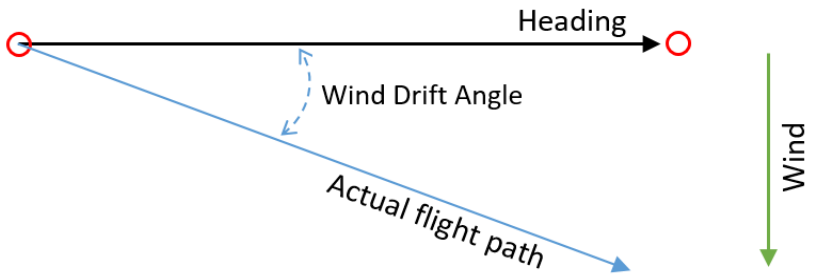


**Figure 3-3: Wind Drift**

However, the previously mentioned wind estimations can be calculated in various ways to compensate for, or minimize the amount of drift. In the paper by Liu *et al.* (2013), wind estimations are implemented into a controller designed for a UAV following a path. The wind estimations are mainly based on the assumption of constant wind disturbances in the calculation of the error constant. This error constant is used by the controller to adjust the UAV flight in order to compensate for wind disturbances perpendicular to the flight by flying at an angle (Liu *et al.*, 2013). This angle is described as the Wind Correction Angle (WCA) and also referred to as "Crab Angle" (Chapman *et al.*, 2008).

WCA or Crab Angle is calculated by determining the angle and speed at which the wind is blowing towards the AV, multiplying the angle in degrees by the speed in knots, and dividing it by the true airspeed to obtain the WCA in degrees to fly into the wind to compensate for wind drift (FAA, 2016). For example, if the wind blows 90º at 5 knots and the true airspeed is 15 knots, (90º x 5 knots / 15 knots), the WCA to be flown into the direction the wind is blowing from will be 30º. The WCA concept is illustrated in Figure 3-4 with reference to the Wind Drift angle illustrated in Figure 3-3. Instead of heading in the direction of the waypoint, the heading is adjusted by the calculated WCA in the direction where the wind is blowing from to compensate for wind drift and arrive at the waypoint as planned.

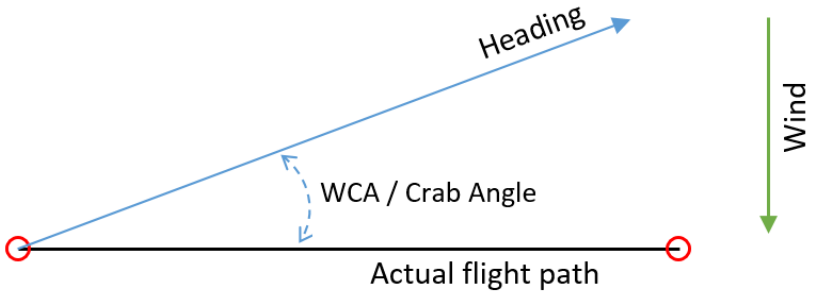


**Figure 3-4: Wind Correction Angle / Crab Angle**

A strategy similar to implementing a WCA to compensate for wind disturbances on a UAV following a specific path is to disregard the relative airspeed of the UAV and focus on its location relative to the ground. According to Liu *et al.* (2013), to disregard the airspeed and focus on the location relative to the ground, the ground velocity and flight-path angles are required. This information can be obtained from the GPS position and various other sensor information, but due to the small size and architecture of commercially available UASs, they generally make use of smaller, low-cost sensors that will not provide accurate information and will produce a larger error margin resulting in inefficient calculations. The results obtained from inaccurate sensor information are therefore inadequate to compensate for the influence of wind disturbances on a UAV flight path.

### 3.4.1 Commercial applications enabling automation

There are a variety of commercially available software applications that support some form of automation. The simplest form of automation supported by most UAS software applications is the RTH functionality that autonomously assists the UAV to fly back to the specific take-off point or explicitly specified home point (DJI, 2017). More advanced software applications have the ability to perform area mapping tasks where a list of waypoints can be specified. Some of the advanced software applications can calculate specific routes and waypoints, to map an area according to the area and flight parameters specified for the task.

The variety of commercially available software applications that enable autonomous tasks each provide their own unique support and capabilities for specific applications. Some of the most popular software applications enabling autonomous UAS tasks include Agrisoft Metashape[1],

[1] Agrisoft Metashape (https://www.agisoft.com/).

Botlink[2], DJI GroundStation Pro[3], DroneDeploy[4], Litchi[5], Pix4D[6], PrecisionHawk[7], Propeller Aero[8], SimActive Correlator3D[9], and UgCS[10].

From the list of available applications that support the implementation of autonomous tasks, UgCS appears to provide the functionality required to perform experimental UAS flights for this study. UgCS is fully functional ground control station software that enables UAS control in order to plan, manage and execute autonomous flight (UgCS, 2019). UgCS allows custom mission planning and the ability to specify exact waypoints for precision flights. UgCS has many flight parameters that can be set according to each specific application. The ability to control the flight speed, specify the height above ground or above mean sea level and the way in which each waypoint is reached can be controlled and specified in UgCS. By making use of UgCS as the ground control station software, experiments can be planned and a flight plan can be generated and autonomously executed by the ground control station software used to plan and manage experiments of this study.

### 3.5 Summary

In this chapter, an overview and discussion of topics relevant to this research study have been discussed. A background on AVs has been provided, as well as the components and technology typically present in UAS. Furthermore, basic UAS control has been described, leading to the discussion on automation and the different levels of UAS automation. The different types of UAS were categorised as recreational or professional UASs, followed by various uses or unique applications of UASs. The environmental factors influencing UAS task automation in dynamic environments have been investigated, which included communications interference, air density, temperature, precipitation, fog, humidity and wind. As discussed in Section 3.4, of all the dynamic factors, wind is the most significant factor that influences UAS task automation.

Now that the most significant factor has been identified as wind, the extent to which the wind influences the UAS task automation in dynamic environments is investigated by performing

---

2 Botlink (https://botlink.com/).
3 DJI GroundStation Pro (https://www.dji.com/ground-station-pro/).
4 DroneDeploy (https://www.dronedeploy.com/).
5 Litchi (https://flylitchi.com/).
6 Pix4D (https://www.pix4d.com/).
7 PrecisionHawk (https://www.precisionhawk.com/).
8 Propeller Aero (https://www.propelleraero.com/).
9 SimActive Correlator3D (https://www.simactive.com/).
10 UgCS (https://www.ugcs.com/).

experiments to demonstrate and support this claim. In the next chapter, the experimental setup is described, providing a description of all the relevant hardware and software used, the process followed to conduct these experiments, as well as a description of the unique experiment types conducted to support this study.

# CHAPTER 4 – EXPERIMENTS

*An introduction to the hardware and software used, as well as how various experiments are implemented to highlight and demonstrate the relevance and effect of wind on UAS task automation.*

## 4.1 Introduction and Background

In this chapter, a description is provided on the equipment used which includes the UAS and its specifications, the specific ground control station software that was used to plan and manage experiments, the weather station to measure the wind speed, direction and other environmental information, along with the process of planning, setting up and performing a test flight. Furthermore, the four specific experiment types conducted to support the study are described, followed by a section concluding the experimental setup and design.

## 4.2 Hardware

The hardware used in this study consisted of a UAS and a weather station. In this section, overviews of the DJI Phantom 3 Professional, the UAS used in this study, as well as the Davis Vantage Vue weather station are presented.

### 4.2.1 UAS

The DJI Phantom 3 Professional was available and used to conduct the necessary experiments and data gathering for this study. The DJI Phantom 3 Professional is a quadrotor UAV that comes ready-to-fly with all the necessary components and is shown in Figure 4-1.

**Figure 4-1: DJI Phantom 3 Professional UAS used in this study**

The DJI Phantom 3 Professional weighs 1.28 kilogram (kg) with a battery and its propellers attached, has a maximum flight speed of 16 metre per second (m/s), which converts to 57.6 kilometre per hour (km/h). It has a maximum transmission distance of 5 km (free from interference or obstacles) and maximum flight time of approximately 23 minutes from its 4480 mAh (milliamp hour) LiPo (lithium-ion polymer) battery. A detailed specification of the DJI Phantom 3 Professional UAS can be found on their official website at *www.dji.com/phantom-3-pro*.

With the DJI Phantom 3 Professional, a mobile phone or tablet can be connected to the controller via the USB port located at the back to provide the operator with a direct camera feed from the UAV, as well as additional flight telemetry directly to the mobile device. This port also provides a communications channel that allows commands to be sent from the mobile device to the UAS.

### 4.2.2 Weather station

The initial test flights and experiments carried out to obtain sample data and to determine the requirements for adequate and accurate weather measurements posed a challenge. These initial experiments were done by hand with a handheld Kestrel Weather and Wind indicator used for portable and fast weather monitoring. Every few seconds the wind speed and direction were manually noted on a piece of paper. This process proved to be an inefficient and tedious process that would not be suitable to obtain accurate weather information. Researching current weather stations used in agricultural applications, the Davis Vantage Vue weather station was identified as an appropriate tool to measure weather information for the purposes of this study. The weather station components included the weather station itself, the wireless receiver, and the data logger as shown in Figure 4-2.


**Figure 4-2: Davis Vantage Vue weather station used in this study**

Davis instruments (*www.davisinstruments.com*), an important player in the agricultural sector for more than 50 years, manufactures a wide range of unique solutions for weather monitoring as well as marine and outdoor equipment, ranging from hobbyist instruments to large company solutions. The Davis Vantage Vue is a more than capable precision weather station that can wirelessly monitor temperature, humidity, barometric pressure, wind speed and direction, dew point, as well as rainfall (Davis_Instruments, 2019). The anemometer can measure wind speeds of 3 km/h up to 241 km/h, temperature readings range from -40ºC to 65ºC and relative humidity as a percentage from 0 to 100%.

A data logger is a permanent storage device connected to the Davis Vantage Vue providing the ability to store the measured weather data at the remote locations where each experiment is conducted, into a log file. This log file contains all the measured weather data that can be downloaded and analysed afterwards.

### 4.3 Ground control station software

UgCS (*www.ugcs.com*), provides fully functional ground control station software that enables UAS control in order to plan, manage and execute autonomous flight. UgCS allows custom mission planning and the ability to specify exact waypoints for precision flights. UgCS has many flight parameters that can be set according to each specific application. For the purpose of this study the main parameters that were of importance were the ability to specify exact GPS waypoints, to control the flight speed, to specify the height above ground or above mean sea level and to control the way each waypoint is reached. A screen capture of the UgCS software during experiment planning is shown in Figure 4-3.


**Figure 4-3: UgCS interface during experiment planning**

The UgCS ground control station software consists of two core components that are required for the specific UAS used in this study, the desktop software and the mobile companion application. The UgCS desktop software can be downloaded from their official website for free, but will have limited functionality and will be unable to execute a flight unless a licence has been purchased or trial account is activated. The trial account was sufficient for the purpose of this study, since it provided all the relevant and required features for a period of 14 days. The installation process for the UgCS desktop software is a straightforward process of downloading the latest installation file from their official website, following the installation wizard while taking note of the server details and IP-addresses for future use. The UgCS desktop software is used to plan and manage experiments by providing GPS waypoints and experiment-specific parameters.

UgCS for DJI is the mobile companion application to establish connection between the UAS and the UgCS desktop software. The mobile device connected to the controller via the USB port should have UgCS for DJI installed and be on the same network as the computer running the UgCS desktop software to enable communication and control. The UgCS for DJI mobile companion application can also be downloaded from their official website or from the Google Play Store (only available for Android devices at the time of writing).

Flight planning can be done “off-line” on the desktop software without having the UAS connected or being in the specific location where the flight is planned. When the planned flight is ready to be executed, the mobile device can be connected to the same network as the computer running the UgCS desktop software, or alternatively, if no network is available, a hotspot on either one of the devices can be created. When the network is set up and the desktop software can successfully communicate with the mobile companion application, a message will appear to confirm the connection and display all the UAS health and sensor information in the top right-hand corner on the desktop software. When the connection has been established, the planned experiment (referred to as the current mission) can be uploaded to the UAS and executed from the desktop software or from the mobile companion application.

Usually, an operator would need to control the UAV-flight by moving the control sticks on the controller, but with UgCS this is not necessary, since the ground control station software can take off, fly and land the UAV without the operator interacting with the controller.

### 4.4 Data acquisition and pre-processing

After each field day of conducting experiments, all the relevant data is consolidated to a central location. The flight log files are downloaded from the DJI Phantom 3 Professional from the USB port located on the front of the UAV. This can be achieved by connecting the mobile device to the

controller and powering on the controller and aircraft, opening the DJI Go mobile application and going to “Advanced Settings”, and activating “Enter flight data mode”. Once flight data mode is activated, the aircraft is connected to a computer via the USB port located on the front of the UAV. These flight log data files are downloaded as a *.DAT* file and converted to an easily readable *.CSV* file through a third-party application called “CSV View” that can be found at (*www.datfile.net/CsvView/downloads*).

Each planned experiment in the UgCS ground control station software can be saved and is exported after each experiment is conducted to a *.KML* file that contains various flight information including, experiment specific parameters, as well as a list of coordinates provided as the planned path to follow. These specified coordinates can later be compared to the flight log data files to determine how much the UAV deviated from these coordinates provided as the planned path to follow.

The data logger connected to the Davis Vantage Vue weather station that provides the weather log file containing all the measured weather data is downloaded in a *.CSV* format. This weather log file is used in conjunction with the planned path and flight log data to determine the potential effects the accumulated weather data may have had on the flight.

All the relevant data files discussed above were consolidated in MATLAB R2018a. For each experiment the planned path co-ordinates, the flight log data file and the weather log data file were imported into MATLAB, consolidated and stored for further analysis.

### 4.5 Planning and setup

It is necessary to always have a detailed plan of where and when the experiments will be conducted, to review the weather forecasted for that location on the particular day and time, to get permission from the relevant land owners, to determine a safe home location (waypoint set as safe lift-off and landing location for the UAS), to set up all the equipment and to conduct a test flight.

The planning of all experiments started off with a clear objective of what the purpose was, as well as what was aimed to be achieved. These objectives were set out as flight plans prepared beforehand on the UgCS ground control station software after a suitable location was identified. The locations for the experiments conducted in this study varied between two farms that were made available where we had permission from the landowners to conduct our experiments. These locations were most suitable since they conform to the regulations stipulated by the South African Civil Aviation Authority (SACAA). Both locations were more than 10 km away from the nearest

airport, did not have any public spaces within 50 m and were open spaces providing direct line of sight to the UAV. The one location was positioned approximately 10 km west of Wesselsbron and the other location was approximately 15 km southeast of Potchefstroom.

Depending on the experiment objectives, different weather conditions were desired. Therefore, the forecasted weather conditions were continuously monitored and reviewed at the planned locations to find the most suitable day and time on which to conduct each experiment.

Flight preparation before leaving the university included checkout and inspection of all equipment and making sure all the necessary electronic devices and batteries were charged. This equipment included the DJI Phantom 3 Professional UAV, controller and extra batteries, the Davis Vantage Vue weather station, feedback console and mounting tripod, a laptop with UgCS ground control station software installed and an Android 4.4+ mobile device with UgCS for DJI mobile application installed. Furthermore, a Google Maps printout of the specific locations for planning and taking notes of important aspects, such as the flight objective and plan, flight speed, turn type, general wind direction, as well as flight starting and ending times was also available in the *.KML* flight planning data file produced by the UgCS ground control station software.

An experiment setup procedure with a checklist for each component of the equipment was compiled to help the researcher set up each experiment quickly and efficiently, and in the same manner each time. A brief description of the setup procedure is discussed below with the complete setup procedure provided in Annexure A.

**Weather station**

The procedure was started by unboxing the weather station equipment, assembling the bottom of the tripod, assembling the measurement device (mounting the device on the pole, inserting the rain meter, attaching the wind cups, attaching the wind indicator arrow, inserting the battery), mounting the measurement device onto the tripod, assembling the console and inserting the battery (correcting the date, time, etc.) and verifying the connection from the measurement device to the console.

**UAS (DJI Phantom 3 Professional)**

The UAS equipment was unboxed, the aircraft was assembled (the propellers were checked for damage and replaced if unsure, the camera cover was removed, a battery was inserted), the mobile device was connected to the controller via USB, the controller was powered on by pressing and holding the power button and the aircraft was powered on by pressing and holding the power button. Once both the controller and aircraft were powered, the DJI Go application was launched

(it was ascertained whether a connection was established, whether the software was up to date, the compass calibrated, whereafter a GPS fix was obtained and the home point updated).

**Ground control station software (UgCS)**

The UgCS desktop application and UgCS for DJI mobile application were launched, whilst making sure that the desktop and mobile application were on the same network and able to communicate. The flight plan for the specific experiment was uploaded by toggling the controller switch to F-mode to accept external commands. The controller manually got the aircraft to take off and hover in order to confirm that everything was operating as expected.

**Test flight**

It is advisable to always perform a test flight prior to executing any planned experiments to ensure that the UAV and all sensory information are in perfect working order. A test flight can be performed by following the steps in the previous sections regarding the UAS. After the UAS setup, a test flight with the proprietary DJI Go mobile application can be performed. The DJI Go application on the mobile device was launched and the propellers started. Take-off was executed and a hover approximately 1.5 metre (m) from the ground was initiated. All the motion controls with the control sticks on the controller were tested by performing a short flight. After a satisfactory test flight, the aircraft was returned to the take-off location and landed.

### 4.6 Description of experiments

Several UAS flights, referred to as experiments, were conducted to support this study. There were four unique experiment types which include the following:

- Experiment 1: RL400
- Experiment 2: RL250
- Experiment 3: RH
- Experiment 4: Circle

Each of these experiments was uniquely set up in the UgCS ground control station software to support the objectives of the research study. The first type of experiment, named RL400, consisted of 400 m long straight flight segments to evaluate the influence of wind over long straight flight segments where waypoints were located far apart. The second type of experiment, named RL250, consisted of 250 m long straight flight segments to evaluate the influence of wind over shorter flight segments where waypoints were not as far apart as in the first experiment. The third type of experiment, named RH, consisted of a series of sharp 90º turns followed by short

10 m and 20 m straight flight segments to evaluate the influence of wind over short flight segments in various directions. The fourth type of experiment, named Circle, was, as its name describes, a circular flight. This experiment was implemented to evaluate the extent to which a constant bank turn is affected by wind.

There were some variations performed on the experiments where different parameters could be specified for each experiment that included: Sub-waypoints, Waypoint approach, Height, Speed and Orientation. Sub-waypoints were provided between the starting and ending waypoints for some flight segments of Experiment 1 to see whether consistent corrections over long periods are favourable to flight automation. The UAV could be controlled by two different waypoint approach strategies. The UAV can stop at a waypoint (possibly hover for a specified time), turn to the next waypoint (S&T) and continue. Alternatively, the UAV could approach a waypoint and perform an adaptive turn towards the next waypoint (Ada) while maintaining flight speed. Each experiment could be conducted on one of two height specifications; the UAV could either be set to maintain a constant height above mean sea level (AMSL) or to maintain a height above ground level (AGL). Variations on the UAV speed could be implemented to see if it had a larger, smaller, or no effect on the deviation from the planned flight path. Three distinct flight speed specifications, 5 m/s, 10 m/s or 15 m/s, were available for the experiments. Lastly, the orientation of the experiment could also be rotated in any direction so that it could be facing directly into the wind, downwind, perpendicular to the wind, or at any angle desired to satisfy the requirements. Each experiment type is described in the sections below.

### 4.6.1 Experiment 1: RL400

The first type of experiment, named RL400, consisted of 400 m and 200 m flight segments to evaluate the influence of wind over long flight segments where waypoints are located far apart. These experiments were provided with five waypoints as objectives. The first waypoint was an initial approach waypoint 10 m from the middle of the path where the second waypoint indicated the starting point of the experiment. Between the second and third waypoints was considered the first flight segment of the experiment which was 200 m in length. After reaching the third waypoint, the UAV would turn around and head towards the fourth waypoint and this was considered the second flight segment of the experiment which was 400 m in length. Similarly, at the fourth waypoint the UAV would turn around and head towards the fifth waypoint which was considered the third flight segment of the experiment which was also 200 m in length. After reaching the fifth waypoint, the UAV would return to the take-off position and land. Figure 4-4 below provides an illustration of the RL400 type of experiment with the waypoints shown in red and flight segments shown in blue with an arrow indicating the direction of the flight.

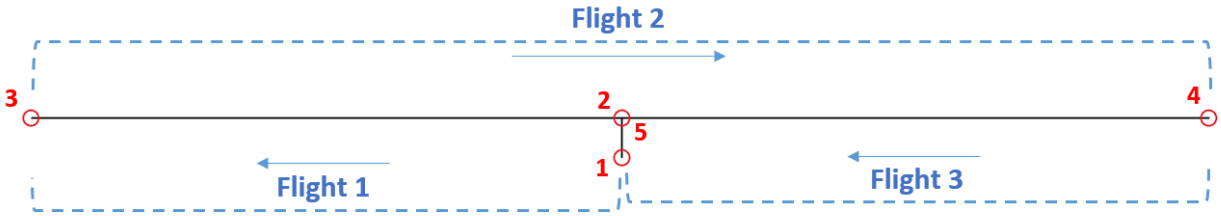


**Figure 4-4: Experiment 1: RL400 waypoint and flight illustration**

The waypoints and flight segments for each of these experiments illustrated in Figure 4-4 are summarised below:

- Waypoint 1 – Initial approach
- Waypoint 2 – Flight 1 Begin
- Waypoint 3 – Flight 1 End, Flight 2 Begin
- Waypoint 4 – Flight 2 End, Flight 3 Begin
- Waypoint 5 – Flight 3 End

Special variations on the RL400 type of experiment was to provide sub-waypoints spaced at 10 m intervals between the starting and ending waypoints of each of the three flight segments. These variations were performed to see whether consistent corrections over long flight segments are favourable to flight automation.

### 4.6.2 Experiment 2: RL250

The second type of experiment, named RL250, consisted of 250 m and 125 m flight segments to evaluate the influence of wind over shorter flights where waypoints were not as far apart as in the first experiment. These experiments were also provided with five waypoints as objectives. The first waypoint was an initial approach waypoint 10 m from the middle of the path where the second waypoint indicated the starting point of the experiment. Between the second and third waypoints was considered the first flight segment of the experiment which was 125 m in length. At the third waypoint the UAV would turn around and head towards the fourth waypoint and considered the second flight segment of the experiment which was 250 m in length. Similarly, at the fourth waypoint the UAV would turn around and head towards the fifth waypoint which was considered the third flight segment of the experiment which was also 125 m in length. Figure 4-5 provides an illustration of the RL250 type of experiment with the waypoints shown in red and flight segments shown in blue with an arrow indicating the direction of the flight.

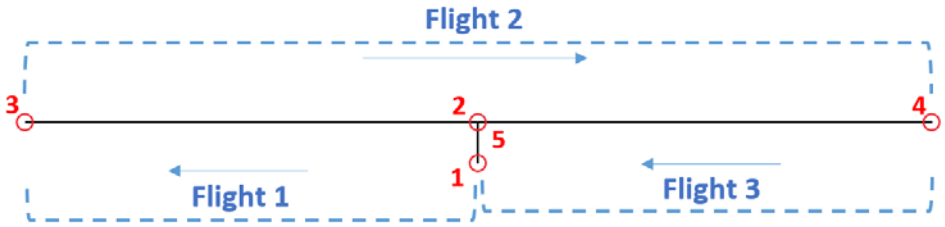


**Figure 4-5: Experiment 2: RL250 waypoint and flight illustration**

The waypoints and flight segments for each of these experiments illustrated in Figure 4-5 are summarised below:

- Waypoint 1 – Initial approach
- Waypoint 2 – Flight 1 Begin
- Waypoint 3 – Flight 1 End, Flight 2 Begin
- Waypoint 4 – Flight 2 End, Flight 3 Begin
- Waypoint 5 – Flight 3 End

There were some special variations performed on the RL250 type of experiment that included specifying faster flight speeds to see whether experiments conducted at faster flights speeds are favourable to flight automation.

### 4.6.3 Experiment 3: RH

The third type of experiment, named RH, consisted of a series of sharp 90º left or right turns followed by short 10 m and 20 m straight flight segments to evaluate the influence of wind over short flight segments in various directions. The RH type of experiment consisted of a total of 30 waypoints as objectives and 28 individual flight segments. The first waypoint was an initial approach waypoint 15 m from a corner in the path where the second waypoint indicated the starting point of the experiment in one of the corners. Between the second and third waypoints was considered the first flight segment of the experiment which was 20 m in length. At the third waypoint the UAV would turn 90º left and head towards the fourth waypoint and this was considered the second flight segment of the experiment which was 10 m in length. At the fourth waypoint the UAV would turn 90º right and head towards the fifth waypoint which was considered the third flight segment of the experiment also 10 m in length. At the fifth waypoint the UAV would again turn 90º right and head towards the sixth waypoint and this was considered the fourth flight segment of the experiment which again was 20 m in length. At the sixth waypoint the UAV would once more turn 90º to the left. This pattern continued throughout the experiment with a total of 28 flight segments and flight distances varying between 10 m and 20 m. Figure 4-6 provides an

illustration of this type of experiment with the 30 waypoints shown in red and 28 flight segments shown in blue with an arrow indicating the direction of the flight.

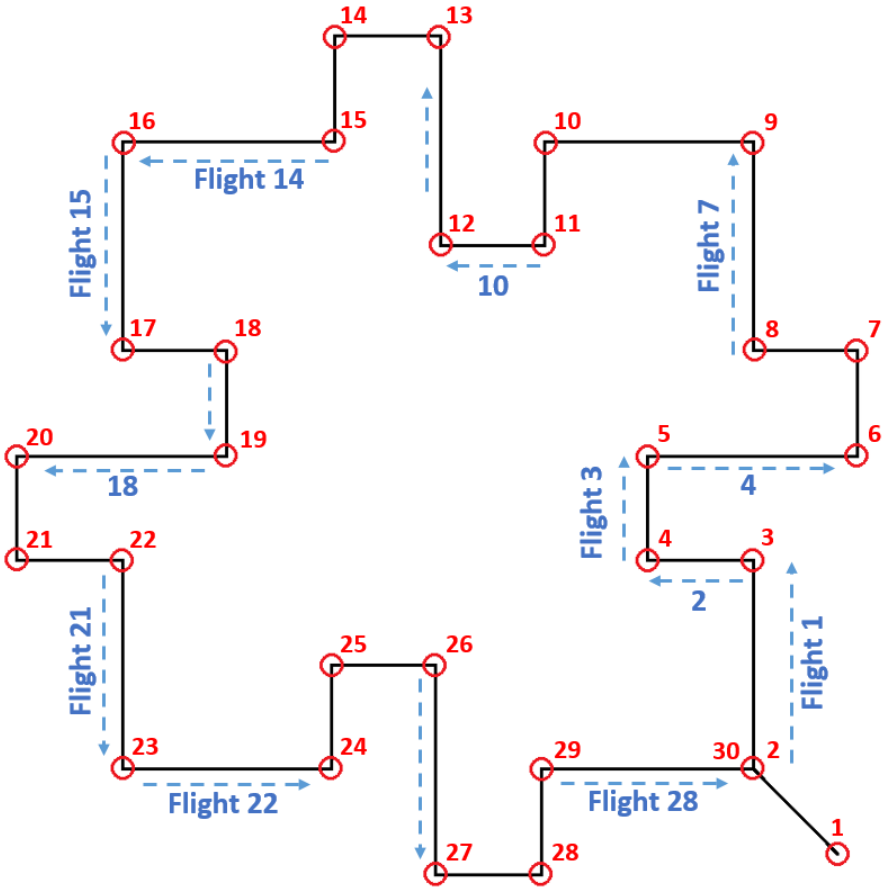


**Figure 4-6: Experiment 3: RH waypoint and flight illustration**

The waypoints and flight segments for each of these experiments illustrated in Figure 4-6 are summarised below:

- Waypoint 1 – Initial approach
- Waypoint 2 – Flight 1 Begin
- Waypoint 3 – Flight 1 End, Flight 2 Begin
- Waypoint 4 – Flight 2 End, Flight 3 Begin
- …
- Waypoint 28 – Flight 26 End, Flight 27 Begin
- Waypoint 29 – Flight 27 End, Flight 28 Begin
- Waypoint 30 – Flight 28 End

There were some special variations performed on the RH type of experiment with different approaches to reaching waypoints. An illustration of the waypoint approach strategies is provided in Figure 4-7 below.

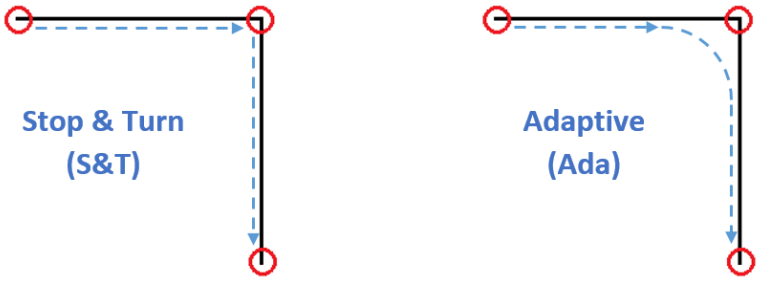


**Figure 4-7: Experiment 3: RH waypoint turn types**

A waypoint could be reached by the UAV having to stop and turn (S&T) towards the next waypoint before proceeding with the flight or by the UAV adaptively (Ada) flying within 2 m of the specified waypoint and “cutting the corner” to the next waypoint.

### 4.6.4 Experiment 4: Circle

The fourth type of experiment, named Circle, was, as its name describes, a circular flight. This experiment was implemented to evaluate the extent to which a constant bank turn is affected by wind perpendicular to the flight path. With this experiment only the initial approach waypoint, the middle, as well as the radius of the circle was specified. The UgCS ground control station software then calculated a flight path with the specified radius around the middle section to form a perfect circular flight path.

Therefore, these experiments consisted of an initial approach waypoint (Waypoint 1) followed by a number of waypoints generated by the UgCS software based on the radius that was provided. The first waypoint was an initial approach waypoint approximately 10 m from a second waypoint on the generated circle that indicated as the starting point of the path. The flight path then moved around the circle through the generated waypoints until it reached that second waypoint on the circle again which was considered a completed flight for this type of experiment. Figure 4-8 provides an illustration of the experiment with the waypoints shown in red, the centre of the circle shown as a black dot surrounded by a red circle, and a blue arrow indicating the direction of the flight.

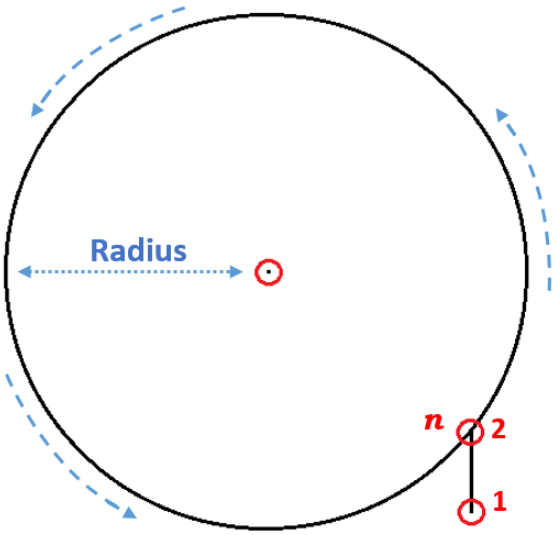


**Figure 4-8: Experiment 4: Circle waypoint and flight illustration**

The waypoints and flights for each of these experiments illustrated in Figure 4-8 are summarized below:

- Waypoint 1 – Initial approach
- Waypoint 2 – Flight 1 Begin
- … (*depending on the radius, the generated number of waypoints will differ*)
- Waypoint $n$ – Flight 1 End

## 4.7 Experiment setup summary

In this chapter, a description was provided on the UAS used and its specifications, the specific ground control station software that was used to plan and manage experiments, the weather station to measure the wind speed, direction and other environmental information along with the process of planning, setting up and executing a basic experiment. The four different experiment types conducted in this study were described, along with the specific variations on these experiments. In the next chapter, the results obtained from the execution of numerous variations and repetitions of the different experiment types are described.

# CHAPTER 5 – RESULTS

*In this chapter, the results of the experiments conducted in the study and how UAS task automation is affected by windy environmental conditions are presented. A description is provided on how the consolidation and segmentation were performed to obtain the relevant data, whereafter a description of the statistical techniques used to analyse the data and a presentation of the results obtained from the analysis are provided.*

## 5.1 Introduction

In this chapter, the results of all the relevant experiments are provided. Firstly, a description is given of how the consolidation and segmentation were performed in order to obtain the relevant data for the analysis. This is followed by a description of the calculations and translations performed on the raw data obtained from the experiments and a presentation of the experimental data. The statistical techniques used to analyse the data are described, followed by the results obtained from the analysis.

## 5.2 Consolidation of acquired data

All the relevant data were consolidated and analysed in MATLAB R2018a. For each experiment, the flight log data file, waypoint data as coordinates, and the weather data were imported into MATLAB R2018a, consolidated and stored for further analysis. These three data files are described briefly with regard to where they are obtained from and the important contents of each.

### 5.2.1 Flight log data

*FLY000.CSV* – The flight log data file is obtained from the UAS as described in Section 4.4. A flight log data file is created for each experiment. If the flight log file obtained from the UAS contained the data of more than one experiment, the flight log data file was split, containing only the data for a single experiment. This might happen when an experiment is started directly after a previous experiment without shutting down the UAV.

The flight log data file contains, amongst other attributes, the GPS longitude and latitude coordinate measurements, the altitude along with the date and time for each data entry indicated by the *Tick#* attribute measured at about 100 millisecond (ms) time intervals. This flight log data file contains several attributes of the UAV, with the important attributes shown in Table 5-1.

| Tick# | Longitude | Latitude | GPS:Date | GPS:Time | GPS:heightMSL |
|---|---|---|---|---|---|
| 62685 | 27.22121543 | -26.77508618 | 20180829 | 61410 | 1415.083 |
| 62706 | 27.22121508 | -26.77508589 | 20180829 | 61411 | 1415.688 |

**Table 5-1: Flight log data example with random location close to Potchefstroom**

The attributes included in Table 5-1 are the only relevant attributes from the flight log data file necessary for calculations and further analysis of the data.

### 5.2.2 Waypoint data

*ExperimentDescription.KML* – The waypoint data file is obtained from the UgCS ground control station software as described in Section 4.4, containing data about the flight plan constructed for each experiment including a list of coordinates in the form of waypoints specified for each experiment. An example of a .KML file with random waypoints close to Potchefstroom is shown in Code Snippet 5-1.

**Code Snippet 5-1: Example of waypoints in .KML file**

```
1  ...
2  <coordinates>
3  27.22119383179502,-26.77511410692382,1435.0 27.22128796809763,-
   26.775072472690443,1435.0 27.219691829911355,-26.771744895838175,1435.0
   27.222898119993747,-26.778399169294378,1435.0 27.22128794014218,-
   26.77507244595521,1435.0
4  </coordinates>
5  ...
```

This .KML file contains the waypoints in the form of a list, with each waypoint separated by a space and the longitude, latitude and height attributes of each waypoint separated by a comma. This .KML file was processed and transformed to be presented as shown in Table 5-2.

| Waypoint# | Longitude | Latitude | Height |
|---|---|---|---|
| 1 | 27.2211938317950 | -26.7751141069238 | 1435.0 |
| 2 | 27.2212879680976 | -26.7750724726904 | 1435.0 |
| 3 | 27.2196918299113 | -26.7717448958381 | 1435.0 |
| 4 | 27.2228981199937 | -26.7783991692943 | 1435.0 |
| 5 | 27.2212879401421 | -26.7750724459552 | 1435.0 |

**Table 5-2: Waypoint data example**

The waypoint data consists of the waypoint index number, longitude, latitude and the height for each waypoint. The data in the table provides an example of the waypoint data specified for the

RL400 type of experiment with a total of five waypoints, with the first waypoint being the initial approach waypoint as described in Section 4.6.1.

### 5.2.3 Weather data

*WeatherExport_YYYY-MM-DD.CSV* – The weather data file is obtained from the Davis Vantage Vue weather station as described in Section 4.4. This data file contains all the measured weather data for the particular day and time on which each experiment was conducted. The timestamp in the flight log data file, described in Section 5.2.1, is matched to the timestamp in the weather data file to obtain the weather data corresponding to the records in the flight log data file for each individual experiment. The weather data are collective measurements available at 1 minute intervals as shown in Table 5-3.

| Date | Time | WindSpeed | WindDir |
|---|---|---|---|
| 2018/08/29 | 9:30 AM | 12.9 | N |
| 2018/08/29 | 9:31 AM | 14.5 | NNE |

**Table 5-3: Weather data example**

The three data files described in Section 5.2 are imported into MATLAB R2018a as *Data* (flight log data), *Waypoint* (waypoint coordinates extracted from .KML file) and *WData* (weather data). After the data have been imported, the workspace is stored as a single consolidated data structure containing the raw data relevant to each specific experiment.

## 5.3 Segmentation

The segmentation process involved separating each unique experiment performed into flight segments. The data for each unique experiment were filtered and segmented according to the number of flight segments, described in Section 4.6, of that particular experiment type. Each experiment consisted of a few properties to describe, and to index all the flight segments of each experiment. These flight segments are located between two waypoints as described in Section 4.6. For flight where the UAV would hover between flight segments, the data would be stored as hover segments according to the time spent hovering between the end waypoint of one flight segment and the begin waypoint of the next segment.

It was easy enough to determine which waypoints are associated with which flight segment, but the challenge was to obtain the specific flight log timestamp on which each flight segment began and ended in order to match those timestamps to the associated waypoints. A MATLAB R2018a program was written to assist in obtaining these timestamp indexes. This program provided a simulation of the experiments that allowed the researcher to visually scan through the

experiments to find the timestamp index on which each flight segment began and ended, as shown in Figure 5-1. Figure 5-1 a) provides an example of the stop and turn (S&T) waypoint approach strategy simulated for one of the RH experiment types, whereas Figure 5-1 b) provides an example of the adaptive (Ada) waypoint approach strategy also simulated for one of the RH experiment types.

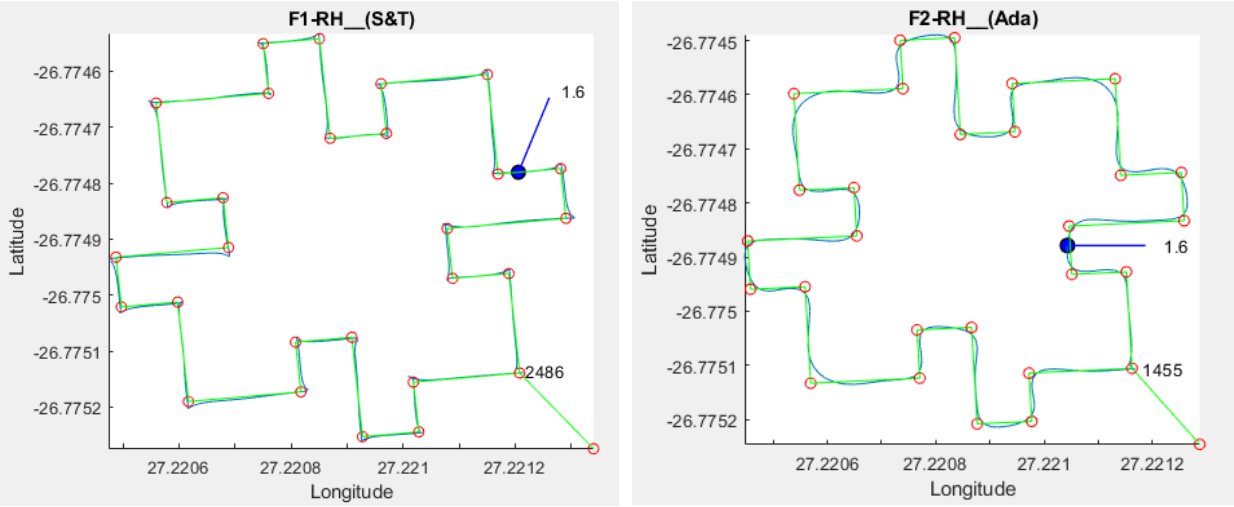


a) Stop and Turn (S&T) example

b) Adaptive (Ada) example

**Figure 5-1: Experiment segmentation simulation**

The simulation shown in Figure 5-1 included the specified path to follow in green, the actual path flown in blue, the wind vector in the direction the wind is blowing, shown as a dot with a line in dark blue, as well as the waypoints indicated with red circles. The wind speed is shown in km/h at the end of the wind vector and the timestamp index at each point in the simulation is shown at the first waypoint of the flight in the bottom right-hand corner of the figure. These timestamp indexes were obtained by the researcher scanning through each experiment, determining the first, nearest coordinate to the specified waypoint and recording the specific flight log timestamp index of that particular segment in the segmentation file described next.

These recorded flight log timestamp indexes were matched with their corresponding waypoints and then indexed into the data structure containing the information of all flight segments of each type of experiment. An example of the flight segment data structure is shown in Code Snippet 5-2 below with a short description of the elements that follow.

**Code Snippet 5-2: Example of segmentation of flights**

```
 1  Experiment(4).Type = "RL400";
 2  Experiment(4).Description = "F4-RL400__[AMSL]";
 3
 4  Experiment(4).Flight(1).Begin = 1041;
 5  Experiment(4).Flight(1).End = 3391;
 6  Experiment(4).Flight(1).WaypointB = Waypoint(2);
 7  Experiment(4).Flight(1).WaypointE = Waypoint(3);
 8
 9  Experiment(4).Flight(2).Begin = 3751;
10  Experiment(4).Flight(2).End = 8431;
11  Experiment(4).Flight(2).WaypointB = Waypoint(3);
12  Experiment(4).Flight(2).WaypointE = Waypoint(4);
13
14  Experiment(4).Flight(3).Begin = 8771;
15  Experiment(4).Flight(3).End = 11201;
16  Experiment(4).Flight(3).WaypointB = Waypoint(4);
17  Experiment(4).Flight(3).WaypointE = Waypoint(5);
```

As shown in Code Snippet 5-2, each *Experiment* object has a *Type*, *Description* and *Flight* property. The *Type* property indicates the associated type of experiment followed by a short description to provide the researcher with more information and notes about the variations and properties of the experiment. The description “F4-RL400 [AMSL]” indicates that it is the fourth experiment of the RL400 type of experiment that is conducted at a constant height above mean sea level (AMSL) at the default speed of 5 m/s (since no speed alterations are indicated). Thereafter, each *Flight* (flight segment) object contains four properties, namely *Begin*, *End*, *WaypointB* and *WaypointE*.

The index values used for the beginning, *Begin* attribute, and ending, *End* attribute of each flight segment in the *Flight* object (shown in line 4 and line 5 of Code Snippet 5-2), are the timestamp index values obtained from the flight log data file for that experiment. The *WaypointB* and *WaypointE* attributes of the *Flight* object (shown in lines 6 and 7 of Code Snippet 5-2) indicate the unique waypoint number associated with the starting and ending waypoint of that segment, obtained from the waypoint data file (*.KML*) for the specific experiment.

## 5.4 Calculations and translations

Calculations need to be performed in order to obtain the correct wind data for each particular flight segment in the preferred format so that it can easily be understood and interpreted. These calculations are done to express wind data relevant to the specific analysis being performed.

For the analysis on the left-right deviation from the flight path, the component of the wind vector perpendicular to the flight path needs to be calculated, pushing the UAV left- or right. For the

analysis of flight segment completion time, the component of the wind vector in the direction of the flight needs to be calculated. This component in the direction of the flight indicates wind coming directly from the front, pushing the UAV backwards or coming directly from behind, pushing the UAV forward.

Before the calculations can be performed, the wind direction, as well as the wind speed at a specific timestamp index need to be obtained and converted to a standardised unit of measure. The wind direction in the data obtained from the weather station is expressed in cardinal directions (as described in Section 3.2.2.2), with sixteen points of precision, as shown in in Figure 5-2.

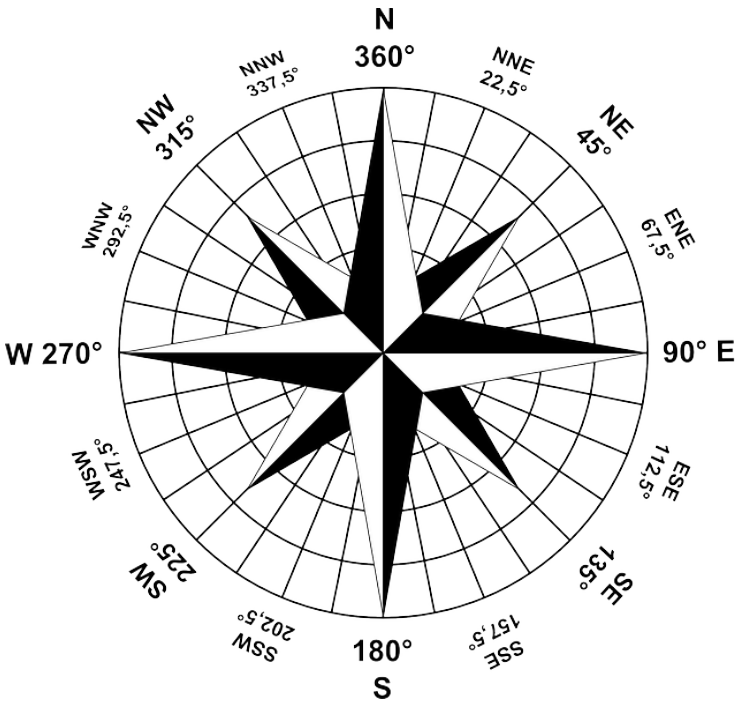


**Figure 5-2: Sixteen points of precision**

To be able to calculate the component of the wind vector in a specific direction, the cardinal directions need to be converted and represented in degrees ranging from 0º to 360º, with North expressed as 360º in aviation terms. Therefore each of the sixteen points of precision represent an interval of 22.5º, as shown in Figure 5-2, where, for example, NE will be translated to 45º, NW will be translated to 315º, and so forth. The collected wind speed was expressed in km/h which was converted to m/s for a standardised unit of measure, as flight lengths will be converted to also be expressed in metres.

Geographic coordinates (latitude and longitude) are customarily used in navigation (Chopde & Nichat, 2013). To calculate the deviation from the flight path, the distance between two

coordinates need to be calculated. These coordinates are two points on a sphere, and the Haversine formula is used in this study to calculate the distance in metre between these points. The calculation of the wind components and the deviation from the flight path are described further and illustrated in Figure 5-3.

Before calculating the component of the wind vector in the relevant directions, as described earlier in this section, the following points need to be described:

- **WP1** - the waypoint where the flight segment begins;
- **WP2** - the waypoint where the flight segment ends;
- **L1** - the current location of the UAV at a specific timestamp index in the flight log;
- **L2** - the point on the line between **WP1** and **WP2**, perpendicular to **L1**;

Using the points described above, the important vector components need to be determined:

- **w** - the vector from **L2**, indicating the current direction and strength of the wind;
- **a** - the vector from **L2** to **L1**, indicating the deviation from the flight plan;
- **p** - a vector from **L2** in the direction of **WP2**;

The three vectors, **w**, **a**, and **p**, determined above, are used to calculate the wind vector components, $\mathbf{w_a}$ and $\mathbf{w_p}$, in the relevant directions, used for further analysis:

The points and the vector components described above are used to calculate the component of the wind vector in the relevant directions:

- $\mathbf{w_a}$ - the vector indicating the component of the wind vector, **w**, in the direction of the deviation, **a**; and
- $\mathbf{w_p}$ - the vector indicating the component of the wind vector, **w**, in the direction of the ending waypoint, **p**.

The first analysis of perpendicular deviation, discussed in Section 5.8, requires the vector **a** and $\mathbf{w_a}$, for all records in each flight segment. The next analysis of flight segment completion time, discussed in Section 5.9, requires the average of the vector $\mathbf{w_p}$ for each flight segment, as well as the time the UAV took to complete the flight segment. The above-mentioned points, vectors, as well as the component of the wind vector in the relevant directions are illustrated in Figure 5-3, and stored for further statistical analysis to be performed.

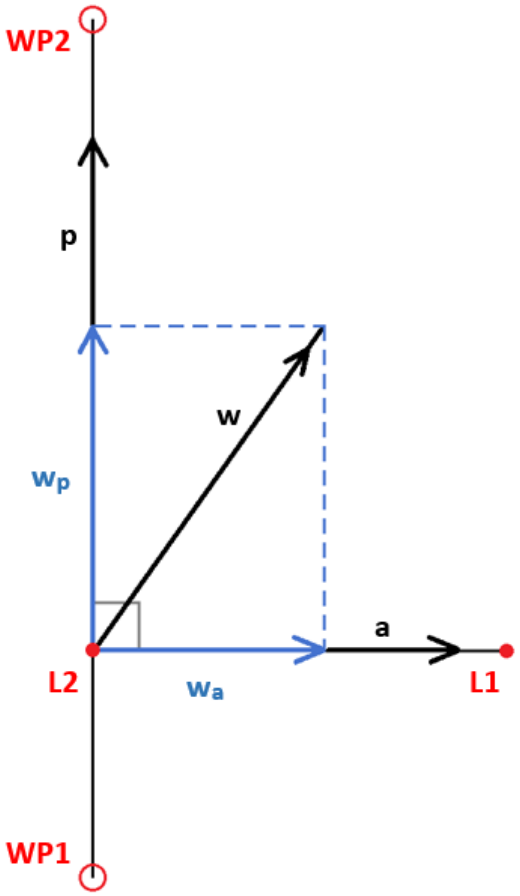


**Figure 5-3: Deviation and wind component calculations**

The time taken to complete each flight segment needs to be calculated next. In order to determine the completion time of each flight segment, the timestamp from the flight log data needs to be obtained for the beginning- and ending waypoints of that flight segment. The time it took to travel from **WP1** to **WP2** is the result of simply subtracting the timestamp at **WP1** from the timestamp at **WP2** for a total completion time of each segment.

After the abovementioned calculations have been performed, all the relevant and calculated data that forms part of each flight segment is stored in a data structure in MATLAB R2018a. The configuration and content of this data structure contains all the relevant data of each flight segment that is used for statistical analysis and is provided in Table 5-4 on the next page. This table contains a description of the attribute, an example of the data and unit of measure, as well as a brief description of each attribute.

| Attribute | Example data | Description |
|---|---|---|
| D | 0.562 m | Deviation from planned flight path |
| WD | 36.71 $^{o}$ | Wind direction at timestamp |
| WS | 7.6 m/s | Wind speed at timestamp |
| $w_a$ | 3.1 m/s | Wind component on deviation plane |
| $w_p$ | 2.7 m/s | Wind component on travel plane |
| T | 84 s | Segment completion time |

**Table 5-4: Summary of data used for statistical analysis**

Statistical analysis is performed on all the relevant and calculated data of each flight segment of every experiment described in Section 4.6. Before the statistical analysis in SPSS, the consolidated data is visually represented in MATLAB R2018a in order to simulate the flight segments and provide a graphical representation of the relationship between the deviation and wind components of any segment of any of the conducted experiments as described in the next section.

## 5.5 Presentation and interpretation

Experiments are graphically presented in terms of graphs and figures in MATLAB R2018a. These graphs assist the researcher to visually cycle through each segment of an experiment to clearly see the deviation and previously calculated wind components of those segments as illustrated in Figure 5-3. To understand and be able to interpret these graphical representations, the key components and logic behind them need to be discussed.

To summarise the key components used in the graphical presentation and interpretation of all experiments and segments, Figure 5-4 is provided for a quick reference to positive and negative values in the data with a short description below.


**Figure 5-4: Wind and deviation sign**

- **Wind** - The wind component on all the relevant figures is shown in the direction in which the wind is blowing or pushing the flight segment. Therefore, a positive wind value indicates that the wind is blowing to the left of the path, and a negative wind value indicates the wind is blowing to the right of the path.

- **Deviation** - The deviation values on all the relevant figures and data sets indicate on which side of the flight path the deviation occurs, taking into account the direction of travel. Left of the flight path would be presented as a positive value, whereas a deviation to the right of the flight path would be presented as a negative value.
- **Time** – The wind components for the completion time analysis are indicated and measured as positive values when the wind is blowing the UAV forward or in the same direction of travel and negative wind component values indicate that the wind is blowing the UAV backwards.

For each experiment conducted, the entire experiment, along with its waypoints, are shown in the Figure 5-5 a) with the wind vector indicated along the flight path at the specific timestamp index in the experiment. The wind vector is shown as a blue line pointing away from the blue dot in the direction the wind is blowing. In Figure 5-5 a), the wind is blowing in a SSW direction. For the specific experiment "F5-RL250_[AMSL]" shown in Figure 5-5, the experiment simulation is paused during the second segment of the experiment at a specific timestamp (segment) index of 2996 shown at the initial approach waypoint in the middle of Figure 5-5 a). The figure on the right, Figure 5-5 b), indicates the magnitude, measured in metre (m), of the deviation (D) perpendicular to the planned flight path and is shown in blue. The magnitude of the wind vector perpendicular to the flight path, is shown in red and has metre per second (m/s) as the unit of measure.

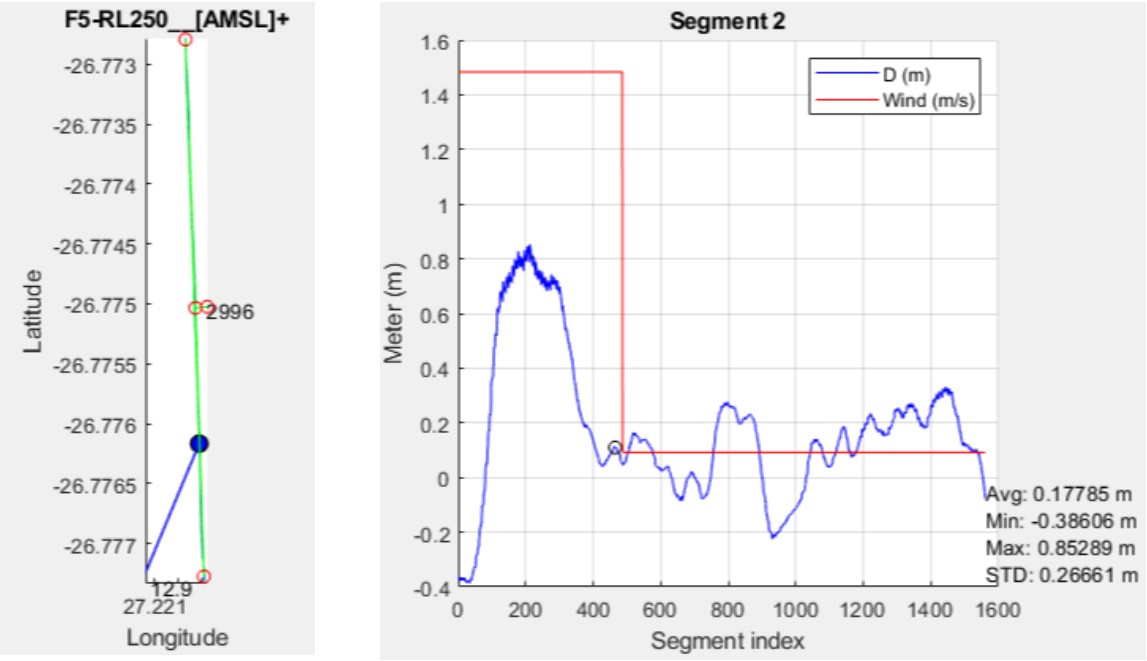


a) Flight simulation

b) Deviation and wind perpendicular to the flight path

**Figure 5-5: Flight segment deviation simulation**

The direction of travel is important in Figure 5-5 a) and Figure 5-5 b). In Figure 5-5 a), the simulation is paused during the second segment of the experiment, therefore travelling from the bottom of the figure to the top of the figure. Figure 5-5 b), the direction of travel is interpreted from the left to the right, starting at the segment index 0, travelling to the last index of that particular segment. A deviation to the left of the flight path would be presented as a positive value, whereas a deviation to the right of the flight path would be presented as a negative value. The positive and negative indication of the component of the wind vector is important, as it is based on the direction of travel and it indicates in what direction the wind is blowing or pushing the UAV. Therefore, the wind component will be a positive value if the component of the wind vector is to the left of the flight path, and a negative value if the component of the wind vector is to the right of the flight path.

In the right-hand bottom corner of Figure 5-5 b), some descriptive statistics for the flight segment are provided for reference. These statistics include the average deviation, minimum deviation (right of the flight path), maximum deviation (left of the flight path), as well as the standard deviation. The statistical analysis and the interpretation of the data are described in the next section.

## 5.6 Synopsis of statistical methods and interpretation

The purpose of this section is to provide background information on the statistical methods used for the exploratory data analysis performed in this study, as well as to provide guidelines on how the results are interpreted. Statistical analysis and interpretation of the experimental data are conducted in the next sections.

Exploratory data analysis is performed to highlight the main characteristics observed in the experimental UAS data where various inferential statistical techniques are used to assist in the analysis of the data to obtain the experimental results. All the statistical techniques are described briefly, based on the purpose and use within the study, and how the results obtained from these techniques are interpreted.

Statistical significance is a measure used to determine whether some effect exists or the likelihood that there is a relationship denoted by the probability p-value. In order to determine whether some effect or relationship is statistically significant, the effect or relationship is compared to a significance level (α) specified by the researcher. The significance level is generally set to 5% ($\alpha = 0.05$), and is compared to the p-value obtained from experiments. If it is true that $p < \alpha$, the effect or relationship is said to be statistically significant, meaning that if there is less than a 5%

chance that the effect or relationship would be rejected or may be caused by chance, it is accepted to be statistically significant.

In this study, the deviation components, completion time and wind components as described previously in Section 5.4 are compared to analyse if some effect or relationship exists and to determine the strength of the relationship by calculating the Spearman correlation coefficient between these components.

### Spearman correlation

The Spearman correlation is calculated and used to determine if there is a relationship between two continuous variables. The strength of the relationship is indicated by the Spearman correlation coefficient which can be interpreted based on the following categories.

| Correlation coefficient | Strength of relationship |
|---|---|
| 0.1 | Small / Weak relationship |
| 0.3 | Medium / Moderate relationship |
| 0.5 | Large / Strong relationship |

**Table 5-5: Spearman correlation categories**

The Spearman correlation categories provided in Table 5-5 are used as guidelines to determine the strength of the relationships between the deviation components, the flight segment completion time and the wind components based on the specific analysis performed. The wind speeds are categorised in order to see if there is a difference between wind speed groups. These wind speed groups are then analysed to determine if they statistically differ from one another by performing ANOVA tests.

### ANOVA

Analysis of variance (ANOVA) is used to measure variation between group means. In this study, the ANOVA tests are mainly calculated with the wind grouped from -6 m/s to 6 m/s in integer groups referred to as wind speed categories, to see how the wind speed categories differ. These wind speed categories are obtained by rounding the wind speed component to the nearest integer and is used in order to determine the significance of the variance between these categories.

Games-Howell Post Hoc tests are performed in order to determine if the related wind categories differ statistically from one another. These tests can also be used to determine if some wind categories should rather be combined to represent a single wind category instead. The practical

significance of the observed effect or relationship between these wind speed categories can be determined by calculating effect sizes.

**Effect size**

The effect size is used to determine the practical significance of an effect and is the standardised measure to determine the extent of the effect. Cohen's d-value is calculated to determine effect sizes by comparing the change in mean values to determine the extent, magnitude or practicality of the observed effect. In this study, the effect size is used to determine if the strength of the different wind speed categories differ practically significantly. The practical significance is indicated by the effect size value obtained by calculating the absolute difference between the sample means and can be interpreted based on the following main classifications.

| Effect size | Practical significance |
|---|---|
| 0.2 | Small |
| 0.5 | Medium |
| 0.8 | Large |

**Table 5-6: Effect size categories**

The effect size categories provided in Table 5-6 are used as guidelines to determine if the observed effect is practically significant. Therefore, in this study, the effect sizes are mostly used to determine if the influence of wind has a noteworthy effect or influence on the deviation from the flight path, the segment completion time or the deviation observed when hovering during flights.

An overview of all the experiments conducted is provided next, followed by the statistical analysis of the experimental data where the abovementioned measurements and techniques are used to obtain the statistical results. Although ANOVA tests are performed on the wind speed categories, this study is concerned with obtaining the descriptive statistical results of the data acquired from conducting the experiments described in Section 4.6.

## 5.7 Experiment results

There were four unique experiment types as discussed in Section 4.6. These unique experiment types, namely Experiment 1: RL400, Experiment 2: RL250, Experiment 3: RH and Experiment 4: Circle, were each conducted a number of times with variations to the attributes of the experiments that included: Sub-waypoints, Waypoint approach (S&T, Adaptive), Height (AMSL, AGL), Speed (5m/s, 10m/s, 15m/s) and Orientation as discussed in Section 4.6. A table summarising all the

unique experiments conducted in this study along with the specific attributes of each experiment is provided in Table 5-7 for reference.

| Ex | Type | Experiment Description | Sub-waypoints | Way-approach | Wait (s) | Height | Speed (m/s) |
|---|---|---|---|---|---|---|---|
| 1 | RL400 | F1-RL400 | No | S&T | 10 | AGL | 5 |
| 1 | RL400 | F2-RL400_Way(S&T) | Yes | S&T | - | AGL | 5 |
| 1 | RL400 | F3-RL400_Way(Ada) | Yes | Ada | - | AGL | 5 |
| 1 | RL400 | F4-RL400_[AMSL] | No | S&T | 10 | AMSL | 5 |
| 1 | RL400 | F5-RL400_Way(S&T)_[AMSL] | Yes | S&T | - | AMSL | 5 |
| 1 | RL400 | F6-RL400_Way(Ada)_[AMSL] | Yes | Ada | - | AMSL | 5 |
| 2 | RL250 | F1-RL250(S&T) | No | S&T | 10 | AGL | 10 |
| 2 | RL250 | F2-RL250 | No | S&T | - | AGL | 10 |
| 2 | RL250 | F3-RL250 | No | S&T | 10 | AGL | 10 |
| 2 | RL250 | F4-RL250 | No | S&T | 10 | AGL | 10 |
| 2 | RL250 | F5-RL250_[AMSL]+ | No | S&T | 10 | AMSL | 10 |
| 2 | RL250 | F6-RL250_[AMSL]++ | No | S&T | 10 | AMSL | 15 |
| 2 | RL250 | F7-RL250_[AMSL]++ | No | S&T | 10 | AMSL | 15 |
| 2 | RL250 | F8-RL250_[AMSL]++ | No | S&T | 10 | AMSL | 15 |
| 3 | RH | F1-RH_(S&T) | No | S&T | - | AGL | 5 |
| 3 | RH | F2-RH_(Ada) | No | Ada | - | AGL | 5 |
| 3 | RH | F3-RH_(S&T)_[AMSL] | No | S&T | - | AMSL | 5 |
| 3 | RH | F4-RH_(Ada)_[AMSL] | No | S&T | - | AMSL | 5 |
| 4 | Circle | F1-Circle_(Ada) | Yes | Ada | - | AGL | 5 |
| 4 | Circle | F2-Circle_(Ada)_[AMSL] | Yes | Ada | - | AMSL | 5 |

**Table 5-7: Experiments conducted**

For all the unique experiments conducted, there are a number of flight segments in each, depending on the type of experiment. The experiment types RL400 and RL250 consisted of three segments each, the RH type of experiment consists of 28 segments and the Circle type of experiment has a number of segments depending on the radius specified, as described in Section 4.6.

Therefore, from all the unique experiments listed in Table 5-7, data for a total of 154 straight line flight segments are available for analysis from the RL400, RL250, and RH experiment types, and the segments of the Circle experiments used only for the analysis of perpendicular deviation. In the subsections that follow, the statistical analysis will be provided on the deviation perpendicular to the flight path, an analysis on the segment completion time and an analysis of the deviation observed when hovering between flight segments.

## 5.8 Analysis of perpendicular deviation (LR)

This analysis is carried out to determine if there is a correlation between the wind and the perpendicular deviation left and right (LR) from the UAS flight path. The wind component perpendicular to the flight path is used for this analysis to determine if the wind influences the UAS flight path, and to what extent the deviation in the flight path can be explained by the influence of wind.

| Section | Analysis | Description | Reason |
|---|---|---|---|
| 5.8.1 | LR | All flight segments | Overall view of combined data |
| 5.8.2 | LR | All flight segments split by type | Comparison of each type of experiment |
| 5.8.3 | LR | All flight segments split by speed | Compare flight speeds of all experiments |
| 5.8.4 | LR | RL400 split by waypoint specification | Normal waypoint specification compared to sub-waypoint specification |

**Table 5-8: Overview of perpendicular deviation analysis**

An overview of the perpendicular deviation analysis is provided in Table 5-8. This table contains a brief outline of each analysis for reference, whereby a more detailed description is provided in the associated subsections of each.

### 5.8.1 LR - All flight segments

All experiment types are included in this analysis (RL400, RL250, RH, and Circle) in order to have an overall view of the combined data. The absolute deviation (D_Abs) and absolute wind categories (W_Cat_Abs) are used for this analysis. Firstly, a Spearman correlation is performed to determine the degree of association for all the combined data as shown in Table 5-9 below.

| | | | W_Cat_Abs |
|---|---|---|---|
| Spearman's rho | D_Abs | Correlation Coefficient | .050** |
| | | Sig. (2-tailed) p-value | **0.000** |
| | | N | 93969 |
| **. Correlation is significant at the 0.01 level (2-tailed). | | | |

**Table 5-9: Correlation for LR - All flight segments**

Although the relationship between the absolute deviation (D_Abs) and the absolute wind categories (W_Cat_Abs) is statistically significant ($p < 0.001$) on a 0.1% level, there is a correlation coefficient ($r = 0.05$) that is smaller than that in a weak relationship, since $r < 0.1$,

therefore the relationship between the absolute deviation (D_Abs) and the absolute wind categories (W_Cat_Abs) of the combined data is not significant.

To analyse the difference between the absolute wind categories, an analysis of variance (ANOVA) test is performed. The ANOVA p-value (< 0.001) indicates that there is a statistically significant difference between the absolute wind categories, as $p < \alpha$ (0.05). In order to see where the difference between these groups is, Post Hoc tests are performed and effect sizes are calculated for the absolute deviation (D_Abs), as shown in Table 5-10 below.

| W_Cat_Abs (m/s) | N | Mean | Std. Deviation | Std. Error | 95% Confidence Interval for Mean | | Effect size (from 0) |
|---|---|---|---|---|---|---|---|
| | | | | | Lower Bound | Upper Bound | |
| **0** | 38322 | 0.226 | 0.261 | 0.001 | 0.224 | 0.229 | 0.00 |
| **1** | 24521 | 0.196 | 0.201 | 0.001 | 0.193 | 0.198 | 0.12 |
| **2** | 20845 | 0.212 | 0.258 | 0.002 | 0.208 | 0.215 | 0.06 |
| **3** | 6808 | 0.316 | 0.350 | 0.004 | 0.308 | 0.324 | 0.26 |
| **4** | 2893 | 0.517 | 0.451 | 0.008 | 0.501 | 0.533 | **0.65** |
| **6** | 580 | 0.517 | 0.295 | 0.012 | 0.493 | 0.542 | **0.99** |
| Total | 93969 | 0.232 | 0.270 | 0.001 | 0.231 | 0.234 | |

**Table 5-10: Descriptives for LR - All flight segments**

The Games-Howell Post Hoc tests indicate that all wind groups differ from 0. However, effect sizes indicate that only wind categories ≥ 4 have important deviations (where effect sizes are medium to large) and are therefore practically significant. This practical significance trend can also be seen in the means plot as illustrated in Figure 5-6 below.

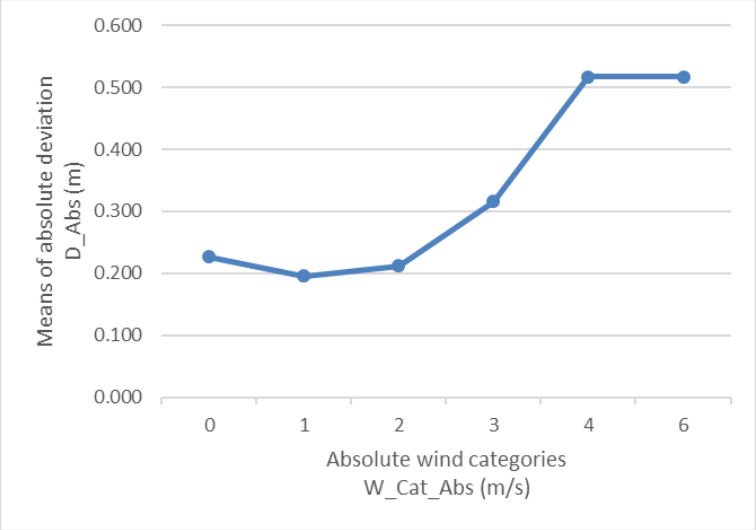


**Figure 5-6: Means plot for LR - All flight segments**

### 5.8.2 LR - All flight segments split by type

This analysis on the data of all the flight segments is split by experiment type (RL400, RL250, RH, and Circle) to observe descriptive statistics for each individual type of experiment. The absolute deviation (D_Abs) and absolute wind category (W_Cat_Abs) are used for this analysis. Firstly, a Spearman correlation is performed to determine the degree of association between the absolute deviation (D_Abs) and the absolute wind category (W_Cat_Abs), to obtain the correlation coefficient for each experiment type, as shown in Table 5-11 below.

| Ex | Type | Correlation type | | | W_Cat_Abs |
|---|---|---|---|---|---|
| 1 | RL400 | Spearman's rho | D_Abs | Correlation Coefficient | -.083** |
| 2 | RL250 | Spearman's rho | D_Abs | Correlation Coefficient | **.463**** |
| 3 | RH | Spearman's rho | D_Abs | Correlation Coefficient | .091** |
| 4 | Circle | Spearman's rho | D_Abs | Correlation Coefficient | **.228**** |
| **. Correlation is significant at the 0.01 level (2-tailed). | | | | | |

**Table 5-11: Correlation for LR - All flight segments split by type**

The degree of association for all experiment types is indicated by the correlation coefficients, as provided in Table 5-11. The relationship between the absolute deviation (D_Abs) and the absolute wind categories (W_Cat_Abs) for all types is statistically significant ($p < 0.001$) on a 0.1% level. The correlation coefficient for the second experiment, RL250, indicates a strong relationship ($r = 0.463$) and the fourth experiment, Circle, indicates a medium relationship ($r = 0.228$) between the absolute deviation (D_Abs) and the absolute wind categories (W_Cat_Abs).

ANOVA tests are performed to analyse the difference between the absolute wind groups for all types. The ANOVA p-values of all of the different experiment types were < 0.001, indicating that there is a statistically significant difference between the wind groups in all experiments. In order to find out where the difference between these groups is, Post Hoc tests are performed and effect sizes for each individual type are calculated, as shown in Table 5-12.

The Games-Howell Post Hoc tests indicate that all wind categories differ from 0. The effect sizes (from 0) indicate that larger wind speed categories are practically significant as they tend to have larger deviations, since effect sizes of larger wind speed categories tend to be medium to large, as indicated in Table 5-12 and clearly observed in RL250 experiment types. This analysis can be extended to ascertain if there is a practical significance between the same wind categories of different experiment types. In order to find out if there is a practical significance between the different experiment types and the wind categories. Effect sizes are calculated between these

wind categories of the experiment types for the absolute deviation (D_Abs), as provided in Table 5-12.

| Ex | Type | W_Cat_Abs (m/s) | N | Mean | Std. Deviation | Effect size (from 0) | Effect size (between Ex 1) | Effect size (between Ex 2) | Effect size (between Ex 3) |
|---|---|---|---|---|---|---|---|---|---|
| **1** | **RL400** | 0 | 20531 | 0.235 | 0.277 | 0.00 | | | |
| | | 1 | 13100 | 0.154 | 0.138 | 0.29 | | | |
| | | 2 | 17544 | 0.174 | 0.224 | 0.22 | | | |
| | | 3 | 4238 | 0.134 | 0.097 | **0.36** | | | |
| | | 4 | 1665 | 0.266 | 0.285 | 0.11 | | | |
| | | 6 | 580 | 0.517 | 0.295 | **0.96** | | | |
| | | Total | 57658 | 0.194 | 0.231 | | | | |
| **2** | **RL250** | 0 | 9619 | 0.133 | 0.118 | 0.00 | **0.37** | | |
| | | 1 | 8797 | 0.227 | 0.225 | 0.42 | 0.32 | | |
| | | 2 | 2 | 0.332 | 0.005 | **1.68** | **0.70** | | |
| | | 3 | 2006 | 0.697 | 0.409 | **1.38** | **1.38** | | |
| | | 4 | 1228 | 0.857 | 0.409 | **1.77** | **1.44** | | |
| | | Total | 21652 | 0.265 | 0.312 | | | | |
| **3** | **RH** | 0 | 7115 | 0.338 | 0.312 | 0.00 | 0.33 | **0.66** | |
| | | 1 | 2302 | 0.293 | 0.297 | 0.14 | **0.47** | 0.22 | |
| | | 2 | 2836 | 0.440 | 0.335 | 0.30 | **0.79** | 0.32 | |
| | | 3 | 564 | 0.329 | 0.218 | 0.03 | **0.89** | **0.90** | |
| | | Total | 12817 | 0.352 | 0.315 | | | | |
| **4** | **Circle** | 0 | 1057 | 0.160 | 0.154 | 0.00 | 0.27 | 0.17 | **0.57** |
| | | 1 | 322 | 0.305 | 0.307 | **0.47** | **0.49** | 0.25 | 0.04 |
| | | 2 | 463 | 0.231 | 0.168 | **0.43** | 0.25 | **0.60** | **0.62** |
| | | Total | 1842 | 0.203 | 0.201 | | | | |

**Table 5-12: Descriptives for LR - All flight segments split by type**

The effect sizes calculated between the same wind categories of the different experiment types also tend to be higher at higher wind speed categories, especially evident in the RL250 and RH experiment types. The RL250 experiments have a medium to large effect size in almost all wind categories when compared to the wind categories of the RL400 type of experiment and are therefore regarded as a significant effect in practice. The means plot for each type of experiment is illustrated on a single graph to show how the means vary across the wind groups of the different experiment types, also clearly showing the increased deviation at higher wind speed categories, especially when comparing the means of the RL250 and RL400 experiment types.

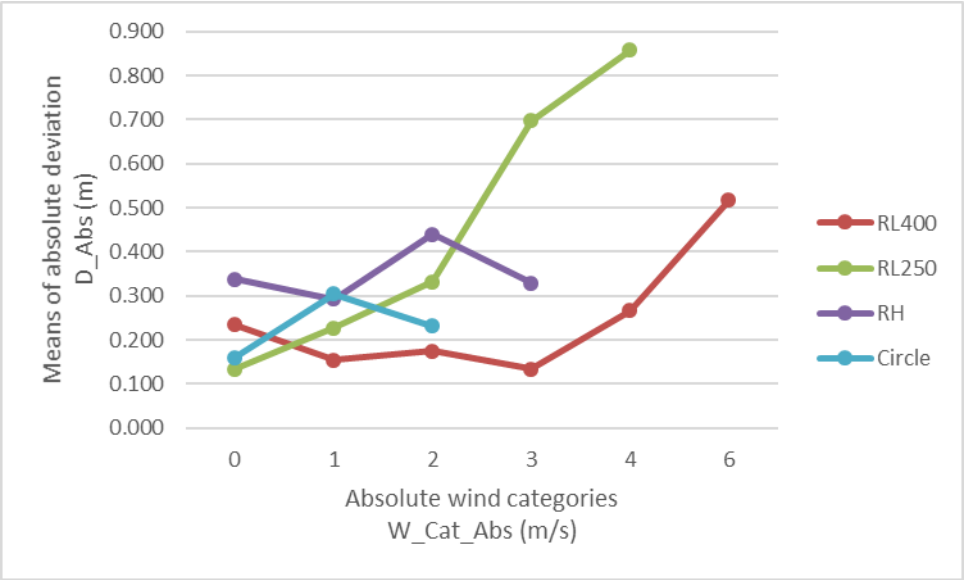


**Figure 5-7: Means plot for LR - All flight segments split by type**

### 5.8.3 LR - All flight segments split by speed

This analysis is performed on all experiment types (RL400, RL250, RH, and Circle), split by the flight speed of the experiment (5 m/s, 10 m/s and 15 m/s) to obtain descriptive statistics for the different flight speeds of all the experiments. The absolute deviation (D_Abs) and absolute wind categories (W_Cat_Abs) are used for this analysis. Firstly, a Spearman correlation, provided in Table 5-13, is performed to determine the degree of association.

| Speed | Correlation type | | | W_Cat_Abs |
|---|---|---|---|---|
| **5 m/s** | Spearman's rho | D_Abs | Correlation Coefficient | -.080** |
| **10 m/s** | Spearman's rho | D_Abs | Correlation Coefficient | .154** |
| **15 m/s** | Spearman's rho | D_Abs | Correlation Coefficient | **.477**** |
| **. Correlation is significant at the 0.01 level (2-tailed). | | | | |

**Table 5-13: Correlation for LR - All flight segments split by speed**

The relationship between the absolute deviation (D_Abs) and the absolute wind categories (W_Cat_Abs) for all speeds is statistically significant ($p < 0.001$) on a 0.1% level. However, the correlation coefficient seems to increase as the flight speed is increased and indicates a strong relationship ($r = 0.477$) between the absolute deviation (D_Abs) and the absolute wind categories (W_Cat_Abs) for flight speeds of 15 m/s.

The ANOVA p-values of the different flight speeds were all < 0.001, indicating that there is a statistically significant difference between the absolute deviation (D_Abs) and absolute wind

categories (W_Cat_Abs) at different flight speeds. In order to establish where the difference between these wind categories is, Post Hoc tests are performed and effect sizes for each flight speed are calculated for the absolute deviation (D_Abs), as shown in the table below.

| Speed | W_Cat_Abs (m/s) | N | Mean | Std. Deviation | Std. Error | 95% Confidence Interval for Mean | | Effect size (from 0) | Effect size (between 5 m/s) |
|---|---|---|---|---|---|---|---|---|---|
| | | | | | | Lower Bound | Upper Bound | | |
| **5 m/s** | 0 | 28703 | 0.257 | 0.287 | 0.002 | 0.254 | 0.261 | 0.00 | |
| | 1 | 15724 | 0.178 | 0.183 | 0.001 | 0.175 | 0.181 | 0.28 | |
| | 2 | 20843 | 0.212 | 0.258 | 0.002 | 0.208 | 0.215 | 0.16 | |
| | 3 | 4802 | 0.157 | 0.133 | 0.002 | 0.153 | 0.160 | **0.35** | |
| | 4 | 1665 | 0.266 | 0.285 | 0.007 | 0.252 | 0.280 | 0.03 | |
| | 6 | 580 | 0.517 | 0.295 | 0.012 | 0.493 | 0.542 | **0.88** | |
| | Total | 72317 | 0.223 | 0.255 | 0.001 | 0.221 | 0.224 | | |
| **10 m/s** | 0 | 8998 | 0.121 | 0.098 | 0.001 | 0.119 | 0.123 | 0.00 | **0.48** |
| | 1 | 6795 | 0.175 | 0.158 | 0.002 | 0.171 | 0.179 | 0.34 | 0.02 |
| | 2 | 2 | 0.332 | 0.005 | 0.004 | 0.285 | 0.379 | **2.15** | **0.47** |
| | Total | 15795 | 0.144 | 0.130 | 0.001 | 0.142 | 0.146 | | |
| **15 m/s** | 0 | 621 | 0.315 | 0.203 | 0.008 | 0.299 | 0.331 | 0.00 | 0.20 |
| | 1 | 2002 | 0.406 | 0.311 | 0.007 | 0.392 | 0.419 | 0.29 | **0.73** |
| | 3 | 2006 | 0.697 | 0.409 | 0.009 | 0.679 | 0.715 | **0.93** | **1.18** |
| | 4 | 1228 | 0.857 | 0.409 | 0.012 | 0.834 | 0.880 | **1.33** | **1.71** |
| | Total | 5857 | 0.590 | 0.410 | 0.005 | 0.580 | 0.601 | | |

**Table 5-14: Descriptives for LR - All flight segments split by speed**

The Games-Howell Post Hoc tests indicate that all wind groups differ from 0. The effect sizes (from 0) for all the different flight speeds indicate that larger wind speed categories are practically significant, as they tend to have larger deviations since effect sizes are medium to large as indicated in Table 5-14. Furthermore, by calculating the effect sizes between wind categories of different flight speeds, it is shown that faster flight speeds tend to have larger effect sizes and therefore important deviations that are practically significant, especially evident in the 15 m/s flight speeds when compared to the 5 m/s flight speeds. The means plot for each flight speed is illustrated below to show how the means vary across the wind groups at different flight speeds and also that higher wind speed categories tend to have larger mean deviations.

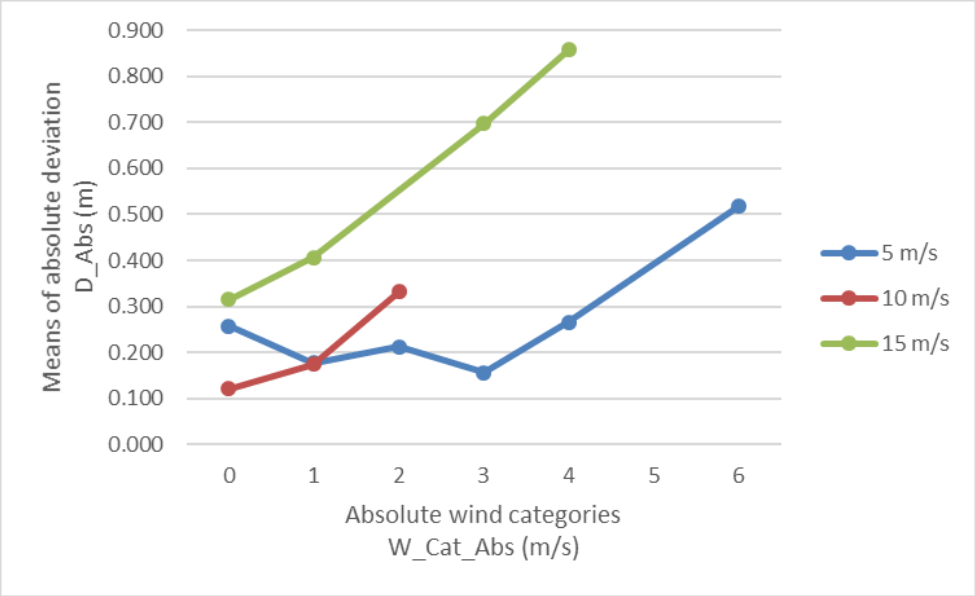


**Figure 5-8: Means plot for LR - All flight segments split by speed**

### 5.8.4 LR - RL400 split by waypoint specification

This analysis is performed on the RL400 type of experiment to calculate the difference between normally specified waypoints that are far apart and sub-waypoint specification. The absolute deviation (D_Abs) and absolute wind category (W_Cat_Abs) are used for this analysis. Firstly, a Spearman correlation is performed to determine the degree of association.

| | Sub-waypoint specification | | | W_Cat_Abs |
|---|---|---|---|---|
| Spearman's rho | No | D_Abs | Correlation Coefficient | -.130** |
| | Yes | D_Abs | Correlation Coefficient | -.057** |
| **. Correlation is significant at the 0.01 level (2-tailed). | | | | |

**Table 5-15: Correlation for LR - RL400 split by waypoint specification**

The results of the Spearman correlations show that the relationship between the absolute deviation (D_Abs) and the absolute wind categories (W_Cat_Abs) for the RL400 split by sub-waypoints is statistically significant ($p < 0.001$) on a 0.1% level. However, the correlation coefficient indicates that both normal ($r = -0.130$), and sub-waypoint specifications ($r = -0.057$) for RL400 types have a weak relationship between the absolute deviation (D_Abs) and the absolute wind categories (W_Cat_Abs).

ANOVA tests are performed to analyse the difference between the absolute wind groups for all types. The ANOVA p-values of the normal and sub-waypoint specification of the RL400 type of

experiment were < 0.001, indicating that there is a statistically significant difference between the wind groups. In order to find out where the difference between these groups is, Post Hoc tests are performed and effect sizes for normal and sub-waypoint specification for RL400 flights are calculated for the absolute deviation (D_Abs), as shown in the table below.

| Sub-waypoint specification | W_Cat_Abs (m/s) | N | Mean | Std. Deviation | Std. Error | 95% Confidence Interval for Mean | | Effect size (from 0) |
|---|---|---|---|---|---|---|---|---|
| | | | | | | Lower Bound | Upper Bound | |
| No | 0 | 5142 | 0.176 | 0.157 | 0.002 | 0.172 | 0.180 | 0.00 |
| | 1 | 3704 | 0.145 | 0.137 | 0.002 | 0.140 | 0.149 | 0.20 |
| | 2 | 6374 | 0.110 | 0.077 | 0.001 | 0.108 | 0.112 | **0.42** |
| | 3 | 1714 | 0.135 | 0.109 | 0.003 | 0.130 | 0.140 | 0.26 |
| | Total | 16934 | 0.140 | 0.126 | 0.001 | 0.138 | 0.142 | |
| Yes | 0 | 15389 | 0.254 | 0.305 | 0.002 | 0.249 | 0.259 | 0.00 |
| | 1 | 9396 | 0.158 | 0.139 | 0.001 | 0.156 | 0.161 | 0.31 |
| | 2 | 11170 | 0.211 | 0.268 | 0.003 | 0.206 | 0.216 | 0.14 |
| | 3 | 2524 | 0.133 | 0.088 | 0.002 | 0.130 | 0.137 | **0.40** |
| | 4 | 1665 | 0.266 | 0.285 | 0.007 | 0.252 | 0.280 | 0.04 |
| | 6 | 580 | 0.517 | 0.295 | 0.012 | 0.493 | 0.542 | **0.86** |
| | Total | 40724 | 0.217 | 0.260 | 0.001 | 0.215 | 0.220 | |

**Table 5-16: Descriptives for LR - RL400 split by waypoint specification**

The Games-Howell Post Hoc tests indicate that all wind categories differ from 0. The effect sizes (from 0) indicate that for normal waypoint specification only wind category 2 has a medium practical significance, for sub-waypoint specification wind category 3 also has a medium practical significance and wind category 6 has a large practical significance. However, these effect sizes do not seem to show any trend in the practical significance between normal and sub-waypoint specification in the analysed data.

The means plot provided in Figure 5-9 shows a trend that sub-waypoint specification tends to have larger deviations at larger wind speeds. Although the normally specified waypoints do not show this trend, the cause might be the fact that the normally specified waypoint data do not have very high wind speed categories and that the observation might have been similar to that of the sub-waypoint specified flights if these flights were conducted in environments with higher wind speeds.

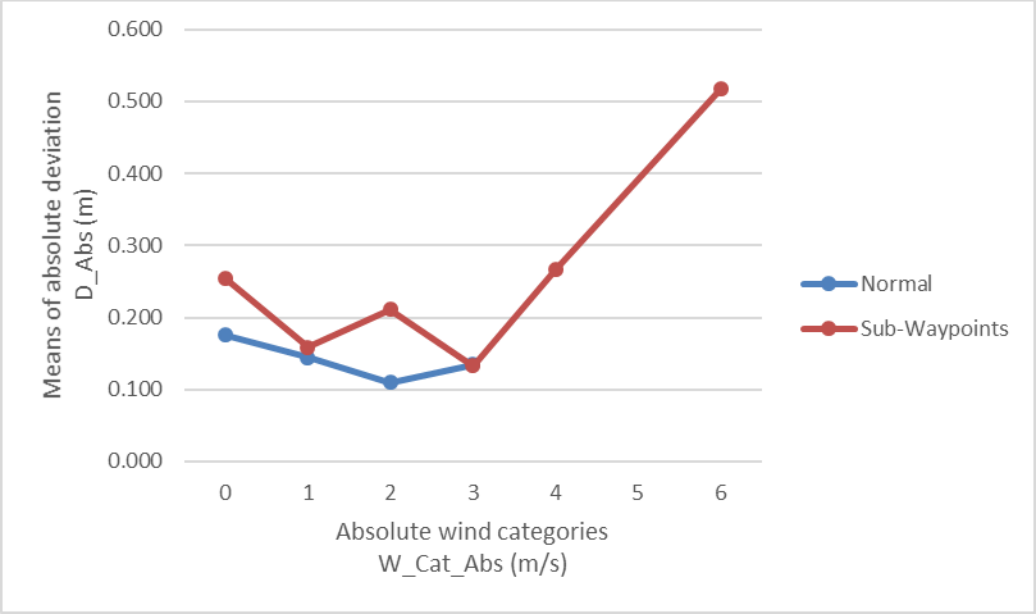


**Figure 5-9: Means plot for LR - RL400 split by waypoint specification**

## 5.9 Analysis of flight segment completion time (Time)

The completion time analysis is performed to determine if there is a correlation between the wind and the time it takes to complete a UAS flight path. The total time taken to complete segments along with the wind component in the direction of the flight path, are used in order to determine if the wind influences UAS flight times, and to what extent the time it takes to complete a flight path can be explained by the influence of wind.

| Section | Analysis | Description | Reason |
|---|---|---|---|
| **5.9.1** | Time | All flight segments split by length | Overall view of different length segments |
| **5.9.2** | Time | All flight segments split by speed | Compare completion times at different flight speeds |
| **5.9.3** | Time | RL250 split by speed | Compare similar length segments when standardised |
| **5.9.4** | Time | RL400 & RL250 split by waypoint specification | Normal waypoint specification compared to sub-waypoint specification |

**Table 5-17: Overview of segment completion time analysis**

An overview of the segment completion time analysis is provided in Table 5-17. This table contains a brief outline of each analysis for reference, whereby a more detailed description is provided in the associated subsections of each.

### 5.9.1 Time - All flight segments split by length

This analysis is conducted on all experiment types that have straight line segments (RL400, RL250, and RH) and are split by the length (10 m, 20 m, 125 m, 200 m, 250 m, and 400 m) of each segment in all those experiments. This analysis is performed to obtain descriptive statistics to see the bigger picture of the segment completion time analysis between different length segments. The total time (T) taken to complete a particular segment and average wind speed categories (W_Cat) are used for this analysis. Firstly, a Spearman correlation is performed to determine the degree of association between the time and wind categories of different length segments.

| Length (m) | Analysis type | | | W_Cat |
|---|---|---|---|---|
| **10** | Spearman's rho | T | Correlation Coefficient | -0.093 |
| | | | Sig. (2-tailed) | 0.465 |
| | | | N | 64 |
| **20** | Spearman's rho | T | Correlation Coefficient | 0.014 |
| | | | Sig. (2-tailed) | 0.924 |
| | | | N | 48 |
| **125** | Spearman's rho | T | Correlation Coefficient | 0.221 |
| | | | Sig. (2-tailed) | 0.449 |
| | | | N | 14 |
| **200** | Spearman's rho | T | Correlation Coefficient | .735* |
| | | | Sig. (2-tailed) | 0.038 |
| | | | N | 8 |
| **250** | Spearman's rho | T | Correlation Coefficient | 0.186 |
| | | | Sig. (2-tailed) | 0.690 |
| | | | N | 7 |
| **400** | Spearman's rho | T | Correlation Coefficient | 0.294 |
| | | | Sig. (2-tailed) | 0.571 |
| | | | N | 6 |

*. Correlation is significant at the 0.05 level (2-tailed).

**Table 5-18: Correlation for Time - All flight segments split by length**

The relationship between the segment completion time (T) and the wind speed categories (W_Cat) does not seem to be statistically significant except for the 200 m segments on a 5% level. The correlation coefficients of only the 125 m, 200 m, and 400 m show a moderate to strong relationship with all the rest showing a weak- or no relationship with low correlation coefficients.

It is also important to take note of the N-values that indicate the amount of data points for different lengths, showing that not much data is available for the time analysis.

To analyse the variance among the different segment lengths, an analysis of variance (ANOVA) test is performed. The ANOVA p-values indicate that there is only a statistically significant difference between the wind speed categories of the 10 m, 200 m, and 250 m flight segments as the p-value for these segments is smaller than the alpha value, $p < \alpha$ (0.05), as shown in the ANOVA table for the completion time (T) provided below.

| Length (m) | Sum of Squares | df | Mean Square | F | Sig. |
|---|---|---|---|---|---|
| **10** | 14.167 | 5 | 2.833 | 2.925 | 0.020* |
| **20** | 9.530 | 5 | 1.906 | 1.556 | 0.194 |
| **125** | 45.357 | 3 | 15.119 | 1.661 | 0.238 |
| **200** | 1876.625 | 3 | 625.542 | 11.011 | 0.021* |
| **250** | 132.464 | 2 | 66.232 | 28.641 | 0.004** |
| **400** | 1237.833 | 3 | 412.611 | 1.503 | 0.423 |
| *. Correlation is significant at the 0.05 level (2-tailed).<br>**. Correlation is significant at the 0.01 level (2-tailed). | | | | | |

**Table 5-19: ANOVA's for Time - All flight segments split by length**

In order to observe where the difference between these wind categories of the different length segments is, Post Hoc tests are performed and effect sizes calculated for the completion time (T), as provided in Table 5-20 below.

| Length (m) | W_Cat (m/s) | N | Mean | Std. Deviation | Std. Error | 95% Confidence Interval for Mean | | Effect size (from 0) |
|---|---|---|---|---|---|---|---|---|
| | | | | | | Lower Bound | Upper Bound | |
| **10** | -2 | 11 | 2.82 | 0.982 | 0.296 | 2.16 | 3.48 | **0.53** |
| | -1 | 5 | 4.00 | 0.707 | 0.316 | 3.12 | 4.88 | **0.57** |
| | 0 | 36 | 3.39 | 1.076 | 0.179 | 3.02 | 3.75 | 0.00 |
| | 1 | 5 | 2.60 | 0.894 | 0.400 | 1.49 | 3.71 | **0.73** |
| | 2 | 5 | 2.20 | 0.447 | 0.200 | 1.64 | 2.76 | **1.10** |
| | 3 | 2 | 4.00 | 0.000 | 0.000 | 4.00 | 4.00 | **0.57** |
| | Total | 64 | 3.20 | 1.057 | 0.132 | 2.94 | 3.47 | |
| **20** | -3 | 1 | 5.00 | | | | | |
| | -2 | 8 | 4.50 | 0.756 | 0.267 | 3.87 | 5.13 | **0.57** |
| | -1 | 1 | 5.00 | | | | | |
| | 0 | 26 | 5.27 | 1.343 | 0.263 | 4.73 | 5.81 | 0.00 |
| | 1 | 6 | 5.50 | 0.548 | 0.224 | 4.93 | 6.07 | 0.17 |

| | | | | | | | | |
|---|---|---|---|---|---|---|---|---|
| | 2 | 6 | 4.17 | 0.408 | 0.167 | 3.74 | 4.60 | **0.82** |
| | Total | 48 | 5.02 | 1.139 | 0.164 | 4.69 | 5.35 | |
| **125** | -3 | 4 | 24.50 | 4.796 | 2.398 | 16.87 | 32.13 | **0.80** |
| | 0 | 6 | 28.33 | 0.516 | 0.211 | 27.79 | 28.88 | 0.00 |
| | 1 | 3 | 27.67 | 3.215 | 1.856 | 19.68 | 35.65 | 0.21 |
| | 2 | 1 | 24.00 | | | | | |
| | Total | 14 | 26.79 | 3.239 | 0.866 | 24.92 | 28.66 | |
| **200** | 2 | 4 | 83.25 | 1.500 | 0.750 | 80.86 | 85.64 | |
| | 3 | 1 | 105.00 | | | | | |
| | 4 | 2 | 94.50 | 14.849 | 10.500 | -38.92 | 227.92 | |
| | 5 | 1 | 130.00 | | | | | |
| | Total | 8 | 94.63 | 17.336 | 6.129 | 80.13 | 109.12 | |
| **250** | -1 | 1 | 41.00 | | | | | |
| | 0 | 4 | 53.75 | 1.258 | 0.629 | 51.75 | 55.75 | 0.00 |
| | 3 | 2 | 52.50 | 2.121 | 1.500 | 33.44 | 71.56 | **0.59** |
| | Total | 7 | 51.57 | 4.860 | 1.837 | 47.08 | 56.07 | |
| **400** | -4 | 1 | 161.00 | | | | | |
| | -3 | 2 | 190.50 | 23.335 | 16.500 | -19.15 | 400.15 | |
| | -2 | 2 | 165.50 | 2.121 | 1.500 | 146.44 | 184.56 | |
| | -1 | 1 | 196.00 | | | | | |
| | Total | 6 | 178.17 | 18.904 | 7.718 | 158.33 | 198.01 | |

**Table 5-20: Descriptives for Time - All flight segments split by length**

The Games-Howell Post Hoc tests could only be computed on the 10 m length segments, since all the others had at least one wind category with fewer than two cases. The effect sizes (from 0) were calculated for all segment lengths that had at least one occurrence with a wind category of 0. The effect sizes for 10 m segments indicated medium to large practical significance between wind categories, showing a larger practical significance when wind categories are positive. However, it is difficult to gauge the practical significance of other segments, since data for the time analysis is sparsely populated. The means plot of the different wind categories and time taken to complete different length segments are provided in Figure 5-10 on the next page.

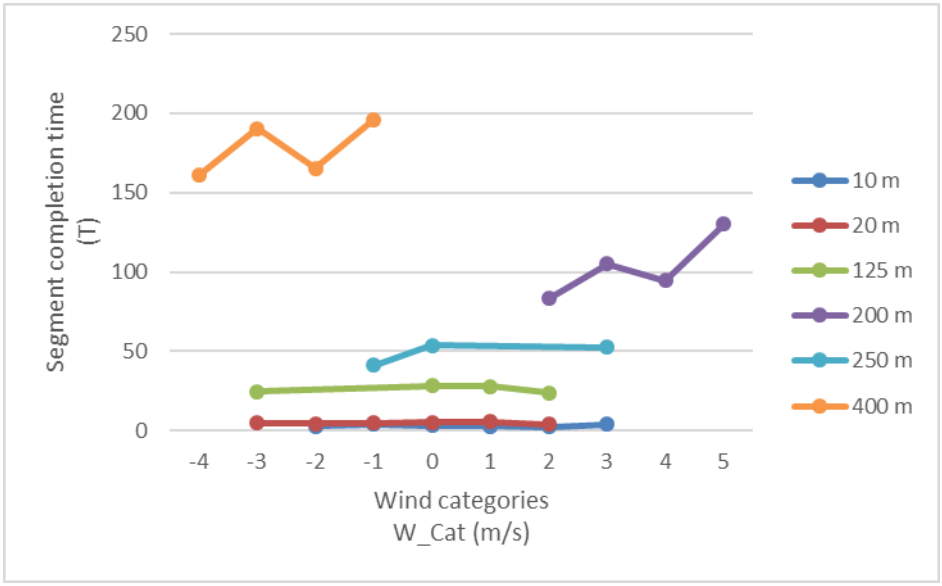


**Figure 5-10: Means plot for Time - All flight segments split by length**

Since the time it takes to complete a segment depends on the length of a segment, the different segments are difficult to illustrate in the means plot shown in Figure 5-10. In order to comparatively illustrate the different length segments, the time taken to complete all segments are standardised, representing the time of all different length segments relative to 10 m segments, as illustrated in the standardised time means plot shown in Figure 5-11 below.

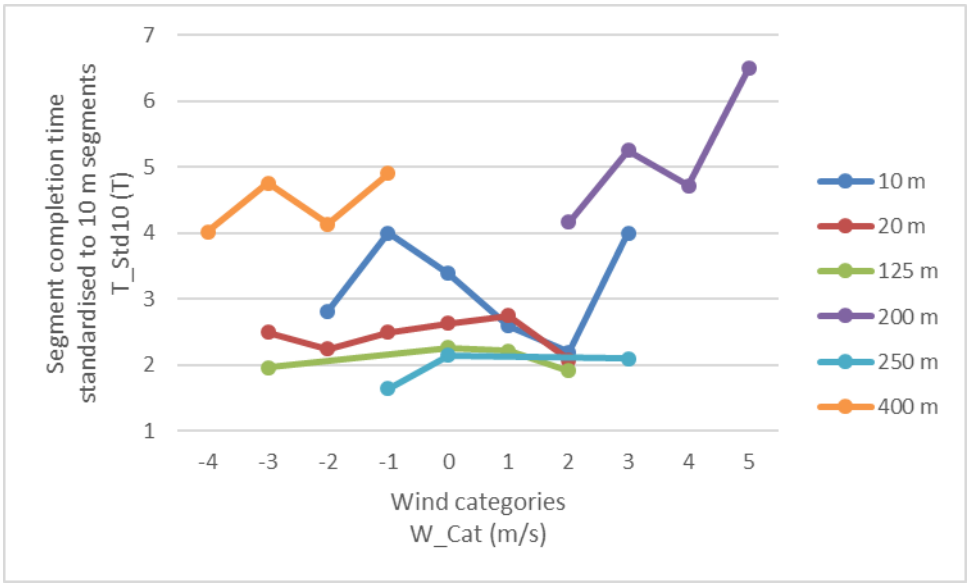


**Figure 5-11: Means plot for Time - All flight segments split by length with standardised times (T_Std10)**

A scatter plot is provided in Figure 5-12 to show the relationship between the total time (T) and wind components (W) of the segments in order to illustrate how data is generally spread among the different length segments.

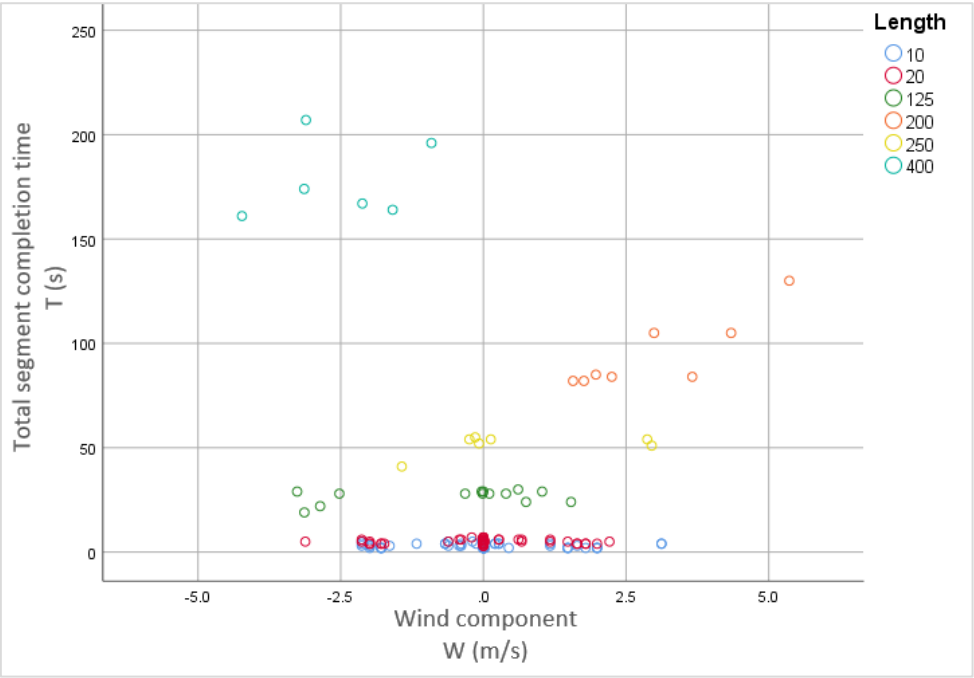


**Figure 5-12: Scatter plot for Time - All flight segments split by length**

Since the time it takes to complete a segment depends on the length of a segment as described previously, the standardised representation of the time relative to 10 m segments is illustrated in the standardised time scatter plot shown in Figure 5-13 below. The scatter plot is fitted with a $R^2$ linear line shown, describing only 1.4% of the variance, therefore a linear relationship cannot be identified in the combined data for segments of all lengths.

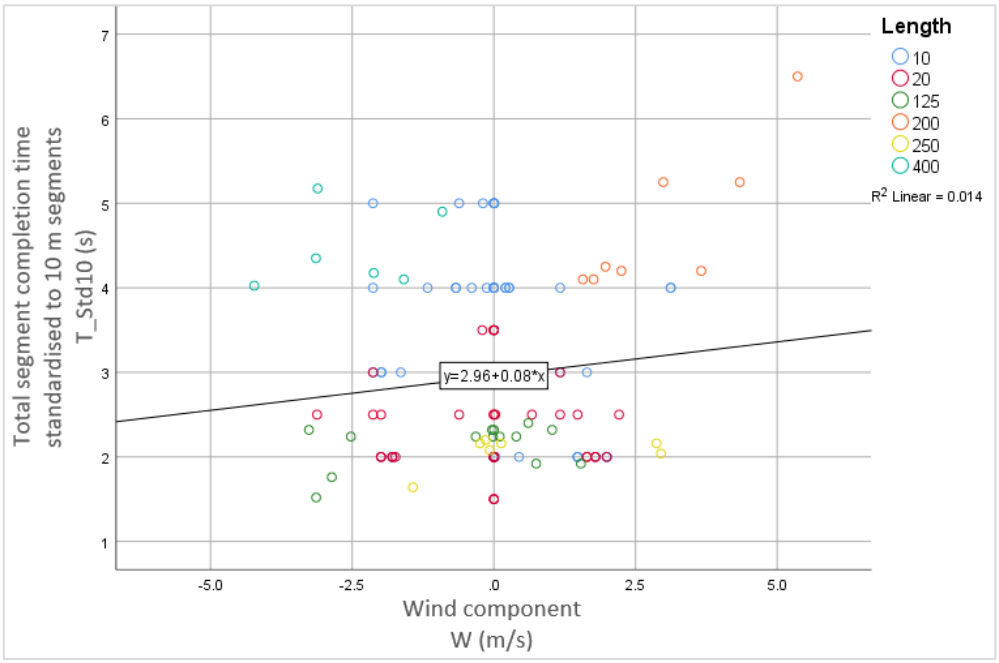


**Figure 5-13: Scatter plot for Time - All flight segments split by length with standardised times (T_Std10)**

### 5.9.2 Time - All flight segments split by speed

This analysis is performed on all experiment types that have straight line segments (RL400, RL250, and RH) and are split by the flight speed of the experiment (5 m/s, 10 m/s and 15 m/s) of each segment in all those experiments. This analysis is performed to obtain descriptive statistics to establish how the completion time compares at different flight speeds. The total time (T) taken to complete a particular segment and average wind speed categories (W_Cat) are used for this analysis. Firstly, a Spearman correlation is performed to determine the degree of association grouped by the different flight speeds.

| Speed (m/s) | Analysis type | | | W_Cat |
|---|---|---|---|---|
| **5** | Spearman's rho | T | Correlation Coefficient | 0.036 |
| | | | Sig. (2-tailed) | 0.689 |
| | | | N | 126 |
| **10** | Spearman's rho | T | Correlation Coefficient | 0.350 |
| | | | Sig. (2-tailed) | 0.201 |
| | | | N | 15 |
| **15** | Spearman's rho | T | Correlation Coefficient | 0.794 |
| | | | Sig. (2-tailed) | 0.059 |
| | | | N | 6 |

**Table 5-21: Correlation for Time - All flight segments split by speed**

The relationship between the segment completion time (T) and the wind categories (W_Cat) does not seem to be statistically significant, although the correlation coefficient for flight speeds of 10 m/s shows a moderate relationship (r = 0.35) and 15 m/s flight speeds show a strong relationship (r = 0.794).

To analyse the variance among the different wind categories of the segment speeds, an analysis of variance (ANOVA) test is performed. The ANOVA p-values indicate that there is only a statistically significant difference in the wind speed categories of only the 5 m/s flight speed segments as $p < \alpha$ (0.05), as shown in the ANOVA table for the completion time (T), provided in Table 5-22.

| Speed (m/s) | | Sum of Squares | df | Mean Square | F | Sig. |
|---|---|---|---|---|---|---|
| **5** | Between Groups | 98507 | 9 | 10945.23 | 9.880 | 0.000 |
| | Within Groups | 128505 | 116 | 1107.80 | | |
| | Total | 227012 | 125 | | | |

| | | | | | | |
|---|---|---|---|---|---|---|
| **10** | Between Groups | 569 | 3 | 189.50 | 1.338 | 0.312 |
| | Within Groups | 1558 | 11 | 141.59 | | |
| | Total | 2126 | 14 | | | |
| **15** | Between Groups | 814 | 4 | 203.58 | 45.241 | 0.111 |
| | Within Groups | 5 | 1 | 4.50 | | |
| | Total | 819 | 5 | | | |

**Table 5-22: ANOVA's for Time - All flight segments split by speed**

In order to observe where the difference between these wind categories of the different flight speeds is, Post Hoc tests are performed and effect sizes for the different flight speeds are calculated, as provided in Table 5-23.

| Speed (m/s) | W_Cat (m/s) | N | Mean | Std. Deviation | Std. Error | 95% Confidence Interval for Mean | | Effect size (from 0) |
|---|---|---|---|---|---|---|---|---|
| | | | | | | Lower Bound | Upper Bound | |
| **5** | -4 | 1 | 161.00 | | | | | |
| | -3 | 3 | 128.67 | 108.362 | 62.563 | -140.52 | 397.85 | **1.15** |
| | -2 | 21 | 18.95 | 48.737 | 10.635 | -3.23 | 41.14 | 0.30 |
| | -1 | 7 | 31.57 | 72.509 | 27.406 | -35.49 | 98.63 | **0.38** |
| | 0 | 62 | 4.18 | 1.510 | 0.192 | 3.79 | 4.56 | 0.00 |
| | 1 | 11 | 4.18 | 1.662 | 0.501 | 3.06 | 5.30 | 0.00 |
| | 2 | 15 | 24.60 | 36.627 | 9.457 | 4.32 | 44.88 | **0.56** |
| | 3 | 3 | 37.67 | 58.312 | 33.667 | -107.19 | 182.52 | **0.57** |
| | 4 | 2 | 94.50 | 14.849 | 10.500 | -38.92 | 227.92 | **6.08** |
| | 5 | 1 | 130.00 | | | | | |
| | Total | 126 | 18.03 | 42.616 | 3.797 | 10.52 | 25.55 | |
| **10** | -3 | 2 | 28.50 | 0.707 | 0.500 | 22.15 | 34.85 | **0.76** |
| | 0 | 10 | 38.50 | 13.151 | 4.159 | 29.09 | 47.91 | 0.00 |
| | 1 | 2 | 29.50 | 0.707 | 0.500 | 23.15 | 35.85 | **0.68** |
| | 3 | 1 | 54.00 | | | | | |
| | Total | 15 | 37.00 | 12.323 | 3.182 | 30.18 | 43.82 | |
| **15** | -3 | 2 | 20.50 | 2.121 | 1.500 | 1.44 | 39.56 | |
| | -1 | 1 | 41.00 | | | | | |
| | 1 | 1 | 24.00 | | | | | |
| | 2 | 1 | 24.00 | | | | | |
| | 3 | 1 | 51.00 | | | | | |
| | Total | 6 | 30.17 | 12.797 | 5.224 | 16.74 | 43.60 | |

**Table 5-23: Descriptives for Time - All flight segments split by speed**

The Games-Howell Post Hoc tests could not be computed for any of the flight speeds, since all speeds had at least one wind category with fewer than two cases. The effect sizes (from 0) were calculated for all flight speeds that had at least one occurrence with a wind category of 0. The effect sizes for 5 m/s segments indicate medium to large practical significance between some of the wind categories, showing a larger practical significance when wind categories are largely positive or largely negative. The 10 m/s segments also indicated large practical significance; however, the data is sparsely populated, making it difficult to gauge the significance. The means plot of the different wind categories and time taken to complete segments at different flight speeds are provided in Figure 5-14.

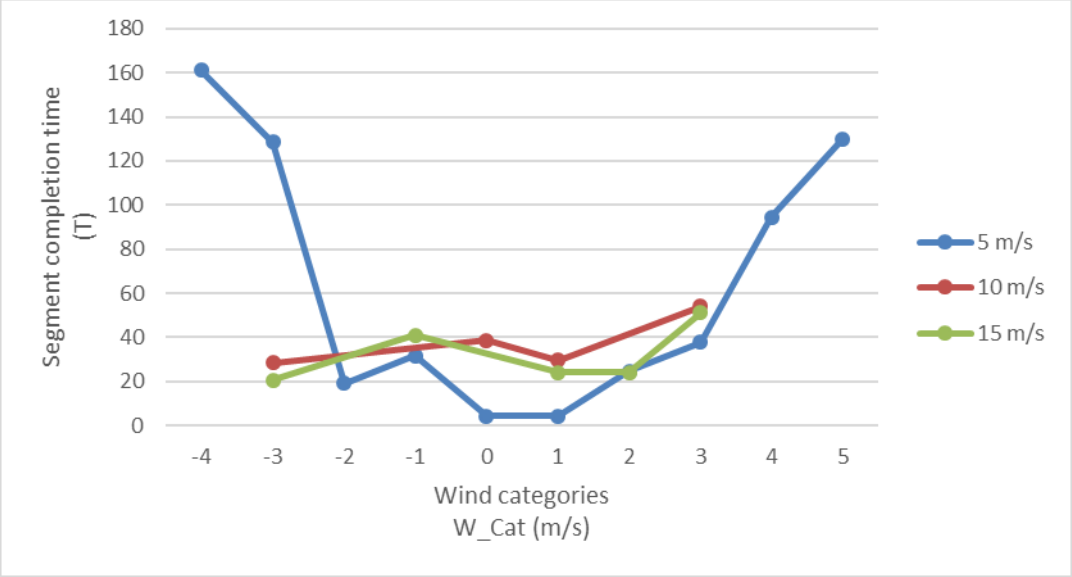


**Figure 5-14: Means plot for Time - All flight segments split by speed**

The means plot for 5 m/s confirms the same phenomena observed as in the effect sizes, showing a larger practical significance when wind categories are largely positive or largely negative. Therefore, the means plot for the 5 m/s flights indicates that there is a non-linear relationship between the wind speed categories and the time it takes to complete a flight segment.

### 5.9.3 Time - RL250 split by speed

This analysis is performed on the RL250 experiment types split by the speed of the experiment (10 m/s and 15 m/s). This analysis is similar to the previous analysis, except that only the segments of RL250 experiments are considered with the time standardised to 200 m segments. The total time taken to complete the segment standardised to 200 m (T_Std200) and average wind speed categories (W_Cat) are used for this analysis. Firstly a Spearman correlation is performed to determine the degree of association grouped by the different flight speeds as provided in Table 5-24.

| | Speed (m/s) | | | W_Cat |
|---|---|---|---|---|
| **Spearman's rho** | 10 | T_Std200 | Correlation Coefficient | 0.020 |
| | | | Sig. (2-tailed) | 0.944 |
| | | | N | 15 |
| | 15 | T_Std200 | Correlation Coefficient | .882* |
| | | | Sig. (2-tailed) | 0.020 |
| | | | N | 6 |
| *. Correlation is significant at the 0.05 level (2-tailed). | | | | |

**Table 5-24: Correlation for Time - RL250 split by speed**

The relationship between the standardised segment completion time (T_Std200) and the wind categories (W_Cat) is statistically significant for flight speeds of 15 m/s with the correlation coefficient for flight speeds of 15 m/s showing a strong relationship (r = 0.882).

To analyse the variance between the different wind categories of the segment speeds, an analysis of variance (ANOVA) test is performed. The ANOVA p-values do not indicate a statistically significant difference in the wind speed categories of 10 m/s or 15 m/s flight speeds as neither of the p-values are larger than alpha (0.05), for the standardised completion time (T_Std200), as shown in Table 5-25.

| Speed (m/s) | | Sum of Squares | df | Mean Square | F | Sig. |
|---|---|---|---|---|---|---|
| **10** | Between Groups | 16.917 | 3 | 5.639 | 2.809 | 0.089 |
| | Within Groups | 22.080 | 11 | 2.007 | | |
| | Total | 38.997 | 14 | | | |
| **15** | Between Groups | 65.280 | 4 | 16.320 | 1.417 | 0.552 |
| | Within Groups | 11.520 | 1 | 11.520 | | |
| | Total | 76.800 | 5 | | | |

**Table 5-25: ANOVA's for Time - RL250 split by speed**

In order to establish where the difference between these wind categories of the different flight speeds is, Post Hoc tests are performed and effect sizes for the different flight speeds are calculated for the standardised completion time (T_Std200), as provided in Table 5-26.

| Speed (m/s) | W_Cat (m/s) | N | Mean | Std. Deviation | Std. Error | 95% Confidence Interval for Mean | | Effect size (from 0) |
|---|---|---|---|---|---|---|---|---|
| | | | | | | Lower Bound | Upper Bound | |
| **10** | -3 | 2 | 45.60 | 1.13 | 0.80 | 35.44 | 55.76 | **0.81** |
| | 0 | 10 | 44.40 | 1.47 | 0.47 | 43.35 | 45.45 | 0.00 |
| | 1 | 2 | 47.20 | 1.13 | 0.80 | 37.04 | 57.36 | **1.90** |
| | 3 | 1 | 43.20 | | | | | |
| | Total | 15 | 44.85 | 1.67 | 0.43 | 43.93 | 45.78 | |
| **15** | -3 | 2 | 32.80 | 3.39 | 2.40 | 2.31 | 63.29 | |
| | -1 | 1 | 32.80 | | | | | |
| | 1 | 1 | 38.40 | | | | | |
| | 2 | 1 | 38.40 | | | | | |
| | 3 | 1 | 40.80 | | | | | |
| | Total | 6 | 36.00 | 3.92 | 1.60 | 31.89 | 40.11 | |

**Table 5-26: Descriptives for Time - RL250 split by speed**

The Games-Howell Post Hoc tests could not be computed for any of the flight speeds, since both flight speeds had at least one wind category with fewer than two cases. The effect sizes (from 0) were calculated for all flight speeds that had at least one occurrence with a wind category of 0. The effect sizes for 10 m/s segments indicate a large practical significance; however, the data is sparsely populated, making it difficult to gauge the significance with the small amount of data available. The means plot of the different wind categories and time taken to complete segments at different flight speeds are provided in Figure 5-15.

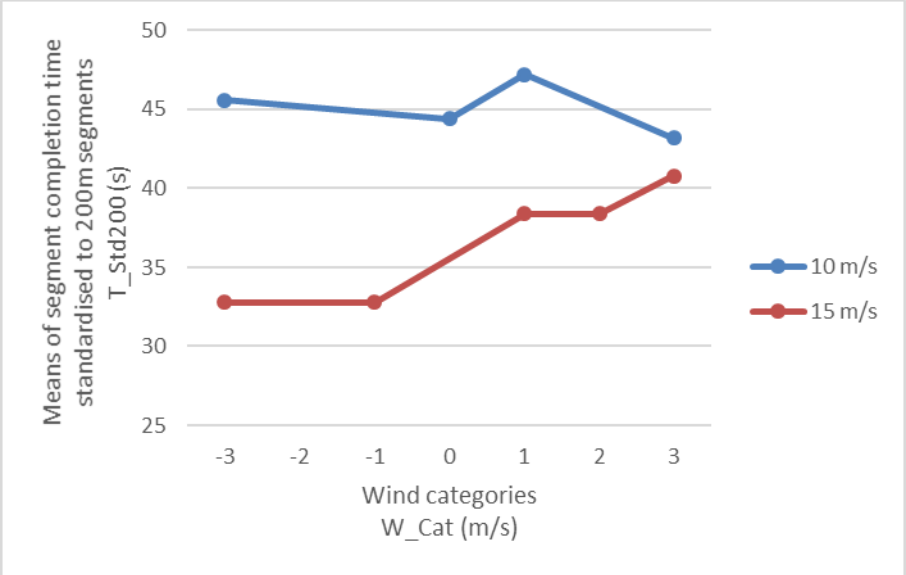


**Figure 5-15: Means plot for Time - RL250 split by speed with standardised times (T_Std200)**

The means plot for 10 m/s shows a negative linear relationship, whereas that for the 15 m/s shows a positive linear relationship. This again, is subject to the sparsely populated data for the time analysis. The scatter plot below is produced with the total time standardised to 200 m segments with the flight speed also standardised to 5 m/s in order to have a comparable scatter plot of the RL250 population by flight speed.

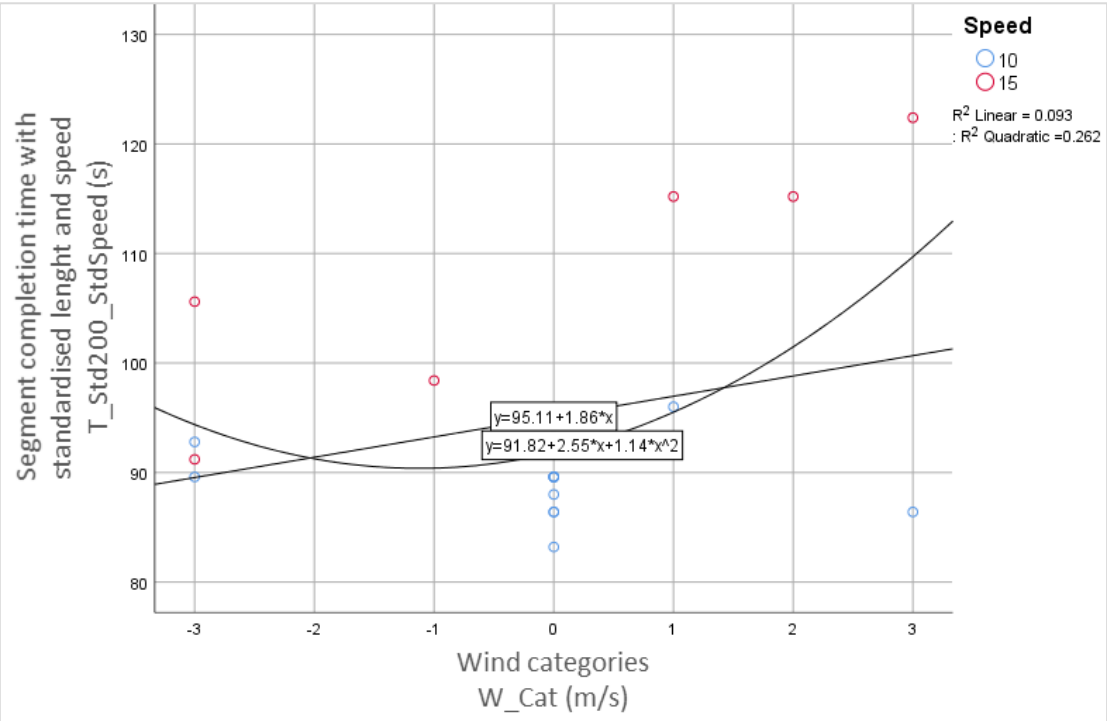


**Figure 5-16: Scatter plot for Time - RL250 split by speed with standardised time and speed (T_Std200_StdSpeed)**

The scatter plot is fitted with a $R^2$ linear line, describing only 9.3% of the variance observed, whereas the $R^2$ quadratic line describes the variance by 26.2%. This indicates that the time analysis of RL250 experiments also show more of a non-linear relationship than a linear relationship that was similarly observed in the previous section, indicated by the means plot shown in Figure 5-15.

### 5.9.4 Time - RL400 and RL250 split by waypoint specification

This analysis is performed on the RL400 and RL250 experiment types to calculate the difference between normally specified waypoints that are far apart and sub-waypoint specification. As described previously, the segment completion time analysis data is sparsely populated, therefore the RL250 experiments that does not contain sub-waypoints are included to have more data for the analysis. The total time taken to complete the segment standardised to 200 m segments that

are also standardised to 5 m/s flight speeds (T_Std200_StdSpeed), along with the average wind speed categories (W_Cat) are used for this analysis. Firstly, a Spearman correlation is performed to determine the degree of association.

| Analysis type | SubWay | | | W_Cat |
|---|---|---|---|---|
| **Spearman's rho** | No | T_Std200_StdSpeed | Correlation Coefficient | 0.039 |
| | | | Sig. (2-tailed) | 0.853 |
| | | | N | 25 |
| | Yes | T_Std200_StdSpeed | Correlation Coefficient | 0.629 |
| | | | Sig. (2-tailed) | 0.051 |
| | | | N | 10 |

**Table 5-27: Correlation for Time - RL400 and RL250 split by waypoint specification**

The relationship between the standardised segment completion time (T_Std200_StdSpeed) and the wind categories (W_Cat) does not seem to be statistically significant, although the correlation coefficient for sub-waypoints shows a strong relationship (r = 0.629). To analyse the variance among the different wind categories, an analysis of variance (ANOVA) test is performed for the standardised segment completion time (T_Std200_ StdSpeed).

| SubWay | | Sum of Squares | df | Mean Square | F | Sig. |
|---|---|---|---|---|---|---|
| **No** | Between Groups | 797.668 | 6 | 132.945 | 1.257 | 0.325 |
| | Within Groups | 1903.365 | 18 | 105.743 | | |
| | Total | 2701.034 | 24 | | | |
| **Yes** | Between Groups | 2034.225 | 7 | 290.604 | 2.612 | 0.305 |
| | Within Groups | 222.500 | 2 | 111.250 | | |
| | Total | 2256.725 | 9 | | | |

**Table 5-28: ANOVA's for Time - RL400 and RL250 split by waypoint specification**

The ANOVA p-values in Table 5-28 indicate that there is no statistically significant difference in the wind speed categories since $p > \alpha$ (0.05). Descriptive statistics and effect sizes can also be calculated to ascertain if some practical significance exists within this particular set of data for the standardised segment completion time (T_Std200_ StdSpeed), as provided in Table 5-29.

| SubWay | W_Cat (m/s) | N | Mean | Std. Deviation | Std. Error | 95% Confidence Interval for Mean | | Effect size (from 0) |
|---|---|---|---|---|---|---|---|---|
| | | | | | | Lower Bound | Upper Bound | |
| **No** | -3 | 5 | 93.24 | 7.23 | 3.24 | 84.26 | 102.22 | **0.61** |
| | -2 | 1 | 82.00 | | | | | |
| | -1 | 1 | 98.40 | | | | | |
| | 0 | 10 | 88.80 | 2.95 | 0.93 | 86.69 | 90.91 | 0.00 |
| | 1 | 3 | 101.33 | 12.12 | 6.99 | 71.24 | 131.43 | **1.03** |
| | 2 | 3 | 94.07 | 18.36 | 10.60 | 48.45 | 139.68 | 0.29 |
| | 3 | 2 | 104.40 | 25.46 | 18.00 | -124.31 | 333.11 | **0.61** |
| | Total | 25 | 93.18 | 10.61 | 2.12 | 88.80 | 97.56 | |
| **Yes** | -4 | 1 | 80.50 | | | | | |
| | -3 | 1 | 103.50 | | | | | |
| | -2 | 1 | 83.50 | | | | | |
| | -1 | 1 | 98.00 | | | | | |
| | 2 | 2 | 83.00 | 1.41 | 1.00 | 70.29 | 95.71 | |
| | 3 | 1 | 105.00 | | | | | |
| | 4 | 2 | 94.50 | 14.85 | 10.50 | -38.92 | 227.92 | |
| | 5 | 1 | 130.00 | | | | | |
| | Total | 10 | 95.55 | 15.83 | 5.01 | 84.22 | 106.88 | |

**Table 5-29: Descriptives for Time - RL400 and RL250 split by waypoint specification**

The Games-Howell Post Hoc tests could not be computed, since both normal and sub-waypoint flights had at least one wind category with fewer than two cases. The effect sizes (from 0) were calculated for all flight speeds that had at least one occurrence with a wind category of 0. The effect sizes for normally specified waypoints indicate a large practical significance for negative, as well as positive wind categories; however, as described previously, the data is sparsely populated, making it difficult to gauge the significance with the small amount of data available. The means plot of the different wind categories and standardised time taken to complete segments at different waypoint specifications is provided in Figure 5-17, showing a large time increase in wind category 5 for sub-waypoint specification, but only indicated by a single data point.

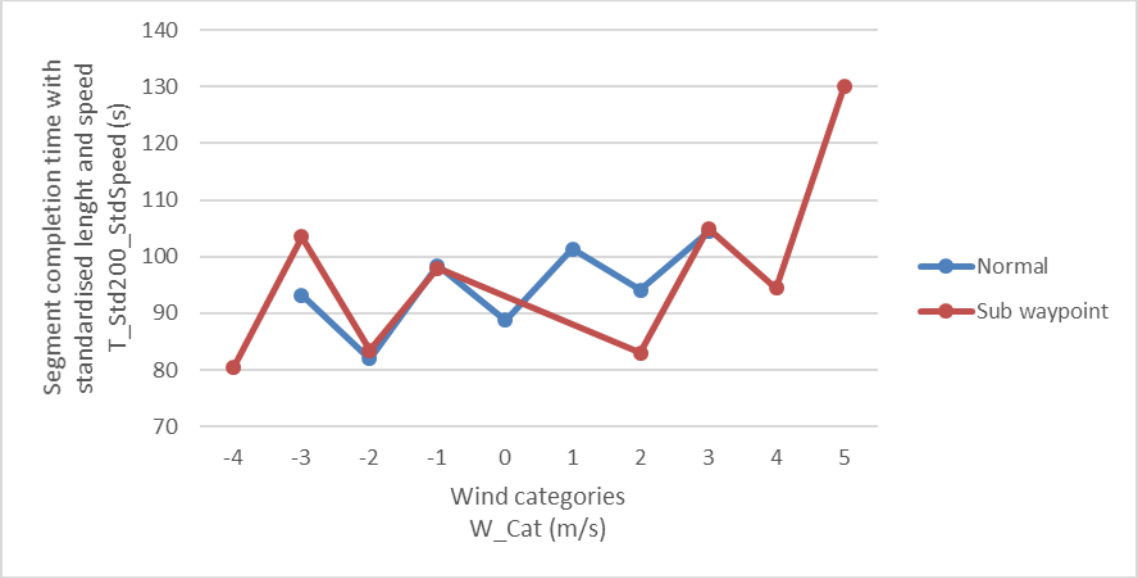


**Figure 5-17: Means plot for Time - RL400 and RL250 split by waypoint specification with standardised time and speed (T_Std200_StdSpeed)**

The scatter plot below is produced with the total time standardised to 200 m segments with the flight speed also standardised to 5 m/s in order to have a comparable population for the scatter plot by waypoint specification.

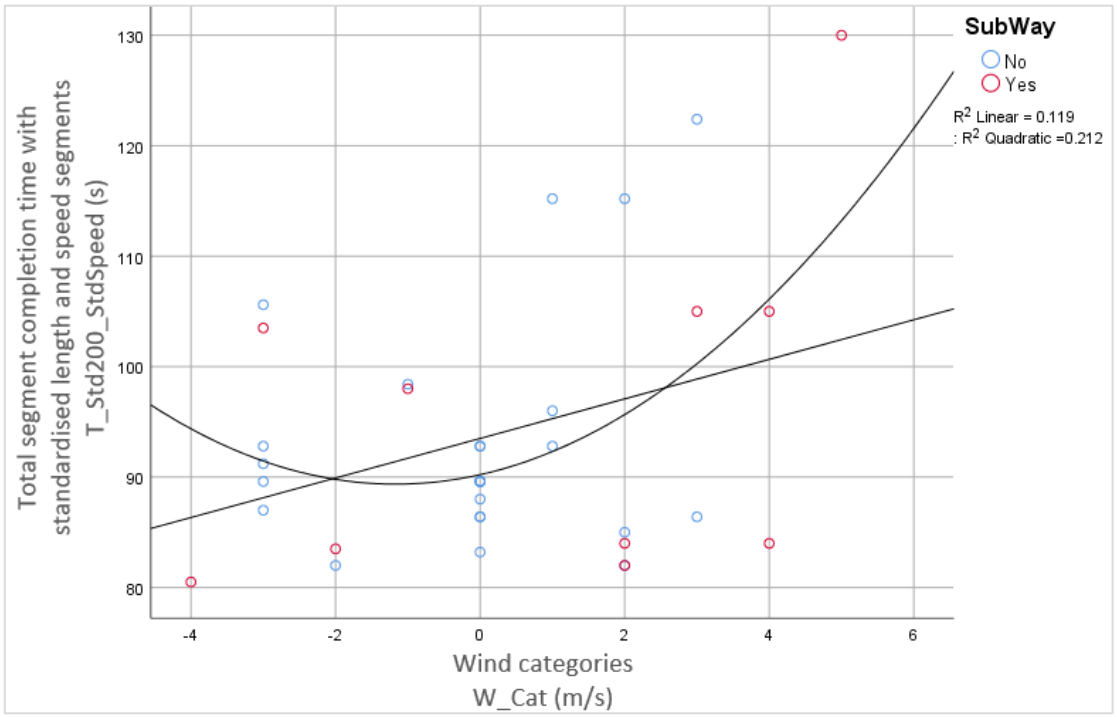


**Figure 5-18: Scatter plot for Time - RL400 and RL250 split by waypoint specification with standardised time and speed (T_Std200_StdSpeed)**

The scatter plot is fitted with a $R^2$ linear line, describing 11.9% of the variance observed, whereas the $R^2$ quadratic line describes the variance by 21.2%. This indicates that the time analysis for these experiments also shows more of a non-linear relationship than a linear relationship that was similarly observed in the previous time analysis sections.

## 5.10 Analysis of deviation during hover (Hover)

This analysis is performed to determine if there is a correlation between the wind and the deviation observed when hovering during UAS flights. The total deviation observed during a hover segment is used, along with the average wind speed during that segment to determine if the wind influences these hover segments, and to what extent the deviation observed when hovering can be explained by the influence of wind.

| Section | Analysis | Description | Reason |
|---|---|---|---|
| **5.10.1** | Hover | All flight segments with S&T | Overall view of deviation during hover segments |
| **5.10.2** | Hover | All flight segments with S&T split by hover duration | View of deviation during longer hover segments |

**Table 5-30: Overview of deviation during hover analysis**

An overview of the deviation during hover analysis is provided in Table 5-30. This table contains a brief outline of each analysis for reference, whereby a more detailed description is provided in the associated subsections of each.

### 5.10.1 Hover - All flight segments with S&T

This analysis is performed on all experiment types that contain hover segments (RL400, RL250, and RH) and makes use of the stop and turn (S&T) waypoint approach strategy to determine if the wind speed is related to the deviation during a hover segment. The total deviation (D) and average wind speed categories (W_Cat) are used for this analysis. Firstly, a Spearman correlation is performed to determine the degree of association between them.

| | | | W_Cat |
|---|---|---|---|
| **Spearman's rho** | D | Correlation Coefficient | .314** |
| | | Sig. (2-tailed) | 0.006 |
| | | N | 74 |
| **. Correlation is significant at the 0.01 level (2-tailed). | | | |

**Table 5-31: Correlation for Hover - All flight segments with S&T**

The relationship between the total deviation (D) and average wind speed categories (W_Cat) is statistically significant at a 1% level with the correlation coefficient indicating a moderate relationship (r = 0.314). To analyse the variance among the different wind speed categories, an analysis of variance (ANOVA) test is performed for the total deviation (D).

| | Sum of Squares | df | Mean Square | F | Sig. |
|---|---|---|---|---|---|
| Between Groups | 150.669 | 5 | 30.134 | 2.593 | 0.033 |
| Within Groups | 790.254 | 68 | 11.621 | | |
| Total | 940.923 | 73 | | | |

**Table 5-32: ANOVA's for Hover - Hover - All flight segments with S&T**

The ANOVA p-value indicates a statistically significant difference in the wind speed categories, as the p-value of 0.033 is smaller than alpha ($p < 0.05$), as shown in Table 5-32. In order to determine where the difference between the wind categories is, Post Hoc tests are performed and effect sizes for the total deviation (D) are calculated, as provided in Table 5-33.

| W_Cat (m/s) | N | Mean | Std. Deviation | Std. Error | 95% Confidence Interval for Mean | | Effect size (from 0) |
|---|---|---|---|---|---|---|---|
| | | | | | Lower Bound | Upper Bound | |
| **0** | 31 | 1.40 | 2.20 | 0.39 | 0.59 | 2.20 | 0.00 |
| **1** | 13 | 2.16 | 2.01 | 0.56 | 0.95 | 3.38 | **0.35** |
| **2** | 12 | 0.90 | 0.34 | 0.10 | 0.68 | 1.11 | 0.23 |
| **3** | 12 | 4.16 | 6.68 | 1.93 | -0.08 | 8.40 | **0.41** |
| **4** | 5 | 5.75 | 5.13 | 2.29 | -0.62 | 12.11 | **0.85** |
| **5** | 1 | 1.14 | | | | | |
| **Total** | 74 | 2.19 | 3.59 | 0.42 | 1.36 | 3.02 | |

**Table 5-33: Descriptives for Hover - All flight segments with S&T**

The Games-Howell Post Hoc tests indicate that all wind categories differ from 0. The effect sizes (from 0) range from a medium practical significance to a large practical significance and indicate the tendency to be larger at higher wind speeds for all flights that contained hover segments where the UAV had to stop and turn (S&T). The increasing effect sizes indicate that the deviation tends to be larger at higher wind speeds and has a significant effect in practice.

The means plot of the different wind categories and the total deviation during hover segments is presented in Figure 5-19 below, also showing the increase in deviation with larger wind speed

categories. Wind category 5 only has a single data point, making it difficult to gauge the difference, but by viewing the trend observed by all the other categories, the trend seems to be positive.

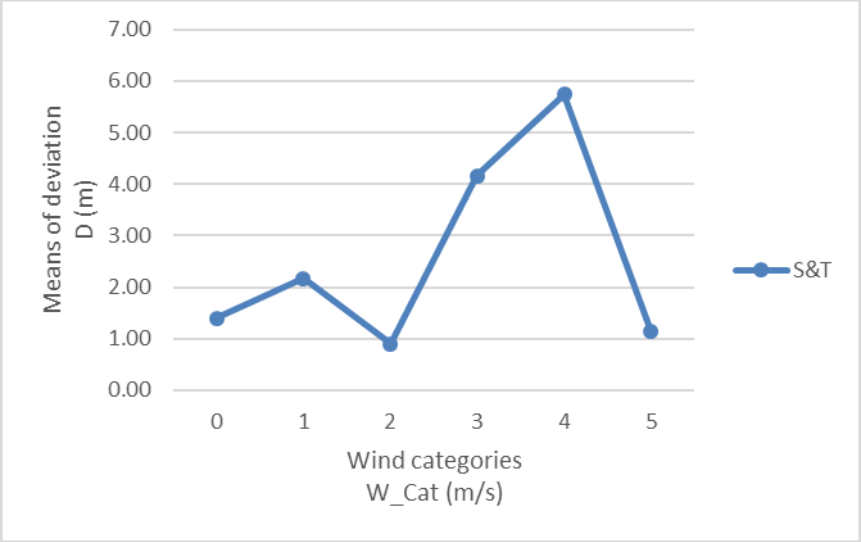


**Figure 5-19: Means plot for Hover - All flight segments with S&T**

The scatter plot provided in Figure 5-20 provides an overall view of the data. The scatter plot is fitted with a $R^2$ linear line, describing only 8.2% of the variance observed, which is not significantly indicative.

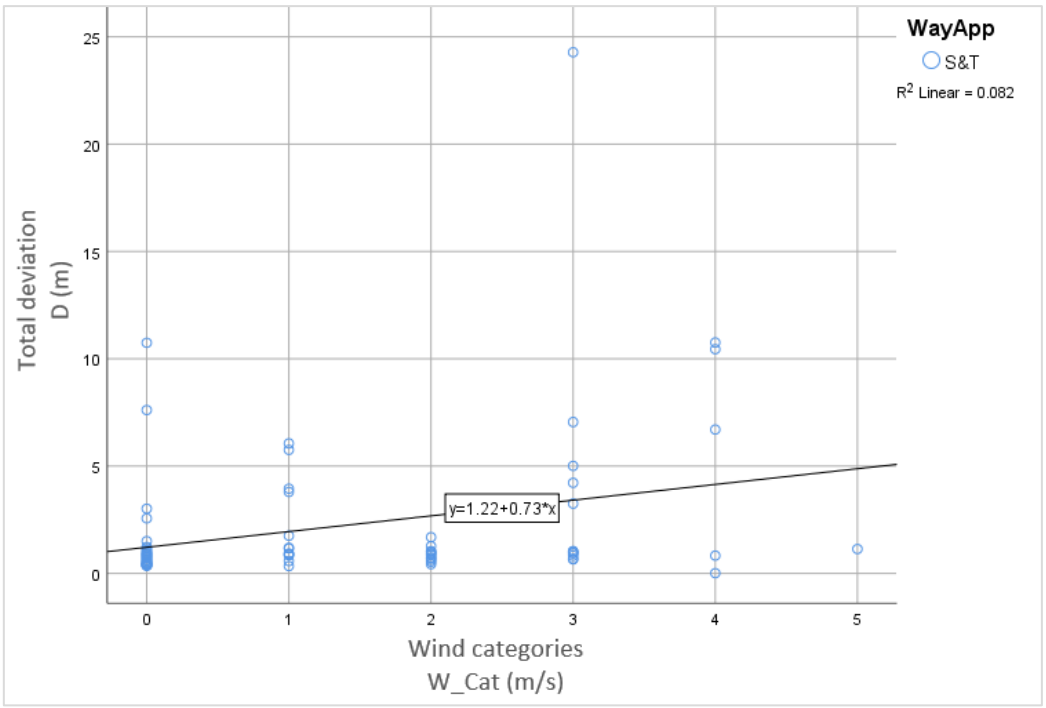


**Figure 5-20: Scatter plot for Hover - All flight segments with S&T**

### 5.10.2 Hover - All flight segments with S&T split by hover duration

This analysis is performed on all experiment types that contain hover segments (RL400, RL250, and RH) using the stop and turn (S&T) waypoint approach strategy to determine if the wind speed is related to the deviation during a hover segment, split by the duration of the hover segment. The total deviation (D) and average wind speed categories (W_Cat) are used for this analysis. Firstly, a Spearman correlation is performed to determine the degree of association.

| Analysis type | Wait (s) | | | W_Cat |
|---|---|---|---|---|
| **Spearman's rho** | 0 | D | Correlation Coefficient | 0.227 |
| | | | Sig. (2-tailed) | 0.084 |
| | | | N | 59 |
| | 10 | D | Correlation Coefficient | 0.011 |
| | | | Sig. (2-tailed) | 0.969 |
| | | | N | 15 |

**Table 5-34: Correlation for Hover - All flight segments with S&T split by hover duration**

The relationship between the total deviation (D) and the wind speed categories (W_Cat) during hover segments split by the duration of the hover does not seem to be statistically significant, although the correlation coefficient for not waiting shows a moderate relationship (r = 0.227). To analyse the variance between the different wind categories, an analysis of variance (ANOVA) test is performed for the total deviation (D).

| Wait (s) | | Sum of Squares | df | Mean Square | F | Sig. |
|---|---|---|---|---|---|---|
| **0** | Between Groups | 0.131 | 5 | 0.026 | 0.105 | 0.991 |
| | Within Groups | 13.267 | 53 | 0.250 | | |
| | Total | 13.399 | 58 | | | |
| **10** | Between Groups | 41.413 | 3 | 13.804 | 0.387 | 0.765 |
| | Within Groups | 392.723 | 11 | 35.702 | | |
| | Total | 434.135 | 14 | | | |

**Table 5-35: ANOVA's for Hover - Hover - All flight segments with S&T**

The ANOVA p-values in Table 5-35 indicate that there is no statistically significant difference in the duration of a hover segment since both p-values are larger than alpha (0.05). Descriptive statistics and effect sizes can be calculated to determine if some practical significance exists within this particular set of data for the total deviation (D).

| Wait (s) | W_Cat (m/s) | N | Mean | Std. Deviation | Std. Error | 95% Confidence Interval for Mean | | Effect size (from 0) |
|---|---|---|---|---|---|---|---|---|
| | | | | | | Lower Bound | Upper Bound | |
| **0** | 0 | 29 | 0.86 | 0.61 | 0.11 | 0.63 | 1.09 | 0.00 |
| | 1 | 9 | 0.95 | 0.40 | 0.13 | 0.65 | 1.26 | 0.15 |
| | 2 | 12 | 0.90 | 0.34 | 0.10 | 0.68 | 1.11 | 0.06 |
| | 3 | 7 | 0.87 | 0.15 | 0.06 | 0.73 | 1.02 | 0.02 |
| | 4 | 1 | 0.83 | | | | | |
| | 5 | 1 | 1.14 | | | | | |
| | Total | 59 | 0.89 | 0.48 | 0.06 | 0.76 | 1.01 | |
| **10** | 0 | 2 | 9.18 | 2.22 | 1.57 | -10.72 | 29.08 | 0.00 |
| | 1 | 4 | 4.89 | 1.18 | 0.59 | 3.01 | 6.77 | **1.94** |
| | 3 | 5 | 8.76 | 8.79 | 3.93 | -2.15 | 19.67 | 0.05 |
| | 4 | 4 | 6.98 | 5.00 | 2.50 | -0.97 | 14.93 | **0.44** |
| | Total | 15 | 7.31 | 5.57 | 1.44 | 4.23 | 10.39 | |

**Table 5-36: Descriptives for Hover - All flight segments with S&T**

The Games-Howell Post Hoc tests could not be computed for S&T hover segments that do not wait 10 seconds, since at least one wind category had fewer than two cases. The effect sizes (from 0) were calculated for all flight speeds that had at least one occurrence with a wind category of 0. The effect sizes are shown to have medium and large practical significance levels at some wind category; however, no trend in the effect sizes is observed and as described previously, the data is sparsely populated, making it difficult to gauge the significance with the small amount of available data.

The means plot of the different wind categories and total deviation during hover segments with S&T waypoint approach strategies is provided in Figure 5-21 on the next page. The means plot indicates that the deviation during hovering segments is generally higher when hovering for longer time periods. However, the wind speed categories show no clear trend as to how it affects the hovering segment which may also be due to the sparsely populated data available to analyse hover segments.

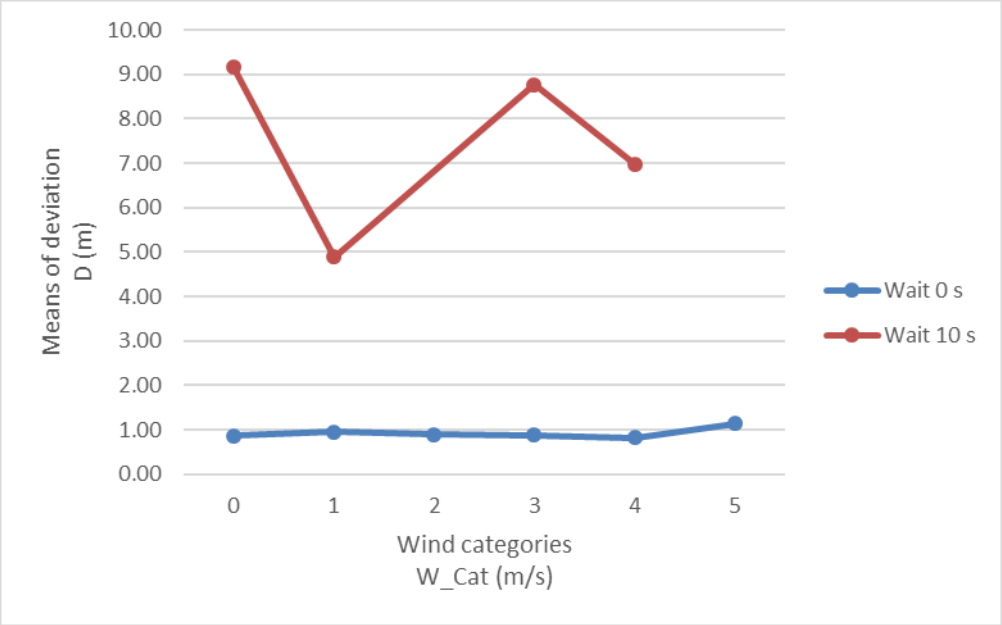


**Figure 5-21: Means plot for Hover - All flight segments with S&T**

## 5.11 Results summary

In this chapter, a description was provided of the consolidation, segmentation, calculations and translations performed on the data obtained from the four different experiment types and variations of those experiments. Statistical techniques used to analyse the experimental data in this study were discussed, along with a detailed description of how these techniques were applied in obtaining the experimental results of the deviation left and right perpendicular to the flight plane, of the completion time of particular flights and of the deviation observed during hover segments.

In the next chapter, a brief summary, discussion and interpretation of the results obtained in this section are presented. The discussion of the results reviews and discusses the practical impact of the results, how UAS task automation was influenced and an attempt is made to provide recommendations for conducting UAS flights in windy conditions.

# CHAPTER 6 – DISCUSSION AND CONCLUSION

*A brief summary of the research, methods and implementation of the study, as well as a discussion and interpretation of the results, what implications these results have on UAS task automation in dynamic environments and opportunities for future work.*

## 6.1 Introduction

With the exponential advancement of UAS technology and improved capability, UASs have gained popularity ranging from recreational to professional purposes. UASs are used for various applications such as agriculture, exploration and mapping, safety and security, as well as disaster and emergency management. The driving force behind the increased commercial interests in UASs is the simplification of tasks and the usefulness in diverse fields for data collection, including image and video collection. Therefore, as described in Section 1.1, specialists are predominantly interested in gathering data for a specific task or field of application rather than in the chore of flying safely and as required.

With the focus on gathering data for the various applications or tasks and the limited availability of trained operators, the need for the autonomous UAS flight emerged as described in Section 3.2.4 in order to alleviate the demanding task of flying safely and as required. The concern, however, is that most UAS tasks are conducted in dynamic, real-world environments where various factors may influence the UAS flight. An investigation into the main factors influencing UAS task automation was performed in Section 3.3 where the factors identified included communications interference, air density, temperature, precipitation, fog and humidity, with the most influential factor identified in literature to be the effect of wind on UAS flight.

Since wind is identified as the most significant factor, the aim is to determine the extent of the effect of wind on UAS task automation by performing various experiment types to demonstrate and support the claim. The experimental setup and design were described in Chapter 4, providing a description of all the relevant hardware and software used, the process followed to conduct these experiments, as well as a description of the unique experiment types conducted with the available equipment to support this study. The unique experiment types were discussed in Section 4.6, which included straight flights of different lengths, performing sharp turns in several directions, as well as circular flights. Several variations on the experiments were performed that included providing sub-waypoints, different waypoint approach strategies, and height, speed and orientation specifications, as discussed in Section 4.6.

The data obtained from the conducted experiments were analysed in Sections 5.8, 5.9, and 5.10 by making use of exploratory statistical techniques to obtain descriptive results of the experiments in order to determine whether the influence of wind on UAS task automation is apparent. The deviations observed were identified to be related to measured wind speeds during experiments.

Furthermore, the purpose was to determine the extent of the effect of wind on UAS task automation through the analysis of the experimental data that was presented in the previous chapter. A summary of the findings is provided in the next section, followed by concluding statements and recommendations on how to perform UAS tasks in windy environments, based on the results obtained from this study.

## 6.2 Summary of findings

The statistical analysis of the data obtained from the experiments was performed in the previous chapter. The analysis included an investigation into the deviation left and right perpendicular to the flight plane, an analysis of the completion time of particular flights and an analysis of the deviation observed during hover segments. From the analysis performed, various important effects and relationships to the measured wind speeds and components have been highlighted and the most important aspects of each are discussed in the subsections below.

### 6.2.1 Perpendicular deviation discussion

The perpendicular deviation analysis was performed in Section 5.8 to determine if there was a correlation between the wind and the deviation left and right from the UAS flight path. The wind component perpendicular to the flight path was calculated and used in order to determine if the wind influenced the UAS flight path, and to what extent the deviation observed in the flight path could possibly be explained by the influence of wind.

The combined analysis which included data from all experiment types, in order to have an overview of the experiments, provided evidence that there was an increase in the deviation observed at higher wind speeds. Although this trend in the deviation was also observed at lower wind speeds, the deviation only became practically significant at wind speeds of 4 m/s and higher. This meant that higher wind speeds have a significant effect that will cause the UAS to drift off its intended flight path thereby opening the possibility for collisions to occur or inaccurate data to be collected if not compensated for or taken into consideration.

The deviations of all experiments were individually compared to the wind speeds and according to this comparison, all individual experiments showed a trending increase in the deviation with an increase in wind speeds. This was most evident in the RL250 and RL400 experiments, since they

were performed during higher wind speeds, clearly showing the extent of the trending effect. The RL250 experiments indicated the largest deviations between different wind speed categories which may be caused by generally faster flight speeds that were specified for this type of experiment. This observation lead to the investigation and analysis of all UAS flights conducted at different flight speeds.

All flight speeds were analysed, which indicated that flight speeds of 15 m/s showed a strong relationship; however, the trend of an increased deviation with higher wind speeds was also observed with faster specified flight speeds. This trend was clearly identified when comparing the practical significance between the 5 m/s and 15 m/s flight speeds where the mean deviation was observed to be much higher at faster flight speeds. Experiments conducted at a flight speed of 5 m/s had a mean deviation of 0.22 m, whereas flights conducted at 15 m/s flight speeds had a mean deviation of 0.59 m as indicated in Table 5-14. This signified that slower flight speeds are less affected by an increase in wind speeds than flights performed at faster specified flight speeds. This observation identified that UAS task automation should consequently be performed at slower flight speeds for more accurate performance, since smaller deviations can be expected.

The specification of sub-waypoints for long flight segments showed no distinguishable difference to normally specified waypoints, further supported by the effect sizes that were scattered, showing no clear trend between wind speed categories for different waypoint specifications. Although this was the case, the same trend in deviations was identified as before, where the means plot showed an increase in the deviation observed when there was an increase in the wind speeds.

### 6.2.2 Completion time discussion

The completion time analysis was performed in Section 5.9 to determine if a correlation exists between the wind speed and the time it takes to complete a UAS flight path or segment. The total time taken to complete segments, along with the wind speed component in the direction of the flight path were used to determine if the wind influenced the UAS flight times, and to what extent the time taken to complete a flight path or flight segment could be explained by the influence of wind.

The Spearman correlations showed that only longer flight segments indicated a moderate to strong relationship between the wind speeds and the time taken to complete a flight segment. Effect sizes, however, showed that there was a definite practical significance in both positive and negative wind speed components, when wind is blowing against or in the direction of travel, negatively affecting the time taken to complete a flight segment. This was most confidently

reported with the results of the 10 m segments since they had the most data to confirm this phenomenon. Although there is a significant variation in the wind speeds, the observation is not unquestionably indicative because of the sparsely populated data making estimates difficult.

All flight segments performed at different flight speeds (5, 10, and 15 m/s) were investigated where an increase in the strength of the relationship between the wind speed categories and the time taken to complete a flight segment was identified as flight speeds increased. The effect sizes also showed that the speed of the UAS flight had a significant practical effect on the time taken to complete flight segments in both positive and negative winds speed components. This observation meant that the speed at which UAS flight was performed had an effect on the time it took to complete a flight segment which seemed quite obvious; however, there was no negative linear relationship observed as logically expected. The variation observed between the relationship of the wind and time taken to complete segments was associated with a non-linear relationship rather than a linear relationship as was shown in the means plot provided in Figure 5-14, specifically for experiments performed at 5 m/s flight speeds. The analysis showed that the time taken to complete segments was negatively affected with negative wind speeds (winds against the direction of travel) and also negatively affected with positive wind speeds (winds in the same direction of travel). This phenomenon supplemented the observation of the non-linear relationship and confirms that both positive and negative winds caused disturbances. These disturbances affected the time taken to complete flight segments negatively, and therefore significantly affect UAS task automation implementations in practice.

### 6.2.3 Hover discussion

The hover analysis was performed in Section 5.10 to determine if a correlation existed between the wind and the deviation observed when hovering during UAS flights. The total deviation observed during a hover segment was used along with the average wind speed during that segment to determine if the wind influenced these hover segments and to determine to what extent the deviation observed when hovering could be explained by the influence of wind.

The results of the analysis confirmed that there was a moderate correlation between the total deviation and the average wind speeds observed in all experiments that contained hover segments. Effect sizes indicated an increase in the practical significance as the wind speed increases. This meant that larger total deviations could be expected when hovering in windy conditions and an increase in wind speeds are associated with an increase in the total deviation during that hover segment.

A comparison of waiting time during hover segments was performed in which hover segments where the UAV simply had to turn into the direction of the next waypoint and continue, were compared to hovering in a specific location for 10 seconds before continuing to the next waypoint. There is no clear indication with waiting time analysis that higher wind speeds are related to larger deviations, only that larger deviations are related to longer hovering times. This comparison undoubtedly indicated that the total deviation observed during long hover segments were higher, as expected, than those where the UAV simply turned and continued to the next waypoint.

It is therefore evident that hovering during UAS flights can be expected to have a deviation; however, the deviation can be minimised by keeping the hovering duration as short as possible in order to not deviate as much, saving flight time and battery power for more important tasks.

### 6.3 Conclusions

This study investigated factors influencing UAS task automation in dynamic real-world environments. Several factors influencing UAS flight and communications have been identified, including communications interference, air density, temperature, precipitation, fog and humidity, whereas the effect of wind was identified in literature as the most significant factor influencing the UAS task environment and therefore UAS task automation in dynamic environments.

In order to confirm this claim, an exploratory study was performed whereby various experiments were conducted in windy conditions. This study provided sufficient evidence with the results of the experiments to substantiate that the automated UAS flights conducted in this study were significantly affected by the influence of wind. The results of the analysis of perpendicular deviation showed that higher wind speeds are related to larger deviations from the intended flight path. The largest mean deviation was approximately 0.9 m, observed in the straight flight segments at a wind speed of 4 m/s. This is, proportionally, not a large deviation, however, when automated tasks that require precision flights are performed, this deviation will have a significant effect.

There was an increase in the time taken to complete flight segments in the presence of wind. It was expected that the time taken to complete flight segments would decrease with wind blowing in the direction of travel and that the time taken would increase with the wind blowing against the direction of travel. However, this was not the case. There was an increase in the time taken to complete flight segments whether the wind blew against the direction of travel or even in the same direction of travel. Therefore, the presence of wind caused the individual segments to take longer, therefore the entire UAS flight took longer because of the disturbance of wind. It seems as if this could be due to the UAV constantly trying to stabilise for the perceived wind.

Hovering during automated UAS flight had a significant influence on the deviation observed. The total deviation observed during long, 10 s, hover segments was much higher (7.31 m) than that where the UAV simply turned and continued to the next waypoint (0.89 m), as shown in Table 5-36. In automated UAS tasks where hover segments are necessary, the duration of hover segments should therefore be kept to a minimum.

When performing automated UAS tasks in windy environments where precision is important, crosswinds will influence the flight path depending on the wind speed, the time taken to complete flight segments will increase, and hover segments will significantly influence the total deviation observed during the UAS flight. Therefore, for precision UAS tasks, it is recommended to make use of UASs equipped with sensors to assist in compensating for the influence of wind, or UASs specifically designed to operate in windy environments.

### 6.4 Future work

Possible future work would be to collect more data to not only determine the wind drift angle after the analysis of flight data, but to determine the possibility of deviations and predict the drift angle, based on historical data in order to recommend a wind correction angle (crab angle) before conducting the flight to be able to compensate for possible deviations in the planned flight.

Another aspect related to the wind, is to not only compensate for wind disturbances, but also to be able to inform the operator or automated system prior to performing the flight that the wind speeds are high compared to the limits of the specific UAV used, and how much the UAV is likely to deviate from the objective in these conditions. This could then be supplemented with a simulation showing the predicted flight path with the affecting wind condition and recommending flight speeds and waypoint approach strategies in order to minimise the deviation likely to occur. In the event that the wind conditions increase sharply and the UAS most likely will not be able to hold a steady position, the software could inform the operator that it is not safe to fly in the current conditions and that a collision or loss of control is most likely to occur.

# BIBLIOGRAPHY


Ackerman, E. and Strickland, E. 2018. Medical delivery drones take flight in east africa. *IEEE Spectrum,* 55(1):34-35.

Adams, S. M. and Friedland, C. J. 2011. A survey of unmanned aerial vehicle (UAV) usage for imagery collection in disaster research and management, (*In* 9th International Workshop on Remote Sensing for Disaster Response, Stanford University: Springer).

Adams, S. M., Levitan, M. L. and Friedland, C. J. 2014. High resolution imagery collection for post-disaster studies utilizing unmanned aircraft systems (UAS). *Photogrammetric Engineering & Remote Sensing,* 80(12):1161-1168.

Ameri, B., Meger, D., Power, K. and Gao, Y. 2009. UAS applications: Disaster & emergency management. (*In* American Society for Photogrammetry and Remote Sensing (ASPRS) Annual Conference, Baltimore, Maryland: Curran Associates, Inc., p. 45-55).

Ayhan, B., Kwan, C., Budavari, B., Larkin, J. and Gribben, D. 2018. Path planning for UAVs with engine failure in the presence of winds. (*In* IECON 2018-44th Annual Conference of the IEEE Industrial Electronics Society: IEEE, p. 3788-3794).

Belkhouche, F. 2009. Reactive path planning in a dynamic environment. *IEEE Transactions on Robotics,* 25(4):902-911.

Bellavia, L., Cinnirella, L., Roccato, P. E., Benedetto, F., Lombardi, A. and Quagliotti, F. 2015. Electromagnetic compatibility tests for multirotor UAS. (*In* 2015 International Conference on Unmanned Aircraft Systems (ICUAS): IEEE, p. 629-638).

Bender, D., Rouatbi, F., Schikora, M., Cremersy, D. and Koch, W. 2016. Scaling the world of monocular slam with ins-measurements for UAS navigation. (*In* 2016 19th International Conference on Information Fusion (FUSION): IEEE, p. 1493-1500).

Biradar, A. S. 2014. Wind estimation and effects of wind on waypoint navigation of UAVs. Arizona: Arizona State University. (Thesis - MSc).

Bohn, D. A. 1988. Environmental effects on the speed of sound. *Journal of the Audio Engineering Society,* 36(4):223-231.

Bouabdallah, S. 2007. Design and control of quadrotors with application to autonomous flying. Tlemcen: University of Abou Bakr Belkaïd. (Thesis - PhD).

Bouabdallah, S., Becker, M., Perrot, V. and Siegwart, R. 2007. Toward obstacle avoidance on quadrotors. (*In* Proceedings of the XII International Symposium on Dynamic Problems of Mechanics (DINAME): ABCM, p. 20-30).

Boucher, P. 2015. Domesticating the drone: The demilitarisation of unmanned aircraft for civil markets. *Science and engineering ethics,* 21(6):1393-1412.

Brandt, S., A. 2015. Small UAV design development and sizing. (*In* Valavanis, K.P. & Vachtsevanos, G.J. eds. Handbook of unmanned aerial vehicles. Dordrecht: Springer. p. 165-180).

Bryson, M. and Sukkarieh, S. 2009. Architectures for cooperative airborne simultaneous localisation and mapping. *Journal of Intelligent and Robotic Systems,* 55(4-5):267-297.

Burzichelli, C. D. 2016. Delivery drones: Will amazon air see the national airspace. *Rutgers Computer and Technology Law Journal,* 42(1):162-195.

Caplinger, T. W. 2015. Path planning and control of an autonomous quadrotor testbed in a cluttered environment. Morgantown: West Virginia University. (Thesis - MSc).

Casbeer, D. W., Kingston, D. B., Beard, R. W. and McLain, T. W. 2006. Cooperative forest fire surveillance using a team of small unmanned air vehicles. *International Journal of Systems Science,* 37(6):351-360.

Chapman, J. W., Reynolds, D. R., Mouritsen, H., Hill, J. K., Riley, J. R., Sivell, D., Smith, A. D. and Woiwod, I. P. 2008. Wind selection and drift compensation optimize migratory pathways in a high-flying moth. *Current Biology,* 18(7):514-518.

Chee, K. Y. and Zhong, Z. W. 2013. Control, navigation and collision avoidance for an unmanned aerial vehicle. *Sensors and Actuators A: Physical,* 190(2013):66-76.

Chopde, N. R. and Nichat, M. 2013. Landmark based shortest path detection by using a* and haversine formula. *International Journal of Innovative Research in Computer and Communication Engineering,* 1(2):298-302.

Cione, J., Kalina, E., Uhlhorn, E., Farber, A. and Damiano, B. 2016. Coyote unmanned aircraft system observations in hurricane edouard (2014). *Earth and Space Science,* 3(9):370-380.

Clothier, R. A., Walker, R. A., Fulton, N. and Campbell, D. A. 2007. A casualty risk analysis for unmanned aerial system (UAS) operations over inhabited areas, (*In* 2nd Australasian Unmanned Air Vehicles Conference, Melbourne, Australia).

Clough, B. T. (2002) *Metrics, schmetrics! How the heck do you determine a uav's autonomy anyway*, Ohio: Air Force Research Laboratory (AFRL) Wright-Patterson Air Force Base.

Dalamagkidis, K. 2015a. Aviation history and unmanned flight. (*In* Valavanis, K.P. & Vachtsevanos, G.J. eds. Handbook of unmanned aerial vehicles: Springer. p. 57-81).

Dalamagkidis, K. 2015b. Definitions and terminology. (*In* Valavanis, K.P. & Vachtsevanos, G.J. eds. Handbook of unmanned aerial vehicles: Springer. p. 43-55).

Dapper e Silva, T., Cabreira, V. and de Freitas, E. 2018. Development and testing of a low-cost instrumentation platform for fixed-wing UAV performance analysis. *Drones,* 2(2):19-32.

Davis_Instruments. 2019. Davis Vantage Vue. https://www.davisinstruments.com/solution/vantage-vue/ Date of access: 5 Nov. 2019.

DJI. 2016. Phantom 3 Professional user manual. https://dl.djicdn.com/downloads/phantom_3/en/Phantom+3+Professional+User+Manual+v1.8_en_20160719.pdf Date of access: 11 Dec. 2016.

DJI. 2017. Inspire 2 user manual. https://dl.djicdn.com/downloads/inspire_2/20171013/INSPIRE_2_User_Manual_EN.pdf Date of access: 2 Jan. 2018.

FAA. 2016. Pilot's handbook of aeronautical knowledge. Oklahoma City: United States Department of Transportation, Federal Aviation Administration.

Fabra, F., Calafate, C. T., Cano, J.-C. and Manzoni, P. 2017. On the impact of inter-UAV communications interference in the 2.4 ghz band. (*In* 2017 13th International Wireless Communications and Mobile Computing Conference (IWCMC): IEEE, p. 945-950).

Fern, L. and Shively, R. J. 2009. A comparison of varying levels of automation on the supervisory control of multiple UASs. (*In* Proceedings of AUVSI's Unmanned Systems North America, Washington, DC: s.n., p. 10-13).

Ganti, S. R. and Kim, Y. 2015. Design of low-cost on-board auto-tracking antenna for small UAS. (*In* 2015 12th International Conference on Information Technology-New Generations: IEEE, p. 273-279).

Gärtner, J. and Johansson, P. 2017. An adaptive control system based on pid, i2pd and rls, a simulated design for UAVs. Västerås, Sweden: Mälardalen University. (Thesis - MSc).

Gerber, A. S. and Green, D. P. 2008. Field experiments and natural experiments. (*In* The oxford handbook of political science: Oxford University Press. p. 1109-1132).

Goodrich, M. A., Morse, B. S., Gerhardt, D., Cooper, J. L., Quigley, M., Adams, J. A. and Humphrey, C. 2008. Supporting wilderness search and rescue using a camera-equipped mini UAV. *Journal of Field Robotics,* 25(1):89-110.

Grenzdörffer, G., Engel, A. and Teichert, B. 2008. The photogrammetric potential of low-cost UAVs in forestry and agriculture. *The International Archives of the Photogrammetry, Remote Sensing and Spatial Information Sciences,* 31(B3):1207-1214.

Guo, Z. and Sheffield, J. 2008. A paradigmatic and methodological examination of knowledge management research: 2000 to 2004. *Decision Support Systems,* 44(3):673-688.

Gutierrez, R. M., Yu, H., Rong, Y. and Bliss, D. W. 2017. Time and frequency dispersion characteristics of the UAS wireless channel in residential and mountainous desert terrains. (*In* 2017 14th IEEE Annual Consumer Communications & Networking Conference (CCNC), Las Vegas: IEEE, p. 516-521).

Hevner, A. and Chatterjee, S. 2010. Design science research in information systems. (*In* Design research in information systems: Theory and practice. Boston: Springer. p. 9-22).

Hofstee, E. 2006. Constructing a good dissertation: A practical guide to finishing a Master's, MBA or PhD on schedule. Johannesburg, South Africa: EPE.

Huang, H.-M., Commerce, D.o. (2004) *Terminology for specifying the autonomy levels for unmanned systems: Version 1.0.* U.S.: National Institute of Standards and Technology (NIST).

Jia, Y., Tu, X., Yan, W., Wang, E., Zhao, Y. and Ding, S. 2019. Study on the influence of electromagnetic pulse on UAV communication link. *American Journal of Electrical and Electronic Engineering,* 7(2):42-48.

Jordan, B. R. 2015. A bird's-eye view of geology: The use of micro drones/UAVs in geologic fieldwork and education. *GSA Today,* 25(7):50-52.

Lee, B., Park, P. and Kim, C. 2015. Power managements of a hybrid electric propulsion system powered by solar cells, fuel cells, and batteries for UAVs. (*In* Valavanis, K.P. & Vachtsevanos, G.J. eds. Handbook of unmanned aerial vehicles: Springer. p. 495-524).

Leong, C. 2015. Eye in the sky. https://issuu.com/wendymaritz/docs/nsri-sea-rescue-autumn-2015 Date of access: 1 Nov 2015.

Leuchter, J. and Bauer, P. 2015. Capacity of power-batteries versus temperature. (*In* 2015 17th European Conference on Power Electronics and Applications, Geneva, Switzerland: IEEE, p. 1-8).

Leuchter, J., Boril, J. and Blasch, E. 2016. Practical considerations of sic technology for UAV. (*In* 2016 IEEE/AIAA 35th Digital Avionics Systems Conference, Sacramento, California: IEEE, p. 1-8).

Liardon, J.-L., Hostettler, L., Zulliger, L., Kangur, K., Shaik, N. S. G. and Barry, D. A. 2018. Lake imaging and monitoring aerial drone. *HardwareX,* 3(2018):146-159.

Lin, J., Matthews, G., Wohleber, R. W., Funke, G. J., Calhoun, G. L., Ruff, H. A., Szalma, J. and Chiu, P. 2019. Overload and automation-dependence in a multi-UAS simulation: Task demand and individual difference factors. *Quaterly Journal of Experimental Psychology: Applied,* 25(3).

Linchant, J., Lisein, J., Semeki, J., Lejeune, P. and Vermeulen, C. 2015. Are unmanned aircraft systems (UAS s) the future of wildlife monitoring? A review of accomplishments and challenges. *Mammal Review,* 45(4):239-252.

Liu, C., McAree, O. and Chen, W. H. 2013. Path-following control for small fixed-wing unmanned aerial vehicles under wind disturbances. *International Journal of Robust and Nonlinear Control,* 23(15):1682-1698.

Månsson, C. and Stenberg, D. 2014. Model-based design development and control of a wind resistant multirotor UAV. Sweden: Lund University. (Thesis - MSc).

Marcaccio, J. V., Markle, C. E. and Chow-Fraser, P. 2016. Use of fixed-wing and multi-rotor unmanned aerial vehicles to map dynamic changes in a freshwater marsh. *Journal of Unmanned Vehicle Systems,* 4(3):193-202.

Martinez, K. 2019. Best drones by category. https://www.dronethusiast.com/best-drones/ Date of access: 1 Nov. 2019.

Metni, N. and Hamel, T. 2007. A UAV for bridge inspection: Visual servoing control law with orientation limits. *Automation in Construction,* 17(1):3-10.

Myers, M. D. 1997. Qualitative research in information systems. *Management Information Systems Quarterly,* 21(2):241-242.

Nekrasov, M., Allen, R. and Belding, E. 2019. Performance analysis of aerial data collection from outdoor iot sensor networks using 2.4 ghz 802.15.4. (*In* Proceedings of The 5th Workshop on Micro Aerial Vehicle Networks, Systems, and Applications (DroNet'19), Seoul, South Korea: ACM, p. 33-38).

Nguyen, H., Troglia Gamba, M., Falletti, E. and Ta, T. 2018. Situational awareness: Mapping interference sources in real-time using a smartphone app. *Sensors,* 18(12):4130-4151.

Oates, B. J. 2006. Researching information systems and computing. London: Sage.

Oncu, M. and Yildiz, S. 2014. An analysis of human causal factors in unmanned aerial vehicle (UAV) accidents. Monterey, California: Naval postgraduate school of business and public policy. (Dissertation - MBA).

Orr, M. W., Rasmussen, S. J., Karni, E. D. and Blake, W. B. 2005. Framework for developing and evaluating mav control algorithms in a realistic urban setting. (*In* American Control Conference, Portland, OR, USA: IEEE, p. 4096-4101).

Pappu, S., Liu, Y., Horn, J. F. and Cooper, J. 2017. Wind gust estimation on a small vtol UAV. (*In* 7th AHS Technical Meeting on VTOL Unmanned Aircraft Systems, Merrifield, Virginia: American Helicopter Society International, p. 1-19).

Patel, A. 2011. UAV collision avoidance: A specific acceleration matching approach. University of Cape Town. (Thesis - MSc).

Pederi, Y. and Cheporniuk, H. 2015. Unmanned aerial vehicles and new technological methods of monitoring and crop protection in precision agriculture. (*In* Actual Problems of Unmanned Aerial Vehicles Developments (APUAVD), Kyiv, Ukraine: IEEE, p. 298-301).

Puri, A. (2005) *A survey of unmanned aerial vehicles (UAV) for traffic surveillance.* Tampa, Florida: Department of computer science and engineering, University of South Florida.

Qian, L. and Liu, H. H. 2019. Path following control of a quadrotor UAV with a cable suspended payload under wind disturbances. *IEEE Transactions on Industrial Electronics,* 67(3):2021-2029.

Quaritsch, M., Kruggl, K., Wischounig-Strucl, D., Bhattacharya, S., Shah, M. and Rinner, B. 2010. Networked UAVs as aerial sensor network for disaster management applications. *Elektrotechnik und Informationstechnik,* 127(3):56-63.

Rasmussen, J., Nielsen, J., Garcia-Ruiz, F., Christensen, S., Streibig, J. C. and Lotz, B. 2013. Potential uses of small unmanned aircraft systems (UAS) in weed research. *Weed Research,* 53(4):242-248.

Rathinam, S., Almeida, P., Kim, Z., Jackson, S., Tinka, A., Grossman, W. and Sengupta, R. 2007. Autonomous searching and tracking of a river using an UAV. (*In* American Control Conference, New York City, USA: IEEE, p. 359-364).

Rizk, M., Al-Deen, T. N., Diab, H., Ahmad, A. M. and El-Bazzal, Z. 2018. Proposition of online UAV-based pollutant detector and tracker for narrow-basin rivers: A case study on litani river. (*In* 2018 International Conference on Computer and Applications (ICCA), Beirut, Lebanon: IEEE, p. 189-195).

Ross, J. A., Geiger, B. R., Sinsley, G. L., Horn, J. F., Long, L. N. and Niessner, A. F. 2008. Vision-based target geolocation and optimal surveillance on an unmanned aerial vehicle. (*In* Proceedings of the AIAA Guidance, Navigation and Control Conference and Exhibit, Honolulu, Hawaii: American Institute of Aeronautics and Astronautics (AIAA)).

Ryaciotaki-Boussalis, H. and Guillaume, D. 2015. Computational and experimental design of a fixed-wing UAV. (*In* Valavanis, K.P. & Vachtsevanos, G.J. eds. Handbook of unmanned aerial vehicles. Dordrecht: Springer. p. 109-142).

Saha, B., Koshimoto, E., Quach, C. C., Hogge, E. F., Strom, T. H., Hill, B. L., Vazquez, S. L. and Goebel, K. 2011. Battery health management system for electric UAVs. (*In* 2011 Aerospace Conference, Montana, USA: IEEE, p. 1-9).

Schiano, F., Alonso-Mora, J., Rudin, K., Beardsley, P., Siegwart, R. and Siciliano, B. 2014. Towards estimation and correction of wind effects on a quadrotor uav. (*In* IMAV 2014: International Micro Air Vehicle Conference and Competition, Delft, The Netherlands: Delft University of Technology).

Selecký, M., Váňa, P., Rollo, M. and Meiser, T. 2013. Wind corrections in flight path planning. *International Journal of Advanced Robotic Systems,* 10(5):248-258.

Shuttleworth, M. and Wilson, L. T. 2008. Definition of research. https://explorable.com/definition-of-research Date of access: 3 Jan. 2018.

Stevenson, A. 2015. Oxford dictionary of english. Research. https://www.oed.com/view/Entry/163432?rskey=wM2s0X&result=1 Date of access: 4 Dec 2019.

Surakul, K., Sodsee, S. and Smanchat, S. 2015. A control of multiple drones for automatic collision avoidance. *Information Technology Journal,* 11(1):91-101.

Tomic, T., Schmid, K., Lutz, P., Domel, A., Kassecker, M., Mair, E., Grixa, I. L., Ruess, F., Suppa, M. and Burschka, D. 2012. Toward a fully autonomous UAV: Research platform for indoor and outdoor urban search and rescue. *IEEE Robotics & Automation Magazine,* 19(3):46-56.

UgCS. 2019. Ground station software UgCS. https://www.ugcs.com/ Date of access: 5 Nov. 2019.

Vaswani, V., Loh, S., Tan, B., Singh, K. and Srigrarom, S. 2014. Modular quadrotor mavs. (*In* IMAV 2014: International Micro Air Vehicle Conference and Competition, Delft, The Netherlands: Delft University of Technology).

Wang, R. and Liu, J. 2018. Trajectory tracking control of a 6-dof quadrotor UAV with input saturation via backstepping. *Journal of the Franklin Institute,* 355(7):3288-3309.

Watts, A. C., Ambrosia, V. G. and Hinkley, E. A. 2012. Unmanned aircraft systems in remote sensing and scientific research: Classification and considerations of use. *Remote Sensing,* 4(12):1671-1692.

Yang, S., Scherer, S. A. and Zell, A. 2012. An onboard monocular vision system for autonomous takeoff, hovering and landing of a micro aerial vehicle. *Journal of Intelligent & Robotic Systems,* 69(1-4):499-515.

Yang, X., Alvarez, L. M., Garratt, M. and Pota, H. 2013. A flight control scheme to improve position tracking performance of rotary-wing UASs. *IFAC Proceedings Volumes,* 46(10):1-8.

Zhang, C. and Kovacs, J. M. 2012. The application of small unmanned aerial systems for precision agriculture: A review. *Precision Agriculture,* 13(6):693-712.

# ANNEXURES

# ANNEXURE A – EXPERIMENT SETUP PROCEDURE

**Weather station**

1. Unbox equipment
2. Assemble bottom of tripod
3. Assemble measurement device
    a. Mount on pole
    b. Insert rain meter
    c. Attach wind cups
    d. Attach wind arrow
    e. Insert battery
4. Assemble top section of tripod with measurement device
5. Assemble console & insert battery (correct the date, time, etc.)
6. Verify connection

**UAS (Phantom 3 Pro)**

1. Unbox equipment
2. Assemble aircraft
    a. Check propellers for damage (replace if unsure)
    b. Remove camera cover
    c. Insert battery
3. Connect controller
    a. Connect mobile device via USB
4. Power ON
    a. Power ON controller (press & hold)
    b. Power ON aircraft (press & hold)
5. Launch DJI Go application
    a. Check software up to date
    b. Calibrate Compass/GPS
    c. Update home point
6. Test Flight

**Ground control station (UgCS)**

1. Launch UgCS desktop application
2. Launch UgCS for DJI android application
3. Upload flight plan / mission (Toggle switch to F-mode)
4. Take off and hover aircraft with remote
5. Execute mission when ready
6. Refrain from the controls until the mission is complete
7. Land the drone
8. * Power off between flights for easier data analysis

**LAST UPDATED: 20 FEBRUARY 2020**